nature chemistry

SUPPLEMENTARY INFORMATION

https://doi.org/10.1038/s41557-018-0155-z

In the format provided by the authors and unedited.

A biomimetic receptor for glucose

Robert A. Tromans[1], Tom S. Carter[2], Laurent Chabanne[2], Matthew P. Crump[1], Hongyu Li[3], Johnathan V. Matlock[2], Michael G. Orchard[2] and Anthony P. Davis[1]*

[1]School of Chemistry, University of Bristol, Bristol, UK. [2]Ziylo Ltd., Unit DX, St Philips Central, Bristol, UK. [3]School of Physiology, Pharmacology and Neuroscience, University of Bristol, Biomedical Sciences Building, University Walk, Bristol, UK. *e-mail: Anthony.Davis@bristol.ac.uk

A biomimetic receptor for glucose

Robert A. Tromans,[1] Tom S. Carter,[2] Laurent Chabanne,[2] Matthew P. Crump[1], Hongyu Li[3], Johnathan V. Matlock,[2] Michael G. Orchard[2] and Anthony P. Davis[1]

[1]School of Chemistry, University of Bristol, Cantock's Close, Bristol, BS8 1TS, UK.

[2]Ziylo Ltd., Unit DX, St Philips Central, Albert Road, Bristol BS2 0XJ.

[3]School of Physiology, Pharmacology and Neuroscience, University of Bristol, Medical Sciences Building, University Walk, Bristol BS8 1TD, UK.

Table of Contents

1. Synthesis and Characterisation of Receptor 2

Synthesis

Commercial reagents were purchased from Sigma-Aldrich, Alfa-Aesar or Acros Organics and were used without further purification unless otherwise specified. Cell culture media were obtained from ThermoFisher Scientific. Human Serum and enzymes were obtained from Sigma Aldrich. All air and moisture sensitive manipulations were carried out using standard vacuum line and Schlenk techniques. Solvents for air and moisture sensitive manipulations were obtained from an Anhydrous Engineering Solvent Purification System[1], distilled and dried over activated molecular sieves, or purchased from Acros Organics.

Flash column chromatography was performed using silica gel 60 Å (Sigma Aldrich, particle size 35-70 micron) and a suitable eluent. Reverse phase flash chromatography was performed on a Biotage Isolera One with Biotage SNAP Ultra C18 25 µm columns, typically with acetone/water eluents. TLC was performed using aluminium backed TLC plates (Merck-Keiselgel 60 F_{254}) and visualised using UV fluorescence (254 or 365 nm) and/or developed using ninhydrin, potassium permanganate, EtOH/H_2SO_4, vanillin, $Pd(OAc)_2/H_2O$ or iodine.

HPLC chromatography was performed using a Waters 600 Controller with a Waters 2998 Photodiode Array Detector. For analytical runs a XSELECT CSH C18 5 µm (4.6 × 150 mm) column was used and for preparative runs a XSELECT CSH Prep C18 5 µm OBD (19 × 250 mm) column was used, normally with an acetone/water or methanol/0.1% trifluoracetic acid (aqueous) solvent mixtures.

^1H and ^{13}C NMR spectra were recorded on Varian VNMR 400 MHz, Bruker 400 MHz, Varian VNMRS 500 MHz, Bruker Advance III HD Cryo 500 MHz and Varian VNMRS (equipped with a ^1H observe cryogenically cooled probe) 600 MHz spectrometers. All spectra were obtained at ambient temperature unless stated otherwise. All ^1H and ^{13}C NMR chemical shifts are reported relative to the ^1H (residual) and ^{13}C chemical shifts of the solvent as standard. The ^1H NMR spectra are provided for all compounds as evidence of purity. NMR spectra for characterisation are listed using individual numbering systems for each compound, not the system employed for the discussion of **2** in the paper (Figs. 1 and S7).

IR spectra were recorded on a Perkin-Elmer Spectrum One FT-IR spectrometer with an ATR accessory and frequencies reported in wavenumbers (cm^{-1}). ESI-HRMS (electrospray ionisation high resolution mass spectrometry) was performed on a Bruker Daltonics micrOTOF II.

Second generation dendritic amine **(5)**[2] and 3-((((9H-fluoren-9-yl)methoxy)carbonyl)amino)-4-aminobenzoic acid **(4)**[3] were prepared according to literature procedures. Receptor **2** was prepared as summarised in Supplementary Supplementary Scheme **1**. The numbering system used to discuss receptor **2** is shown in Supplementary Supplementary Figure **8**. The detailed synthetic procedures and characterisation data for compound in the synthetic sequence towards receptor **2** are given in the following pages, accompanied by the relevant NMR spectra as evidence of purity and characterisation.

[1] Pangborn, A. B., Giardello, M. A., Grubbs, R. H., Rosen, R. K. & Timmers, F. J. Safe and convenient procedure for solvent purification. *Organometallics* **15**, 1518-1520 (1996).
[2] Destecroix, H. et al. Affinity enhancements by dendritic side-chains in synthetic carbohydrate receptors. *Angew. Chem., Int. Ed.* **54**, 2057 –2061 (2015).
[3] Blanco-Canosa, J. B., Dawson, P. E., An Efficient Fmoc-SPPS Approach for the Generation of Thioester Peptide Precursors for Use in Native Chemical Ligation. *Angew. Chem., Int. Ed.* **47**, 6851-6855 (2008).

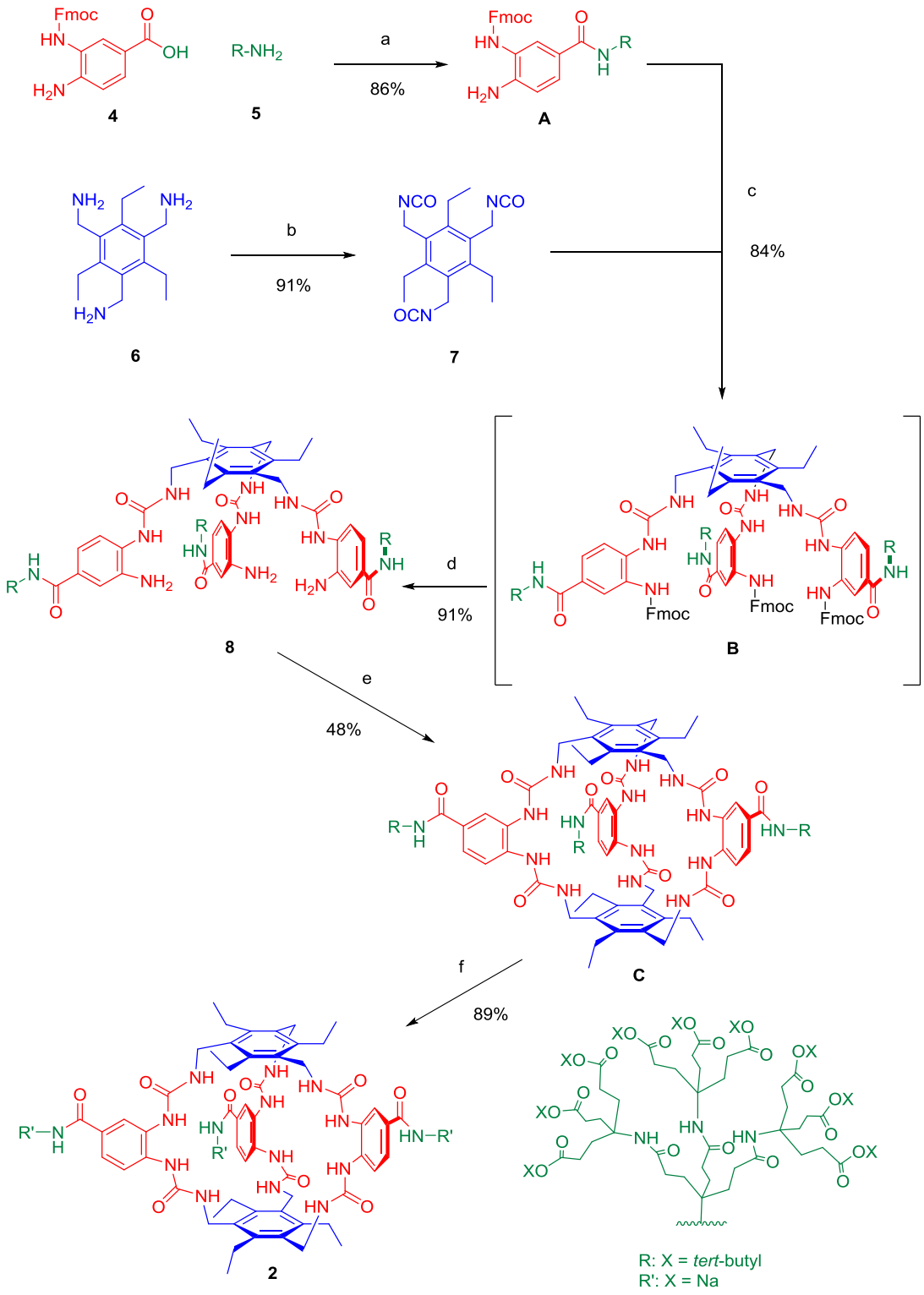

Supplementary Scheme 1| Synthesis of receptor **2**. a) HBTU, HOBt, DIPEA, THF, 25 °C, 16 h, 86%; b) triphosgene, toluene, reflux, 3 h, 91%; c) pyridine, CH_2Cl_2, 34 °C, 84%; d) DBU, CH_2Cl_2, 0 °C, 1 h, 91%; e) octyl β-D-glucoside, DMAP, CH_2Cl_2, 34 °C, 2 days, 48%; f) TFA (20% v/v), CH_2Cl_2, 0 °C then 25 °C, 16 h; then removal of volatiles; then 0.5 M NaOH (aq) to pH 7.4, 89%.

1,3,5-triethyl-2,4,6-tris(isocyanatomethyl)benzene (7)

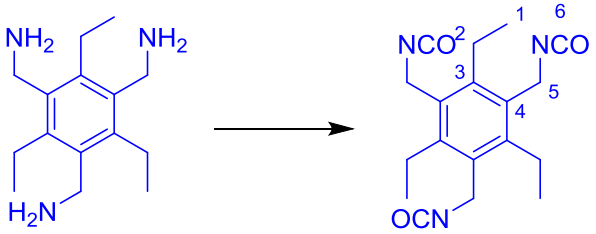

6 **7**

Under an inert N_2 atmosphere, a flask was charged with triphosgene (180 mg, 0.61 mmol) and anhydrous toluene (6 mL). A solution of triamine **6** (50 mg, 0.20 mmol) in anhydrous toluene (6 mL) was added dropwise and the reaction mixture was heated to reflux then stirred for 2 hours. The mixture was cooled and the solvent removed under vacuum. The crude solid was triturated with cold toluene, filtered and the filtrate dried under high vacuum to afford tris-isocyanate **7** (63 mg, 0.20 mmol, 91%) as a colourless oil that crystallised over time.

^{1}H NMR: (400 MHz, ($CDCl_3$): 1.26 (t, *J* = 7.6 Hz, 9H, C(1)H), 2.84 (q, *J* = 7.6 Hz, 6H, C(2)H), 4.50 (s, 6H, C(5)H_2); **^{13}C NMR:** (100 MHz, ($CDCl_3$): δ 16.1 (C(1)H_2), 22.8 (C(2)H), 40.4 (C(5)H), 123.1 (C6), 132.4 (C3), 143.1 (C4); **ν_{max}** 2973, 2933, 2875, 2243, 1495, 1453, 1335, 1042, 856, 577 cm^{-1}; **HRMS:** (ESI^+) calculated for $C_{18}H_{21}N_3O_3Na^+$: 350.1475, found $[M+Na]^+$: 350.1474.

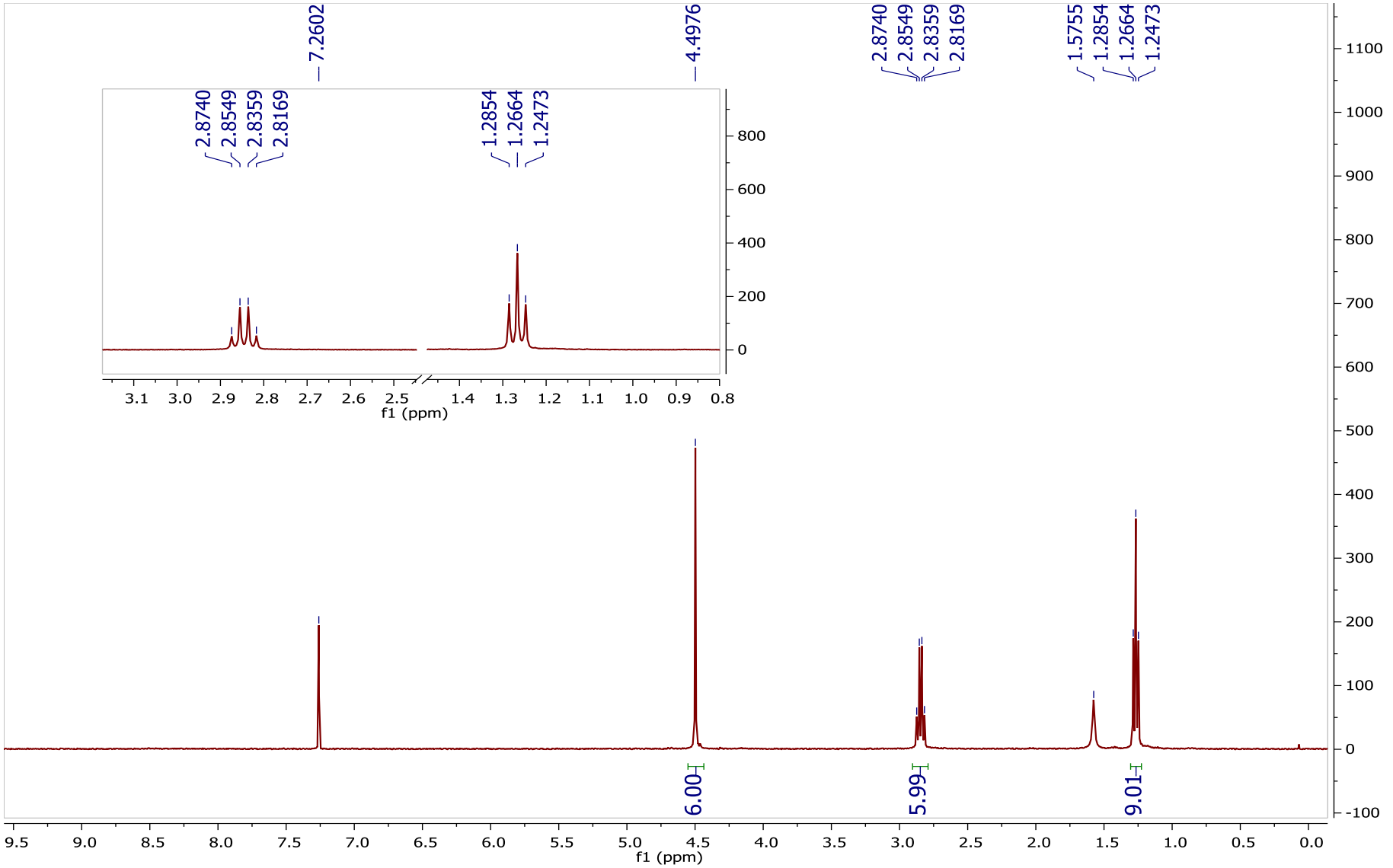

Supplementary Figure 1 | ^{1}H NMR spectrum of **7** in $CDCl_3$ at 298 K.

Fmoc protected spacer unit A

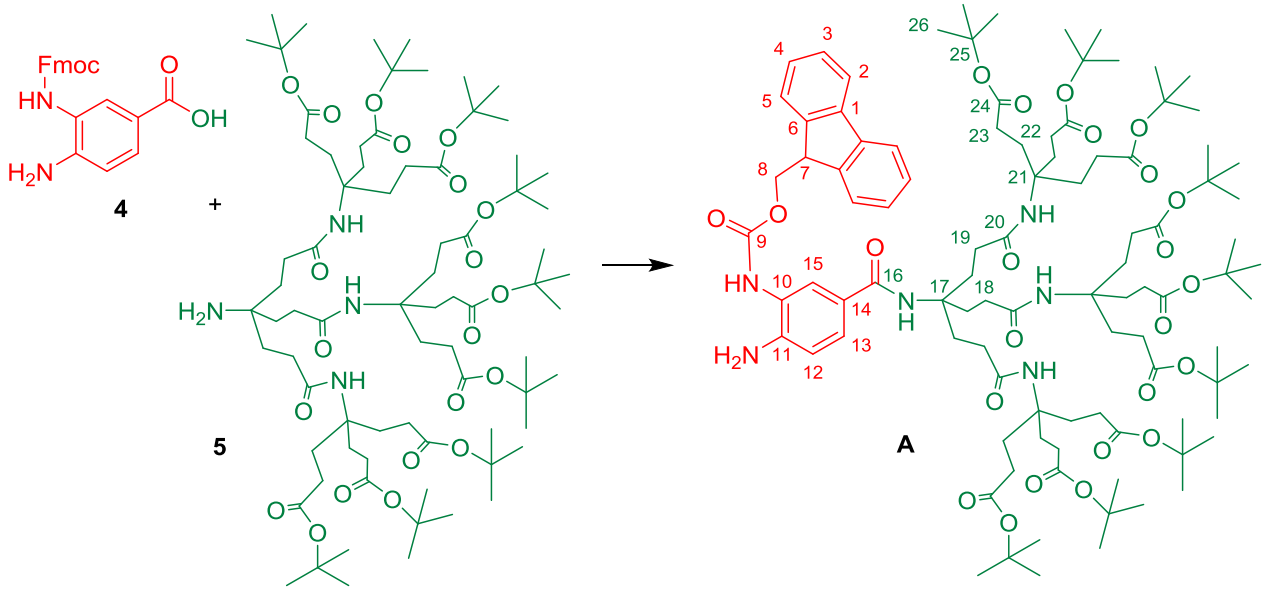

Under an inert N_2 atmosphere, amino acid **4** (5 g, 15.3 mmol), HBTU (5.03 g, 15.3 mmol) and HOBt.H_2O (2.06 g, 15.3 mmol) were suspended in anhydrous THF (60 mL). DIPEA (7.2 mL, 38.3 mmol) was added and the reaction stirred at room temperature for 1 hour. The solvent was removed under vacuum and the crude residue dissolved in ethyl acetate (100 mL) and then poured into water (300 mL). The precipitate was filtered and air dried to afford the crude HOBt ester/tetramethyl urea complex (1:1, 4.36 g, 7.19 mmol, Mw = 607.67 g mol^{-1}) which was used without further purification. The above material was suspended in anhydrous THF (60 mL) and amine **5** (9.4 g, 6.54 mmol) and DIPEA (2.1 mL, 12.3 mmol) were added. The reaction mixture was stirred at room temperature for 24 hours and the solvent removed under vacuum. The residue was then purified by flash column chromatography (5% MeOH:CH_2Cl_2) to afford **A** as an off white solid (9.02 g, 5.19 mmol, 86%). **^{1}H NMR**: (400 MHz, ($CDCl_3$): δ 1.41 (s, 81H, C(26)H_3), 1.95 (m, 18H, C(23)H_2), 2.11 (t, *J* = 7.2 Hz, 6H, C(18)H_2), 2.18 (m, 18H, C(22)H_2), 2.26 (t, *J* = 7.2 Hz, 6H, C(19)H_2), 4.14-4.34 (br m, 3H, C(7)H and NH_2), 4.46 (d, *J* = 7.4 Hz, 2H, C(8)H_2), 6.11 (s, 3H, NH), 6.77 (d, *J* = 8.4 Hz, 1H, C(13)H), 7.26-7.31 (m, 2H, C(4)H), 7.39 (t, *J* = 7.4 Hz, 2H, C(3)H), 7.57-7.69 (m, 2H, C(5)H), 7.72 (d, *J* = 8.7 Hz, 1H, C(2)H), 7.76 (d, *J* = 7.6 Hz, 3H, C(2)H), 7.78 (d, *J* = 2.1 Hz, 1H, C(15)H), 8.59 (s, 1H, NH); **^{13}C NMR:** (100 MHz, ($CDCl_3$): δ 28.0 (C26), 29.8 (C22), 29.9 (C23), 31.8 (C19), 32.2 (C18), 47.2 (C7), 53.4 (C17), 57.4 (C21), 67.3 (C8), 80.6 (C25) 116.6 (C12), 119.9 (C2), 122.6 (C10), 124.6 (C14), 125.3 (C4), 126.0 (C15), 126.8 (C13), 127.0 (C5), 127.6 (C3), 141.3 (C1), 143.8 (C6), 145.3 (C11), 154.9 (C9), 166.6 (C16), 172.7 (C24), 173.1 (C20); **ν_{max}** 2977, 2963, 1752, 1723, 1689, 1637, 1535, 1367, 1242, 1151, 1098, 844 cm^{-1}; **HRMS:** (ESI^+) calculated for $C_{98}H_{150}N_6O_{24}Na_2^{2+}$: 921.0260, found $[M+2Na]^{2+}$: 921.0252.

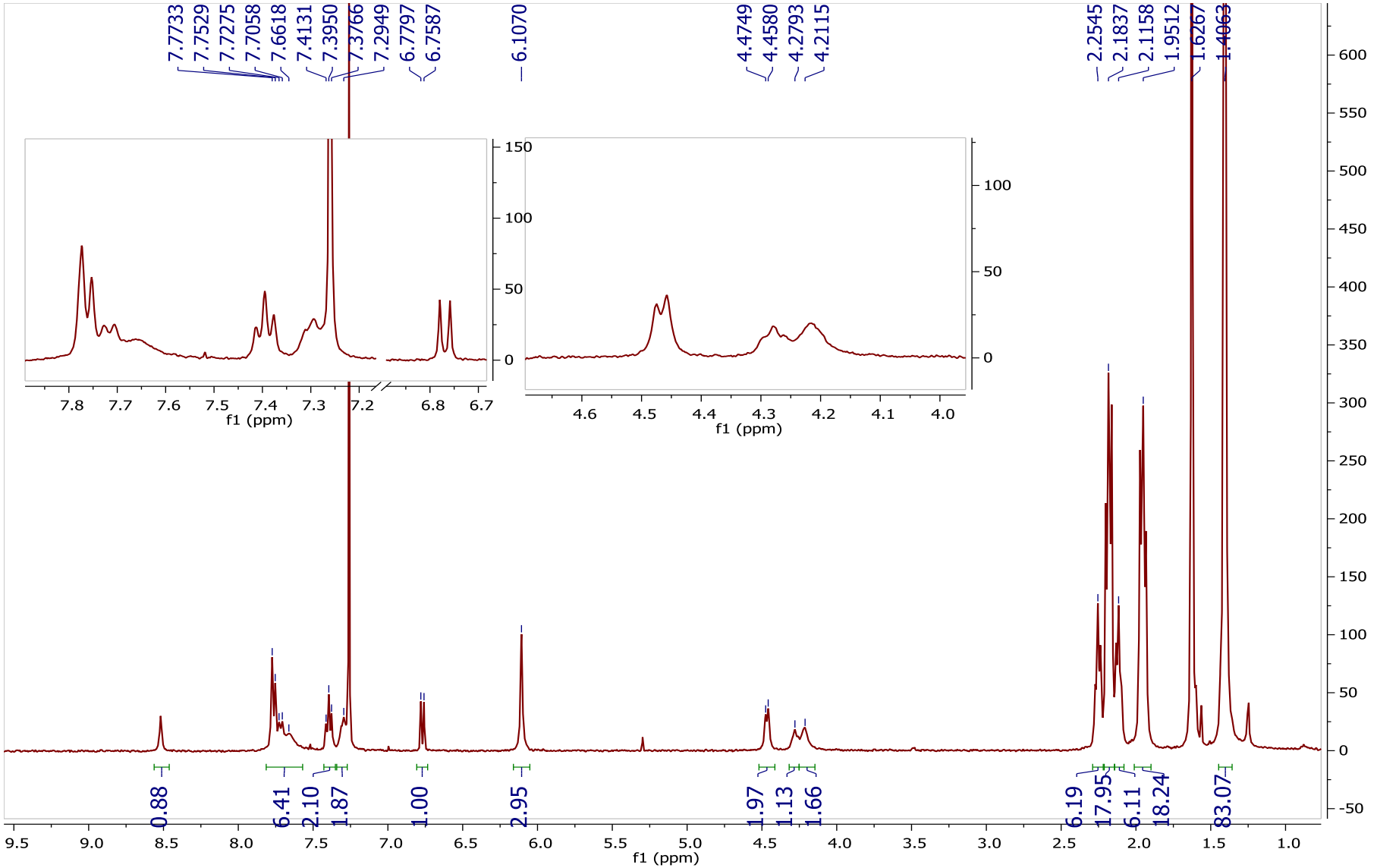

Supplementary Figure 2 | ^{1}H NMR spectrum of amine **A** in $CDCl_3$ at 298 K.

Half-receptor 8

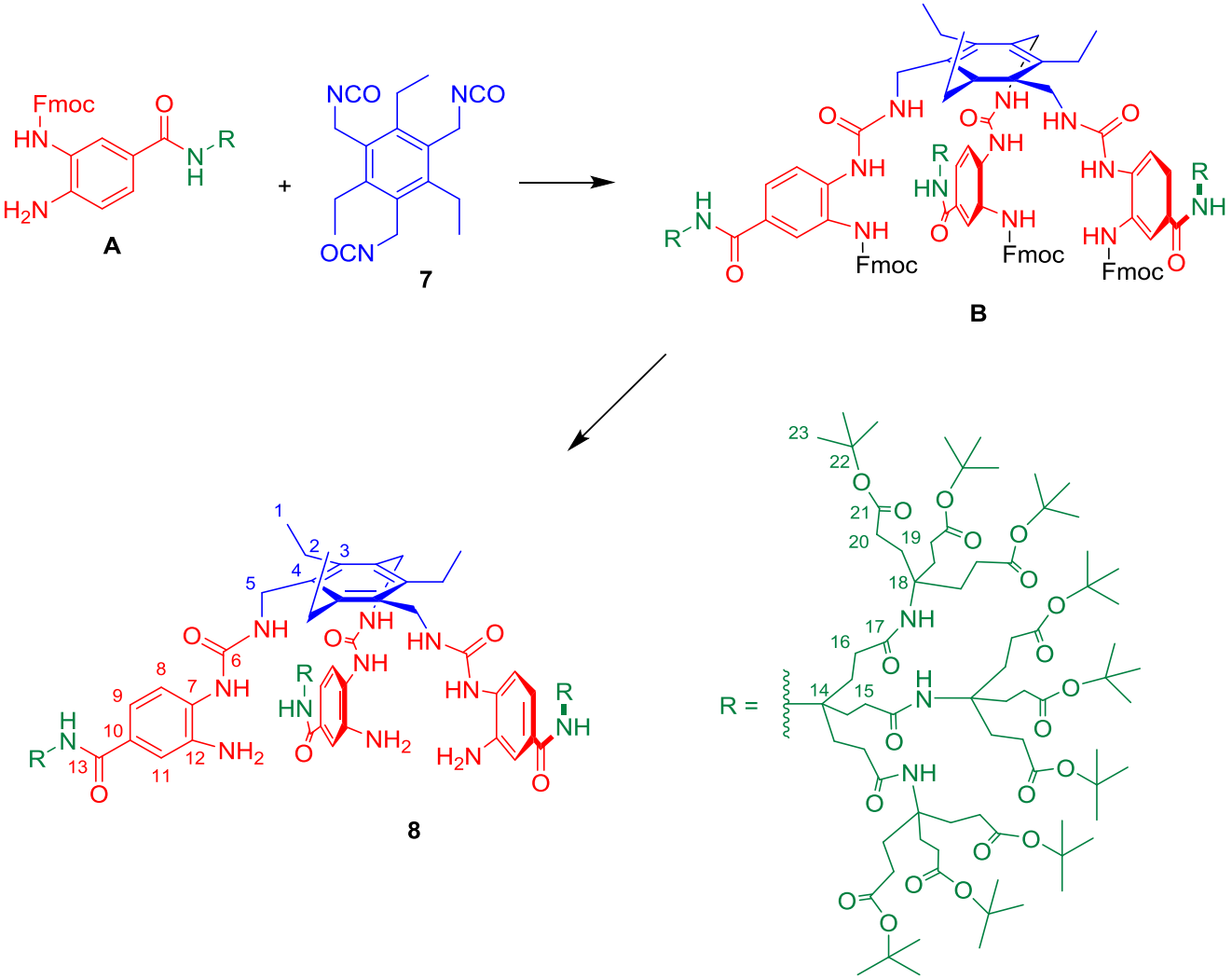

Under an inert N_2 atmosphere, amine **A** (556 mg, 0.31 mmol) was added to a solution of **7** (28 mg, 0.086 mmol) in anhydrous dichloromethane (5 mL). Anhydrous pyridine (40 µL) was added and the reaction heated to 34 °C for 16 hours, after which it was cooled to room temperature and the solvent removed under vacuum. The residue was purified by reverse phase flash chromatography (Biotage SNAP Ultra C18 25 µm) eluting with acetone/water (10:90 → 90:10 over 10 column volumes then 100% acetone over 4 column volumes) to afford the Fmoc-protected half-receptor **B** (400 mg, 0.072 mmol, 84%) as a white solid. Conversion to **B** was confirmed by NMR* and high resolution mass spectrometry (ESI$^+$): m/z calculated for $C_{312}H_{471}N_{21}O_{75}Na_3^{3+}$ 1928.1155, found $[M+3Na]^{3+}$: 1928.1160;

---

* *NMR characterisation was limited by signal broadening, presumably due to slow conformational exchange (see Supplementary Supplementary Figure* **3***)*

calculated for $C_{312}H_{471}N_{21}O_{75}Na_4^{4+}$ 1451.8339, found $[M+4Na]^{4+}$: 1451.8320. Under an inert N_2 atmosphere, **B** (300 mg, 0.052 mmol) was dissolved in anhydrous dichloromethane (8 mL) and cooled to 0 °C. DBU (50 µL, 0.30 mmol) was added dropwise and the reaction mixture stirred at 0 °C for 1 hour. The solvent was removed under vacuum and the crude product purified by flash column chromatography (4% MeOH:CH_2Cl_2) to afford half-receptor **8** as a white solid (238 mg, 0.047 mmol, 91%). **^{1}H NMR:** (400 MHz, (CD_3OD): δ 1.26 (t, *J* = 7.6 Hz, C(1)H$_3$), 1.43 (s, 243H, C(23)H$_3$), 1.94 (m, 54H, C(20)H$_2$), 2.09 (m, 18H, C(15)H$_2$), 2.19 (m, 54H, C(19)H$_2$), 2.24 (m, 18H, C(16)H$_2$), 2.82-2.95 (m, 6H, C(2)H$_2$), 4.52 (s, 6H, C(5)H$_2$), 6.17 (br s, 3H, C(5)H$_2$NH), 7.21 (dd, *J* = 2.1, 8.4 Hz, 3H, C(9)H), 7.30 (d, *J* = 2.1 Hz, 3H, C(11)H), 7.40 (d, *J* = 8.4 Hz, 3H, C(8)H), 7.42 (s, 9H, C(18)NH), 7.93 (s, 3H, OC(13)NH); **^{13}C NMR:** (100 MHz, ($CDCl_3$): δ 17.0 (C1), 22.5 (C2), 28.5 (C23), 30.5 (C19), 30.7 (C20), 32.3 (C15), 32.6 (C16), 37.9 (C5), 58.9 (C18), 59.4 (C14), 81.6 (C22), 117.4 (C11), 118.9 (C9) 124.5 (C8), 130.0 (C10), 132.9 (C3), 133.8 (C7), 141.4 (C12), 145.1 (C4), 157.9 (C6), 170.1 (C13), 174.4 (C21), 175.6 (C17); **HRMS:** (ESI^+) calculated for $C_{267}H_{441}N_{21}O_{69}Na_3^{3+}$ 1706.0472, found $[M+3Na]^{3+}$: 1706.0490.

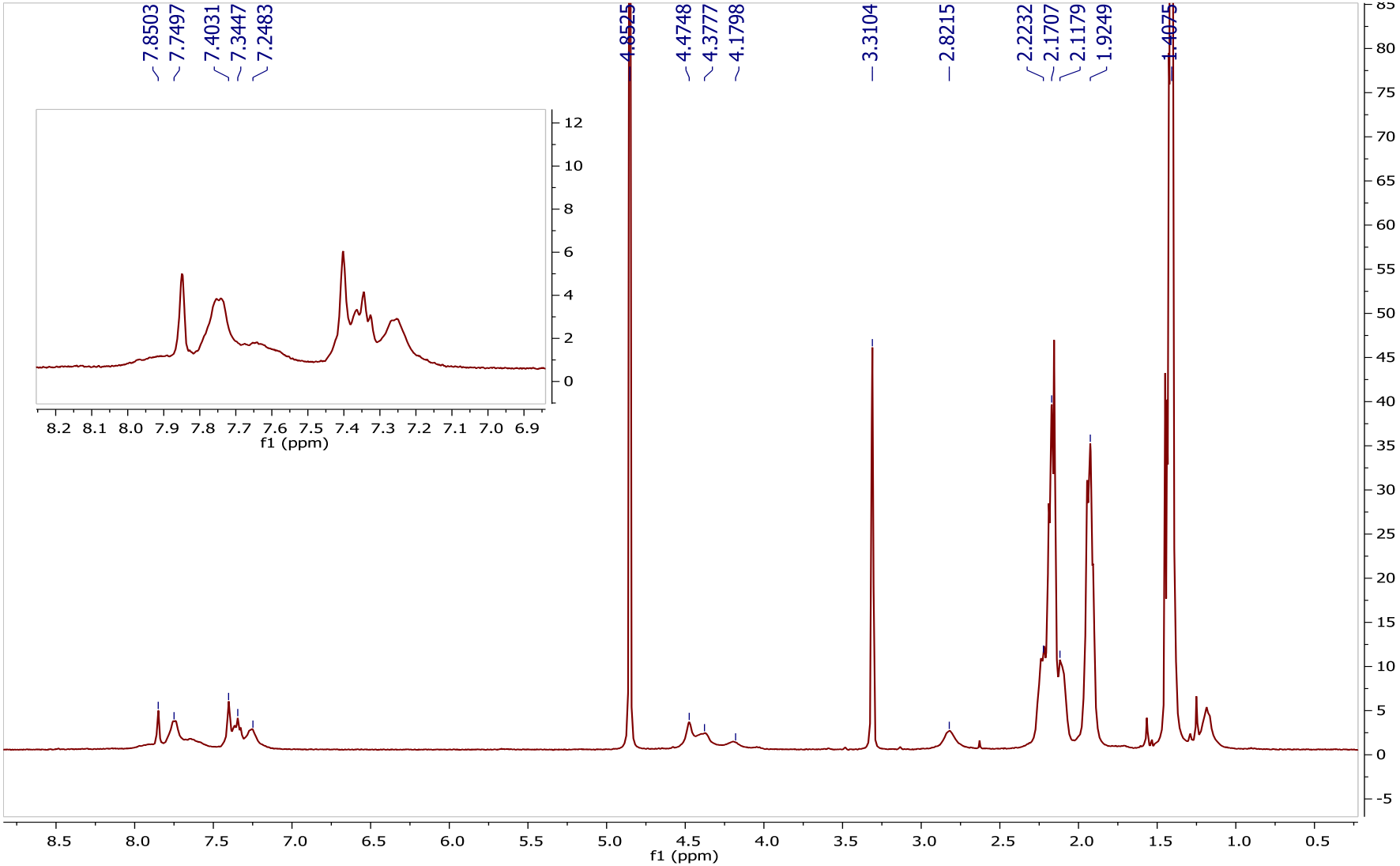

Supplementary Figure 3 | ^{1}H NMR spectrum of Fmoc-protected half-receptor **B** in CD_3OD at 298 K. Signals are broad, most notably in the aromatic region (7-8 ppm).

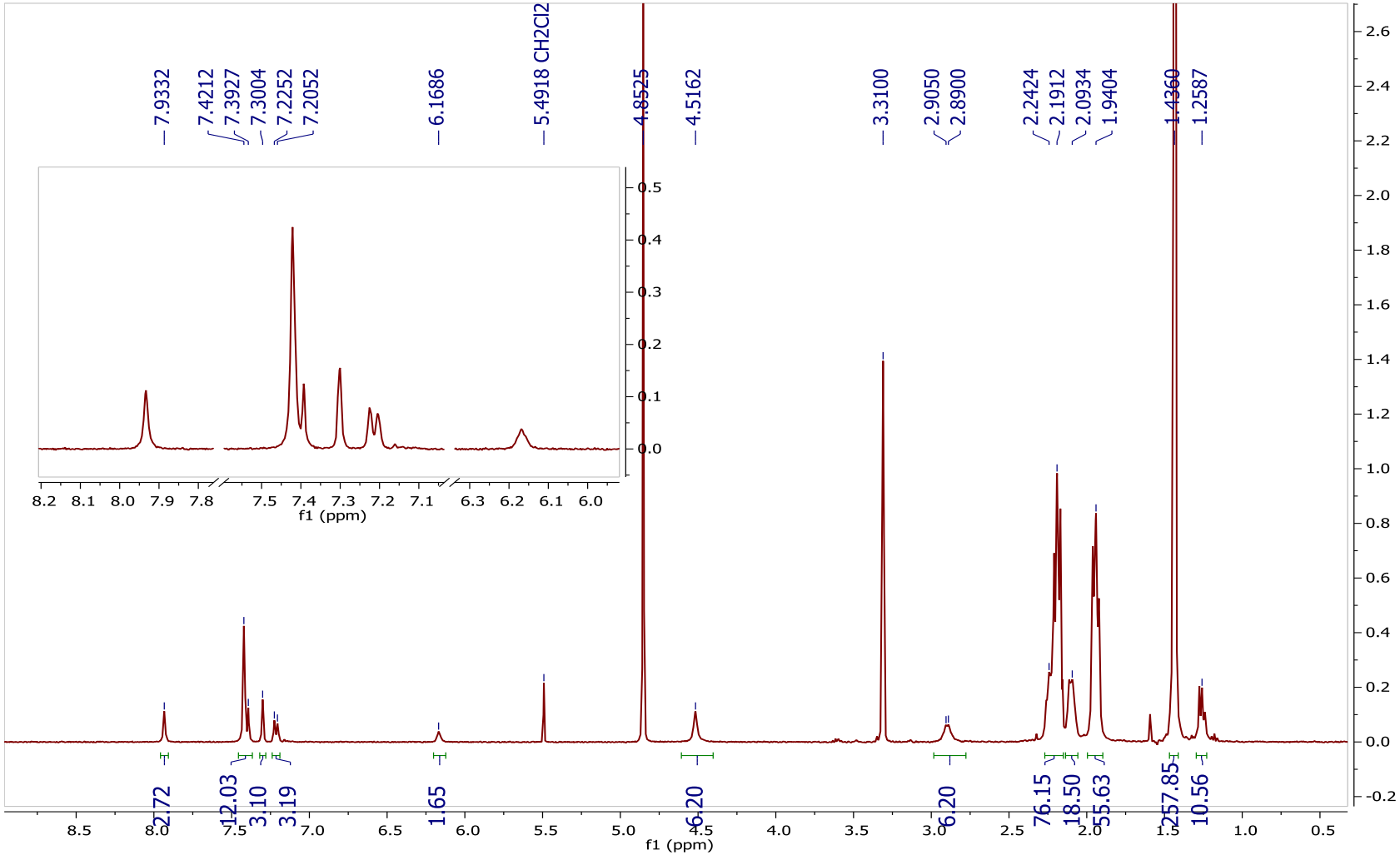

Supplementary Figure 4 | ^{1}H NMR spectrum of half-receptor **8** in CD_3OD at 298 K.

Protected receptor C

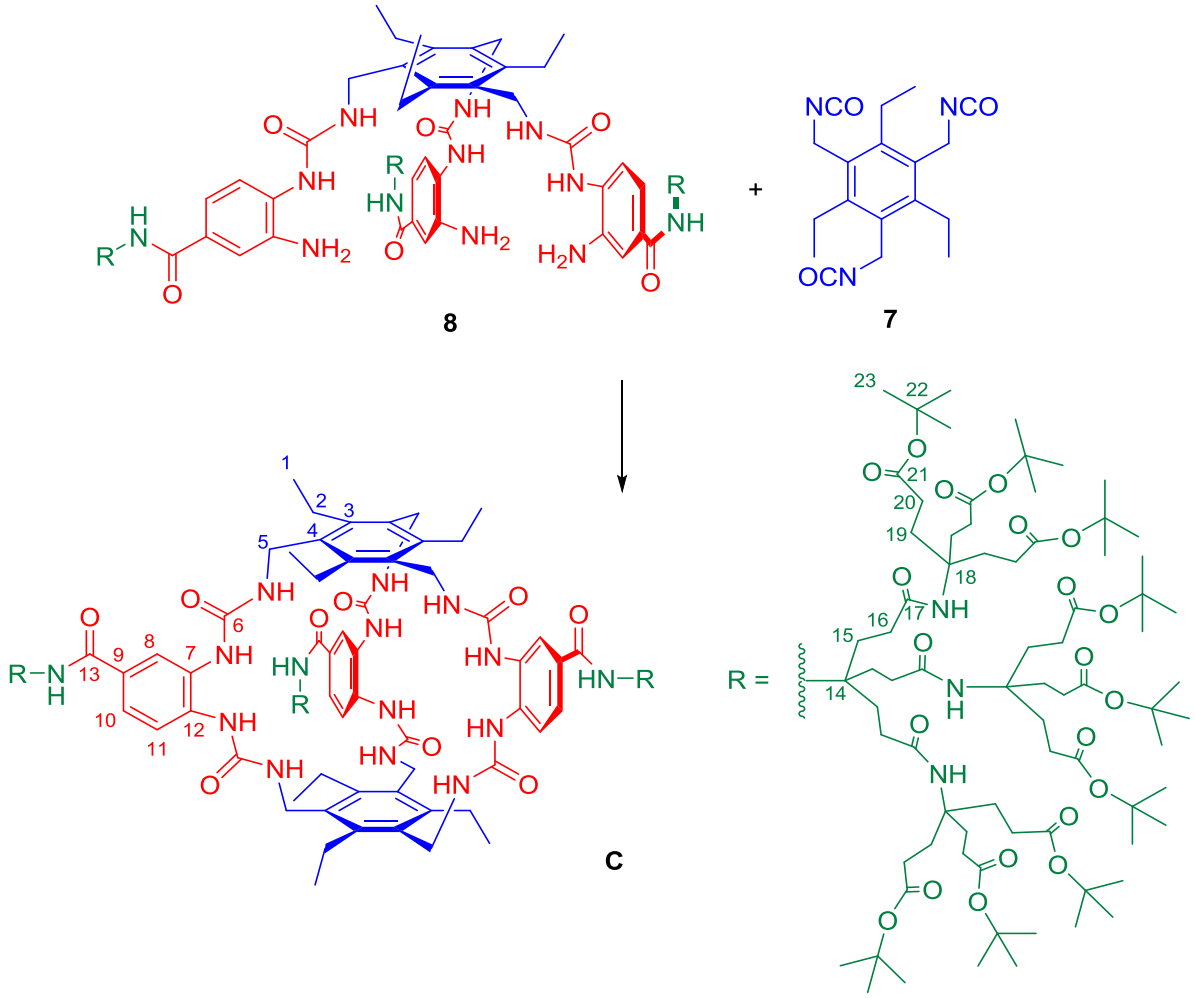

Under an inert N_2 atmosphere, the half-receptor **8** (500 mg, 0.1 mmol), octyl β-D-glucoside **9** (59 mg, 0.2 mmol) and 4-dimethylaminopyridine (37 mg, 0.3 mmol) were dissolved in anhydrous dichloromethane (180 mL). A solution of **7** (33 mg, 0.1 mmol) in anhydrous dichloromethane (20 mL) was added at a rate of 1 mL/hr and the reaction stirred at 34 °C for 2 days. The reaction mixture was cooled to room temperature and the solvent removed under vacuum. The residue was purified by preparative HPLC (Waters CSH C18 5 µm 19 × 250 mm) eluting with acetone/water (70:30 → 96:4 over 30 mins, then 96:4 isocratic over 10 mins, then 100:0 over 5 mins). The solvent was removed under vacuum and the product suspended in water and freeze dried to afford **C** as a white solid (257 mg, 0.048 mmol, 48%). **^{1}H NMR:** (400 MHz, (CD_3OD): δ 1.21 (m, 18H C(1)$\underline{H}_3$), 1.43 (s, 243H, C(23)$\underline{H}_3$), 1.95 (m, 54H, C(20)$\underline{H}_2$), 2.13 (m, 18H, C(15)$\underline{H}_2$), 2.20 (m, 54H, C(19)$\underline{H}_2$), 2.25 (m, 18H, C(16)$\underline{H}_2$), 2.72, 2.83 (br m, 6H, C(2)$\underline{H}_2$), 4.40, 4.49 (br s, 6H, C(5)$\underline{H}_2$), 7.43 (s, 9H, N$\underline{H}$), 7.63 (d, *J* = 8.7 Hz, 3H, C(10)$\underline{H}$), 8.04 (d, *J* = 8.7 Hz, 3H, C(11)$\underline{H}$), 8.06 (s, 3H, C(8)$\underline{H}$); **^{13}C NMR:** (100 MHz, ($CDCl_3$): δ 15.5, 15.6 (C$\underline{1}$), 22.3, 22.5 (C$\underline{2}$), 27.1 (C$\underline{23}$), 29.1 (C$\underline{19}$), 29.3 (C$\underline{20}$), 30.8 (C$\underline{15}$), 31.0 (C$\underline{16}$), 37.5 (C$\underline{5}$), 57.3 (C$\underline{18}$), 58.1 (C$\underline{14}$), 80.2 (C$\underline{22}$), 120.3 (C$\underline{11}$), 123.5 (C$\underline{8}$), 124.1 (C$\underline{10}$), 127.6 (C$\underline{7}$), 129.4 (C$\underline{9}$), 132.0, 132.6 (C$\underline{3}$), 135.0 (C$\underline{12}$), 143.0,

143.2 (C4), 155.8, 156.6 (C6), 168.2 (C13), 173.0 (C21), 174.1 (C17); **HRMS:** (ESI^+) calculated for $C_{285}H_{462}N_{24}O_{72}Na_3^{3+}$ 1816.1084 found $[M+3Na]^{3+}$: 1816.1093.

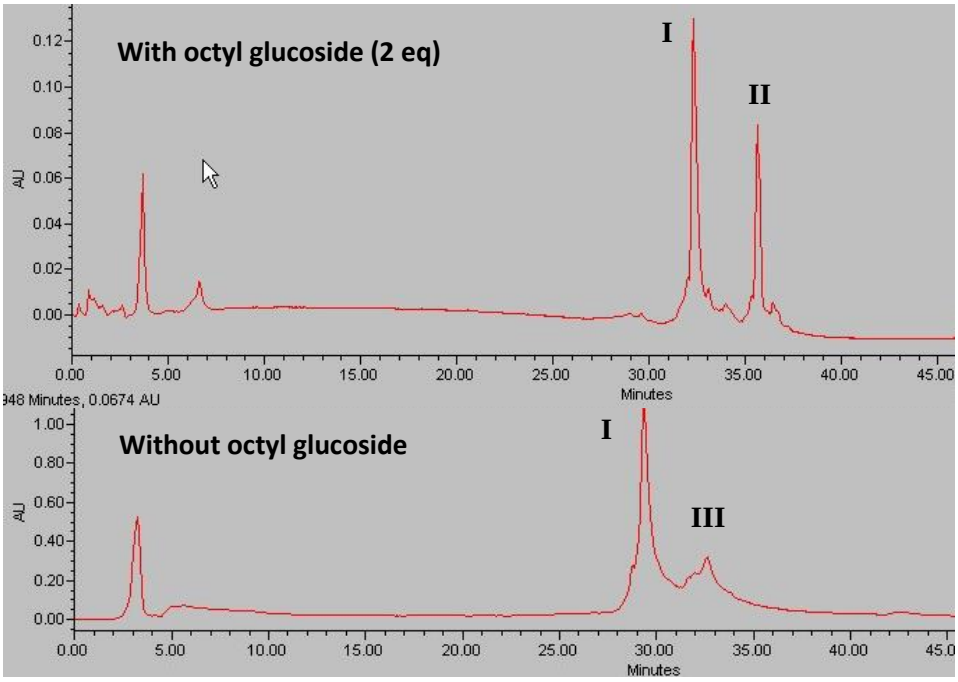

Supplementary Figure 5 | HPLC traces (monitored at 210 nm) for the purification of receptor **C**, showing the effects of templation with octyl glucoside **9**. A typical HPLC trace of the reaction mixture with octyl glucoside present (top) shows two main products: receptor **C** (I) and a side-product (II). According to MS analysis, side product II contains 2 eq of **8** and 1 eq of **7** (see Supplementary Supplementary Figure **6** for hypothesised structure). The isolated yield of **C** is 48%. The reaction was repeated using the procedure outlined above for **C** minus octyl glucoside and at 10 times reduced scale. The HPLC trace of the reaction product without octyl glucoside (bottom) indicates a more complex mixture. The isolated yield of **C** (I) is 12%.

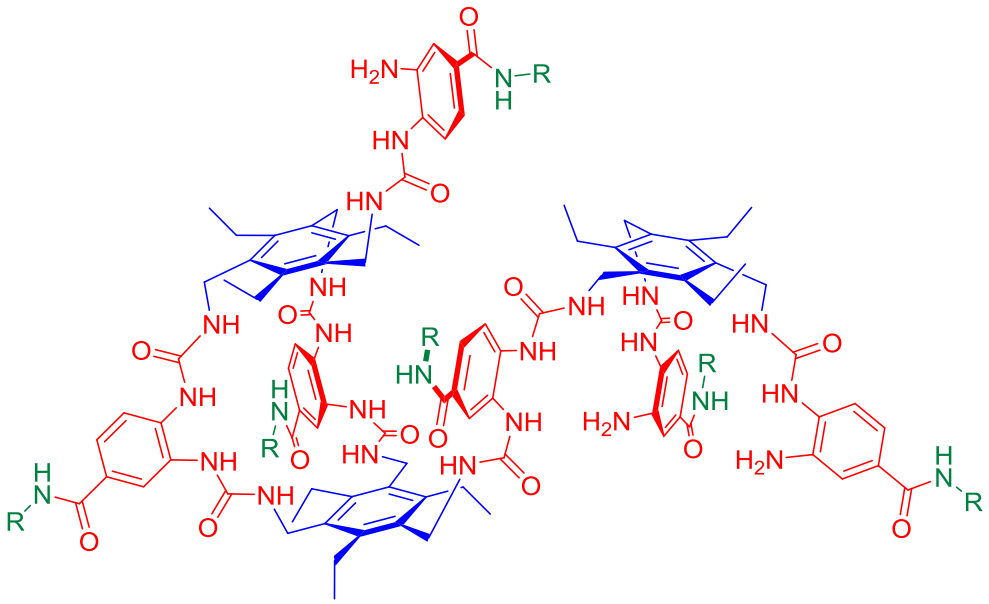

Supplementary Figure 6 | Hypothesised side product (II) consisting of 2 eq of **8** and 1 eq of **7**.

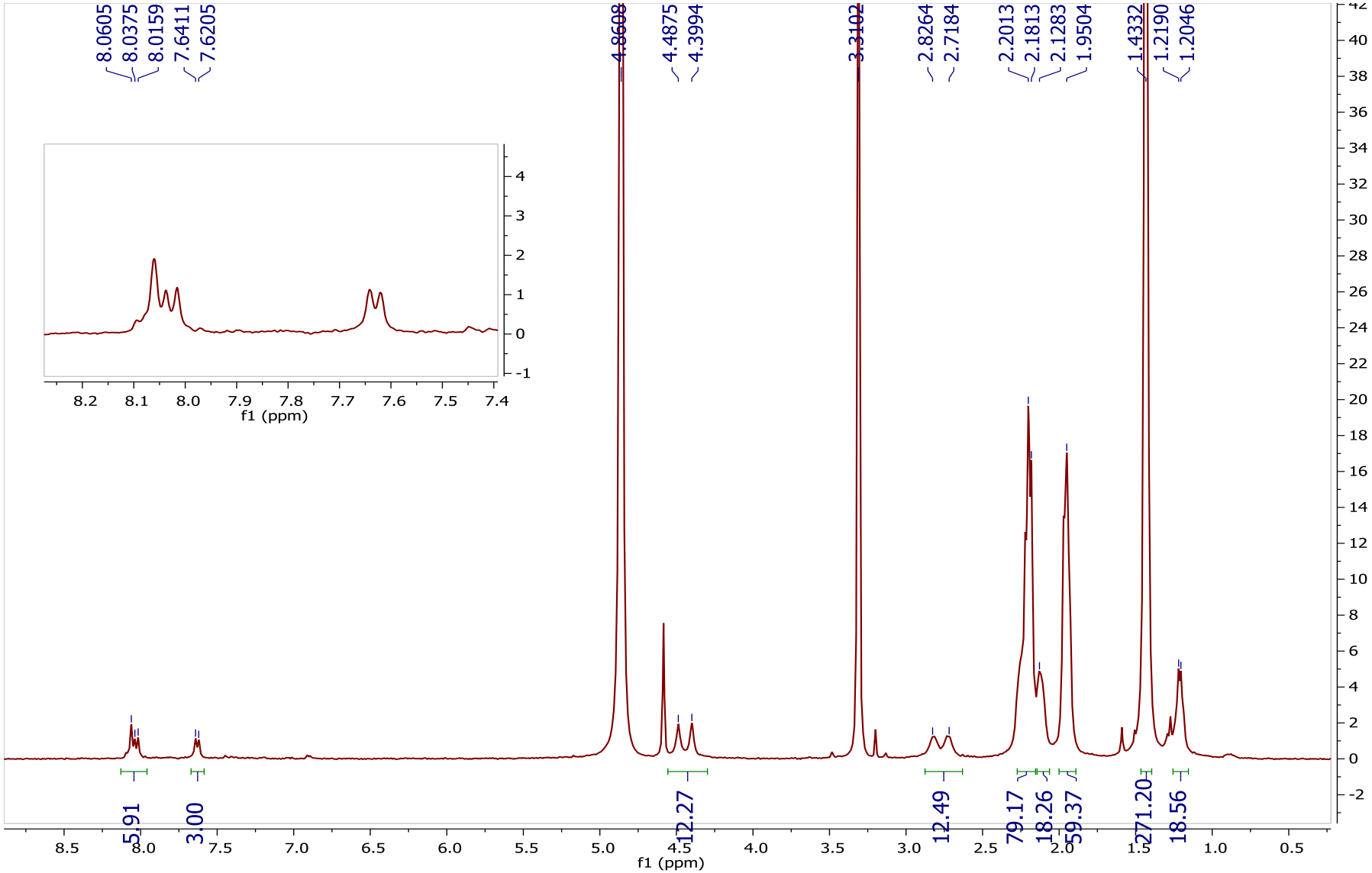

Supplementary Figure 7 | ^{1}H NMR spectrum of protected receptor **C** in CD_3OD at 298 K.

Receptor 2

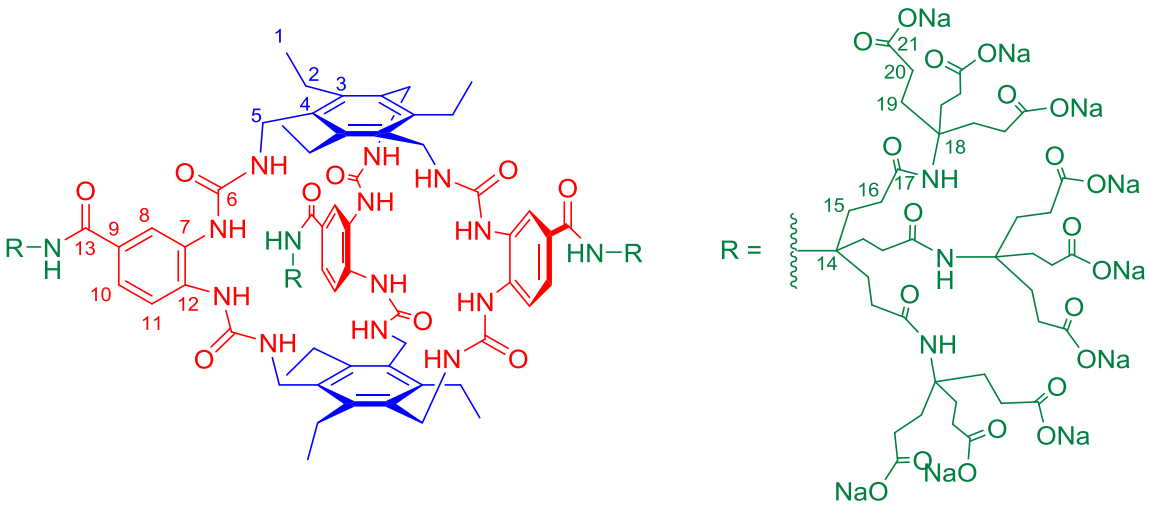

Protected receptor **C** (50 mg, 9.3 µmol) was dissolved in dichloromethane (HPLC grade, 2 ml) and cooled to 0 °C. Trifluoroacetic acid (TFA) (0.5 mL) was added dropwise and the reaction warmed to room temperature and stirred for 16 hours. The solvent was then removed under a flow of nitrogen, then the residue was co-evaporated with toluene (3 x 10 mL) to remove residual TFA, suspended in water and freeze dried. The product was then purified by preparative HPLC (Waters CSH C18 5 µm 19 × 250 mm) eluting with 100% Water (buffered with 0.1 % TFA) → 100% methanol over 40 minutes. The solvent was removed under vacuum, the residue co-evaporated with toluene (3 × 10 mL), the product suspended in water and freeze dried. The solid was then suspended in water, neutralised to pH 7.4 with NaOH (aq), filtered and then freeze dried to afford **2** as a white solid (36.9 mg, 8.3 µmol, 89%). **^{1}H NMR:** (400 MHz, (D_2O): δ 0.93-1.12,1.11-1.25 (br m, 18H, C(1)H_3), 1.89-1.98 (m, 54H, C(20)H_2), 2.08-2.15 (m, 18H, C(15)H_2), 2.13- 2.20 (m, 54H, C(19)H_2), 2.27-2.35 (m, 18H, C(16)H_2), 2.67-2.85 (br m, 12 jH, C(2)H_2), 4.46 (br s, 6H, C(5)H_2), 7.63 (d, *J* = 8.3 Hz, 3H, C(10)H), 7.78 (br s, 3H, C(8)H),7.80-7.85 (br m, 3H, C(11)H); **^{13}C NMR:** (100 MHz, ($CDCl_3$): δ 15.4, 15.5 (C1), 22.4, 22.6 (C2), 30.3 (C19), 30.5 (C15), 30.8 (C16), 31.1 (C20), 37.5, 37.7 (C5), 58.2 (C18), 58.6 (C14),122.4 (C11), 124.9 (C8, C10), 128.4 (C7), 130.0 (C9), 132.0, 132.4 (C3), 135.6 (C12), 144.0, 144.2 (C4), 157.0, 157.7 (C6), 169.6 (C13), 175.2 (C17), 182.1 (C21)

NMR characterisation of receptor 2

The numbering system used to discuss the conformational and binding properties of **2** is shown in Supplementary Supplementary Figure **8**. NMR spectra of receptor **2** taken using 1D and 2D techniques in D_2O or D_2O/H_2O (1:9) are shown in Supplementary Supplementary Figure **9** – Supplementary Supplementary Figure **23**. The interpretation was assisted by a variable temperature ^{1}H NMR study (Supplementary Supplementary Figure **23**). Raising the temperature caused broadened peaks to sharpen, resulting in a spectrum which clearly reflected the symmetry of the molecule. In particular, this confirmed that the two peaks at ~1.05 and 1.2 p.p.m. resulted from the two methyl environments (t1' and t1 respectively). A combination of COSY, NOESY and HMBC methods then resulted in the assignments shown in Supplementary Supplementary Figure **10** (^{1}H) and Supplementary Supplementary Figure **12**(^{13}C). The key conformational question is the orientation of urea NH groups, which could be directed inwards towards the cavity (as represented in Supplementary Supplementary Figure **8**) or outwards, in which case $NH_B/_B$' would approach protons s1 or s3. As shown in Supplementary Supplementary Figure **21**, NOESY spectra showed no correlation between $NH_B/_B$' and either s1 or s3. Correlations which were observed (e.g. NH_C-s1, $NH_B/_B$'-t1') suggest that $NH_B/_B$'-s1/3 cross-peaks could have been detected if the protons were close in space. We therefore conclude that conformations with inward-directed NH groups predominate.

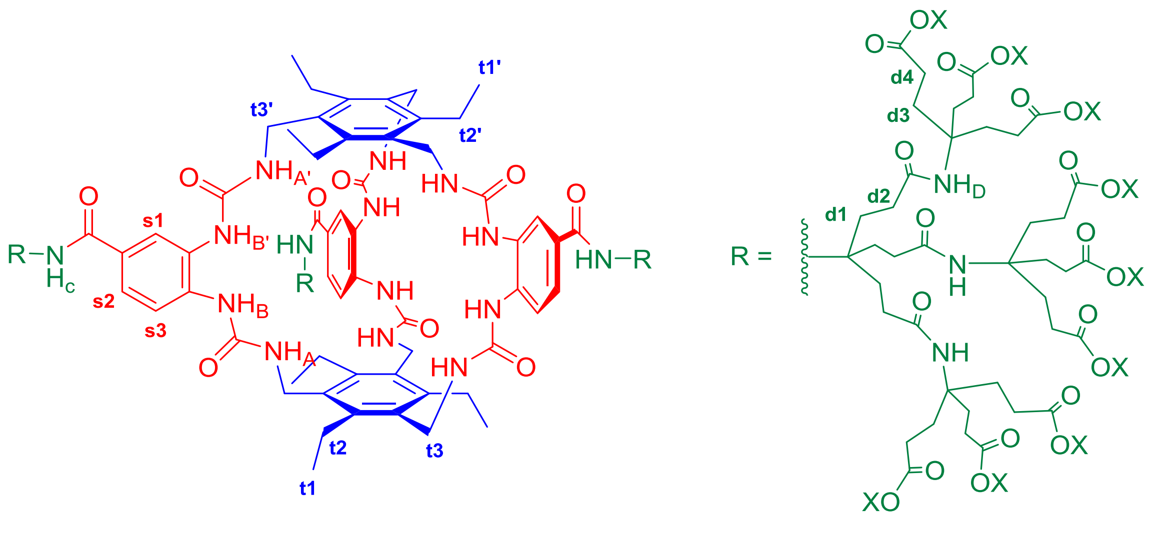

t = "triethylbenzene" **s = "spacer"** **d = "dendrimer", X = *t*-Bu, H, Na**

Supplementary Figure 8| Numbering system used for the discussion of the conformational and binding properties of receptor **2**. Triethylbenzene proton designations (blue) are prefixed with "t" (i.e. t1, t1' etc.), spacer CH protons (red) are prefixed with "s" and protons from the dendritic solubilising groups are prefixed with "d". X can be H, Na, or $C(CH_3)_3$.

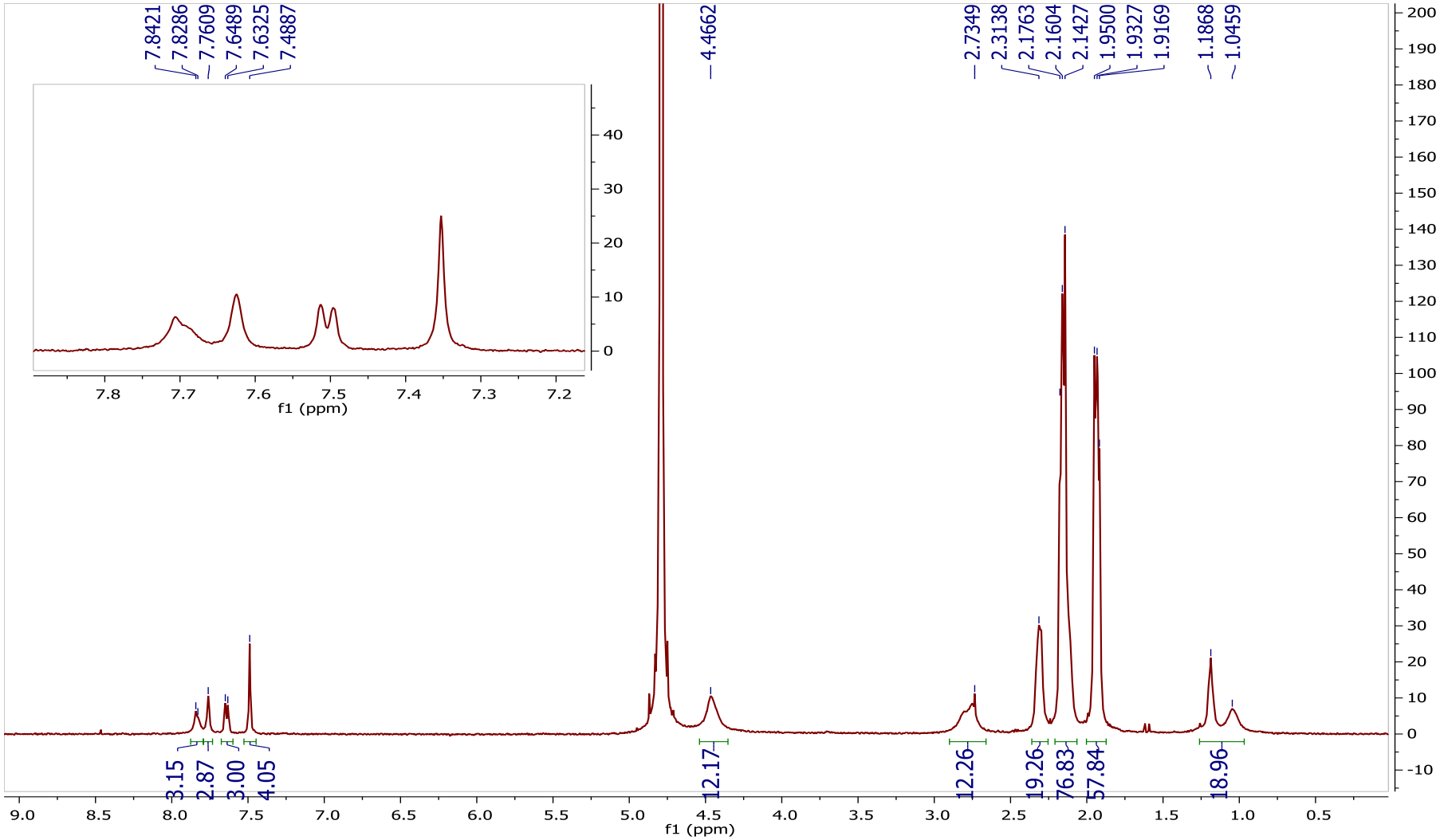

Supplementary Figure 9 | ^{1}H NMR spectrum of receptor **2** (0.5 mM) in D_2O with 10 mM phosphate buffer (pH 7.4) at 298 K.

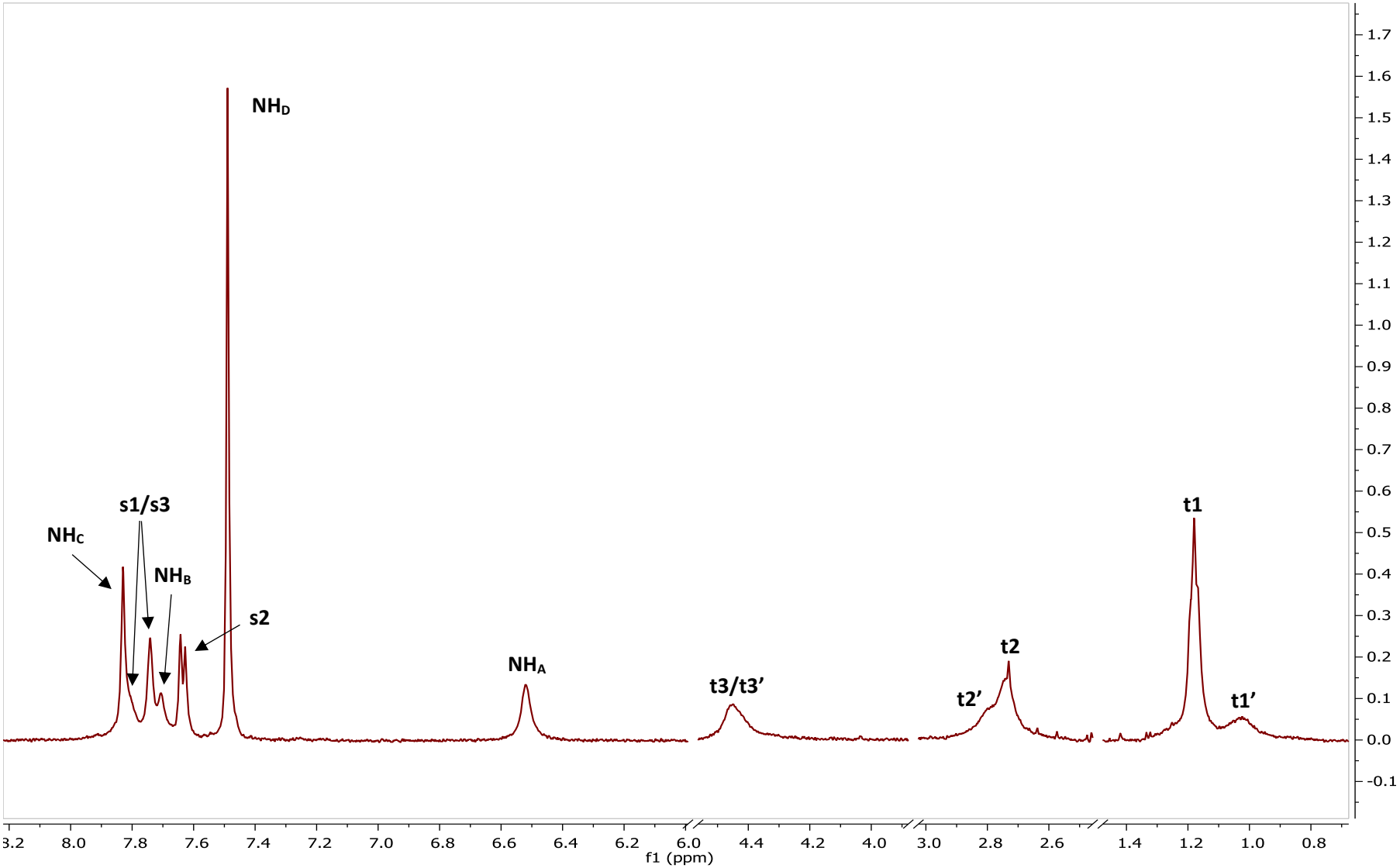

Supplementary Figure 10 | Partial ^{1}H NMR spectra, with assignments, of receptor **2** (0.5 mM) in D_2O/H_2O (1:9) with 10 mM phosphate buffer (pH 7.4) at 298 K.

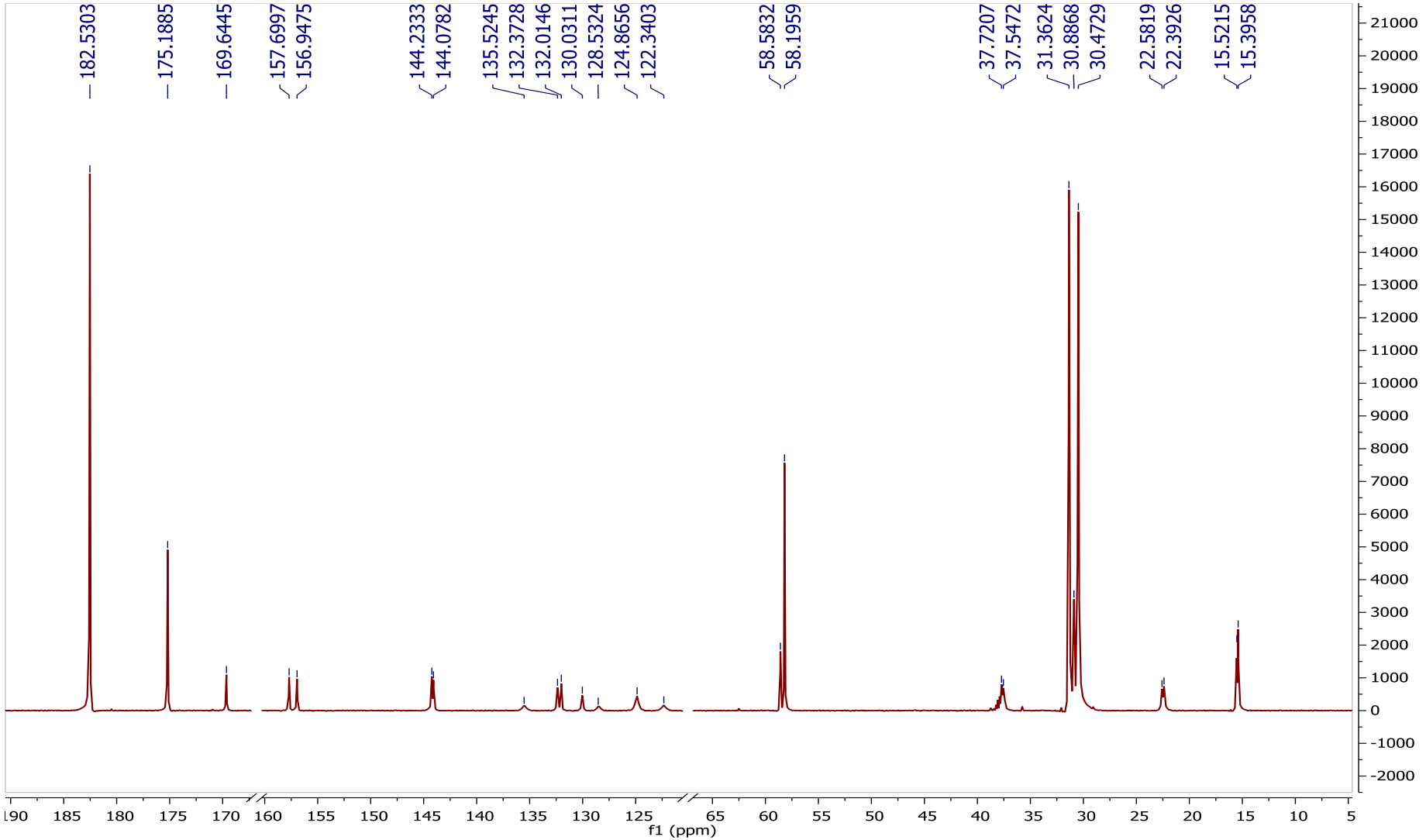

Supplementary Figure 11 | Partial ^{13}C NMR spectra of receptor **2** (10 mM) in D_2O with 10 mM phosphate buffer (pH 7.4) at 298 K.

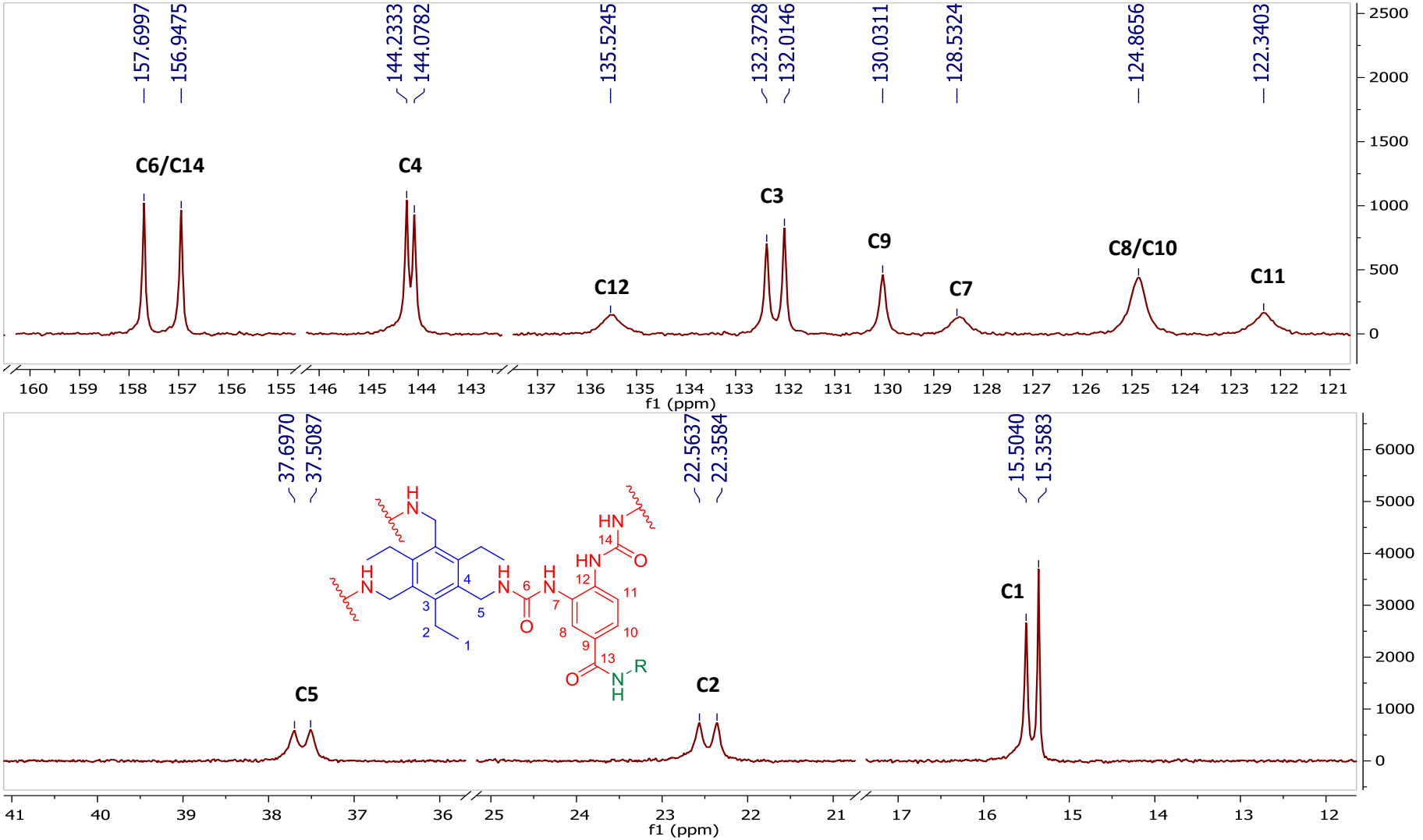

Supplementary Figure 12 | Partial ^{13}C NMR spectra of receptor **2** (10 mM) in D_2O with 10 mM phosphate buffer (pH 7.4) at 298 K. The non-equivalence of the triethylbenzene units is reflected in the pairs of signals observed for C1-C5.

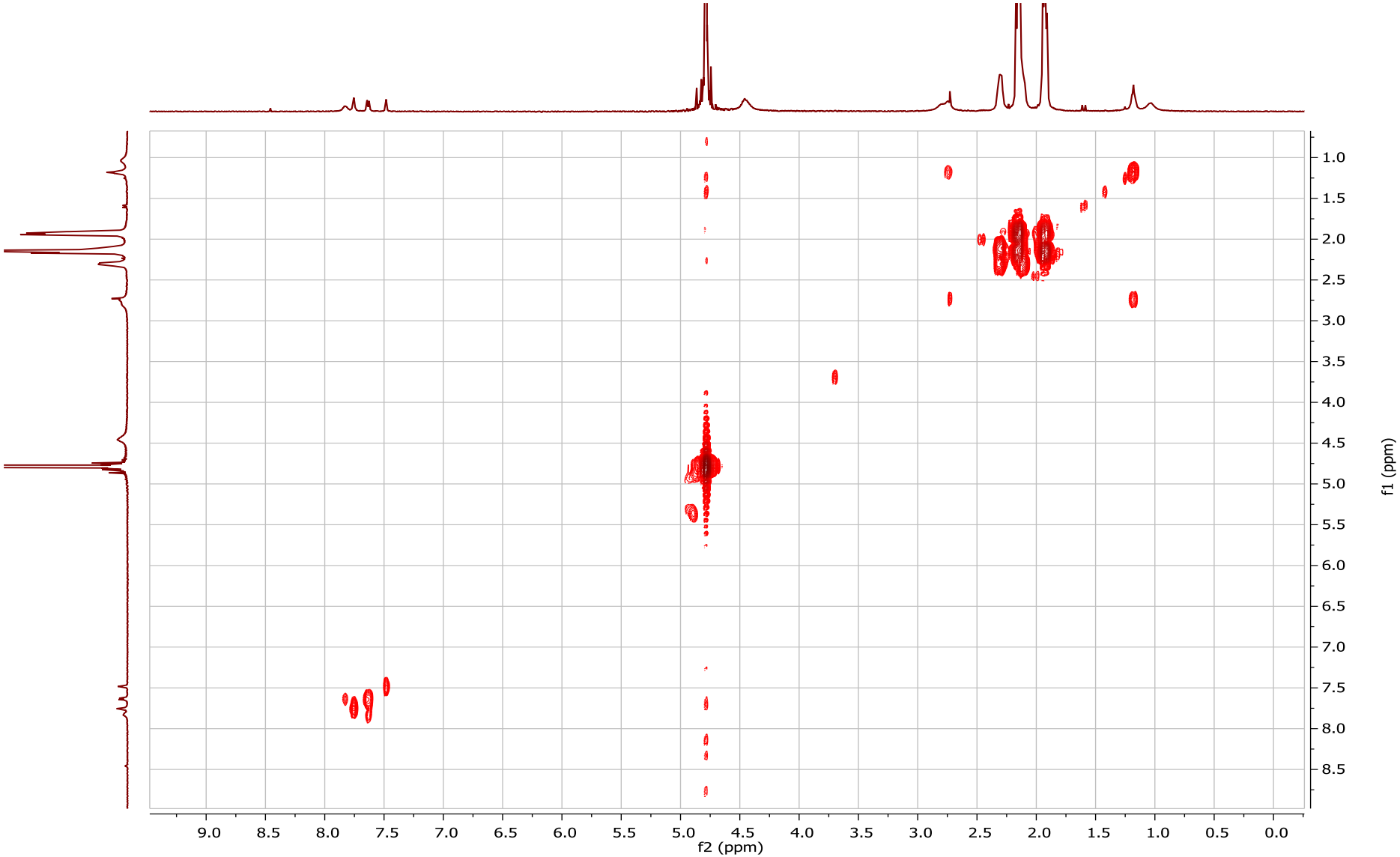

Supplementary Figure 13 | (^{1}H-^{1}H correlation) COSY NMR spectrum of receptor **2** (2mM) in D_2O with 10 mM phosphate buffer (pH 7.4) at 298 K.

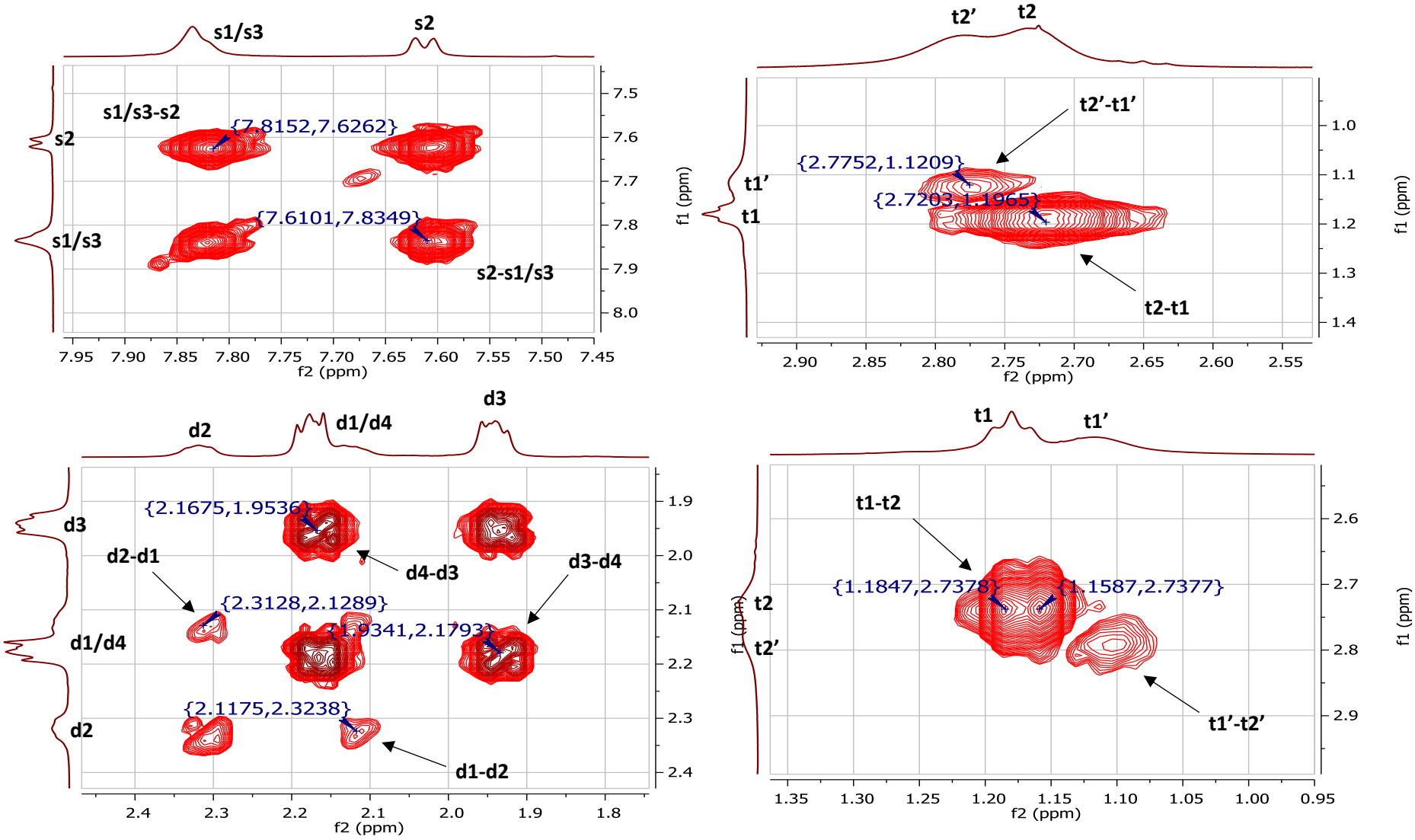

Supplementary Figure 14 | Partial (^{1}H-^{1}H correlation) COSY NMR spectra for receptor **2** (2mM) in D_2O with 10 mM phosphate buffer (pH 7.4) at 298 K.

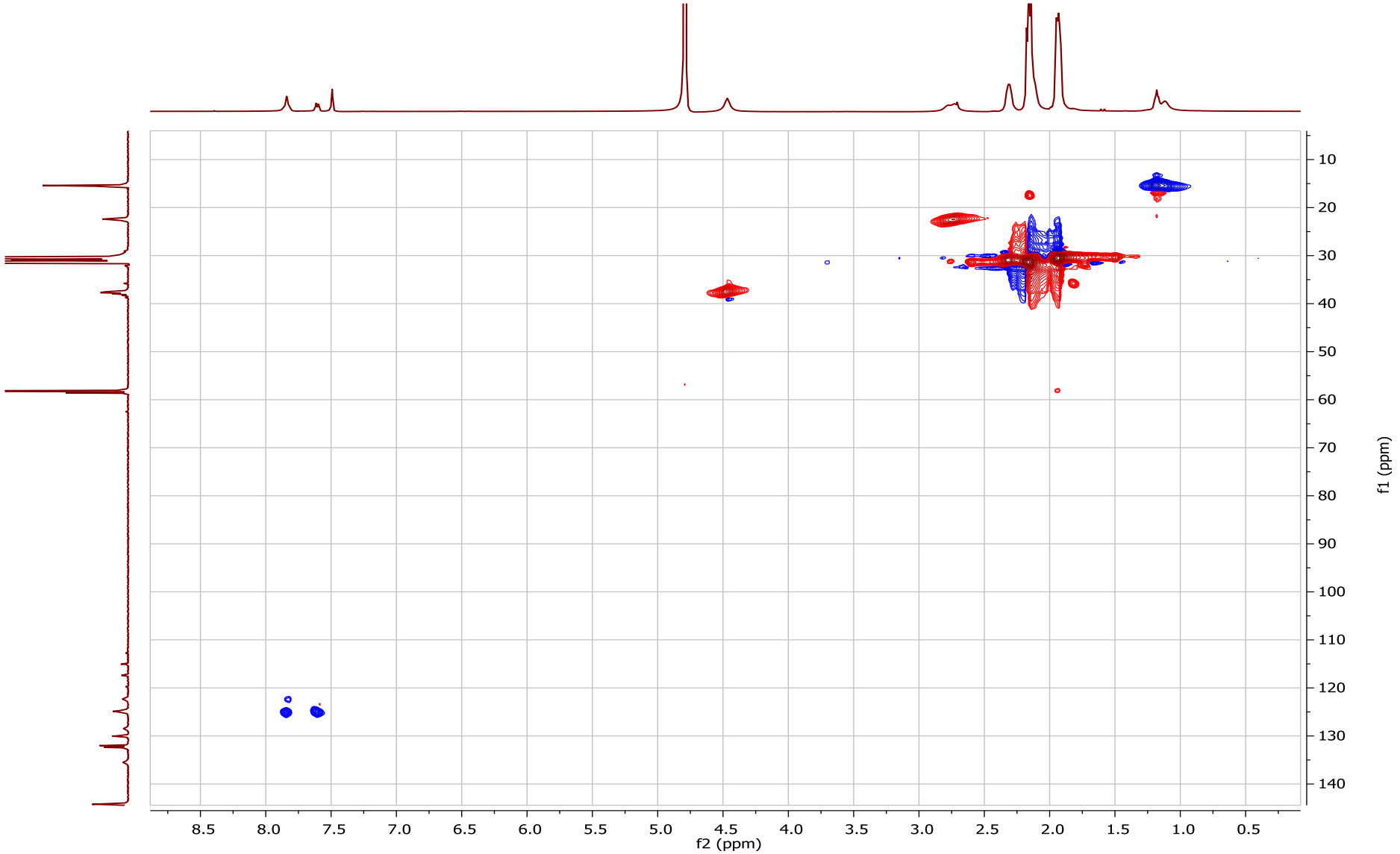

Supplementary Figure 15 | (^{1}H-^{13}C correlation, one bond) HSQC NMR spectrum of receptor **2** (10 mM) in D_2O with 10 mM phosphate buffer (pH 7.4) at 298 K.

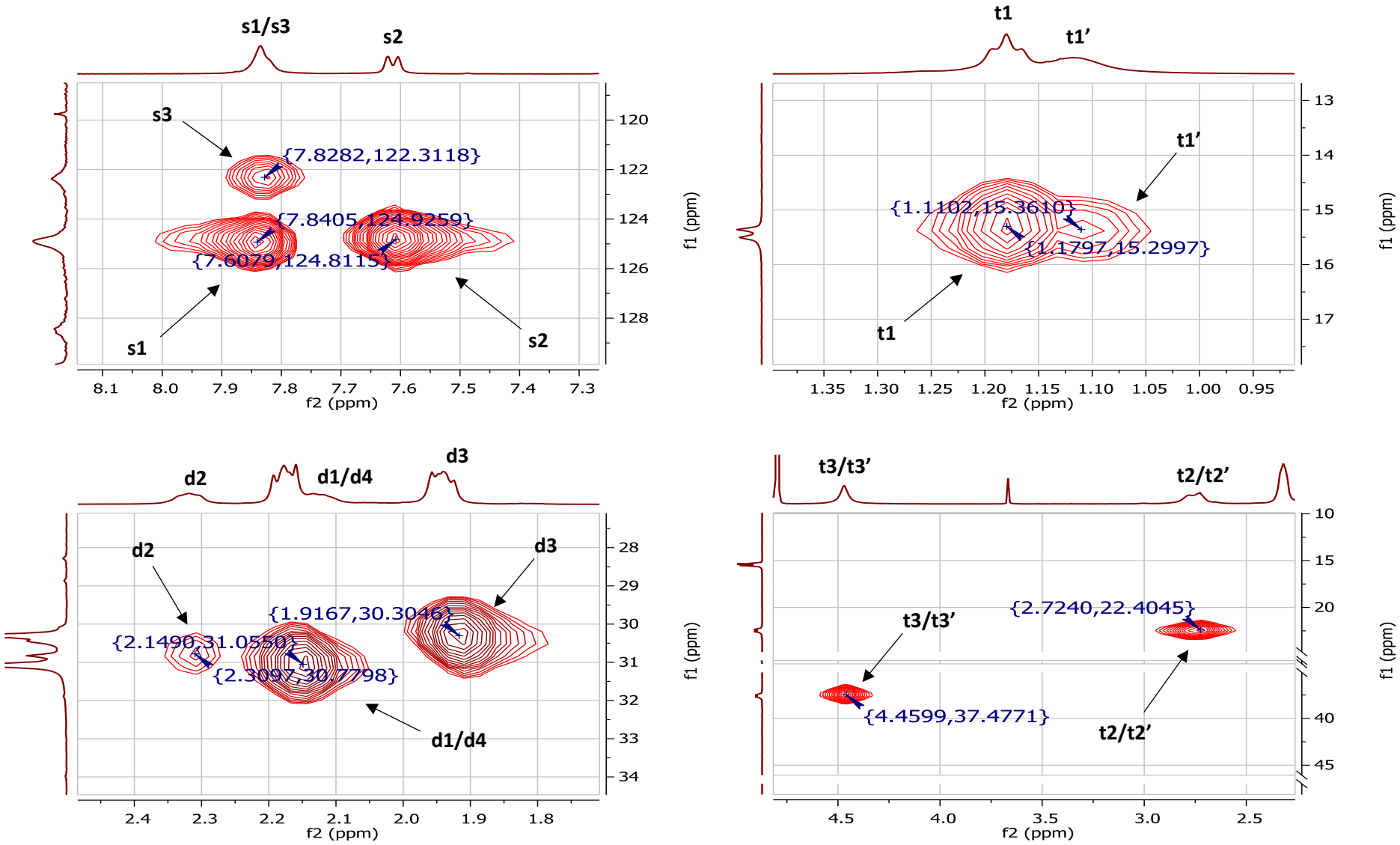

Supplementary Figure 16 | Partial (^{1}H-^{13}C correlation, one bond) HSQC NMR spectra for receptor **2** (10 mM) in D_2O with 10 mM phosphate buffer (pH 7.4) at 298 K

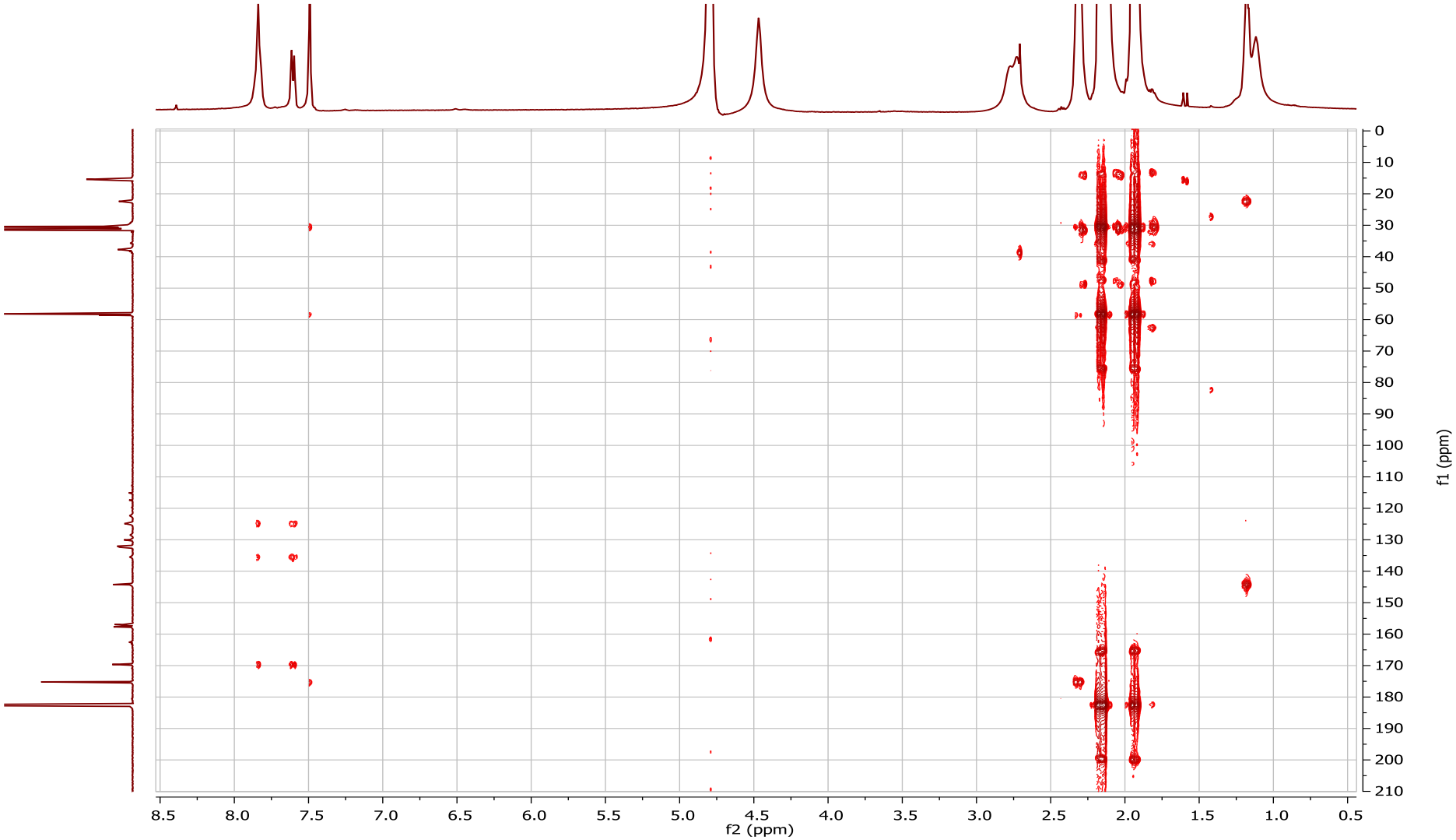

Supplementary Figure 17 | (^{1}H-^{13}C correlation, multiple bond) HMBC NMR spectrum of receptor **2** (10 mM) in D_2O with 10 mM phosphate buffer (pH 7.4) at 298 K.

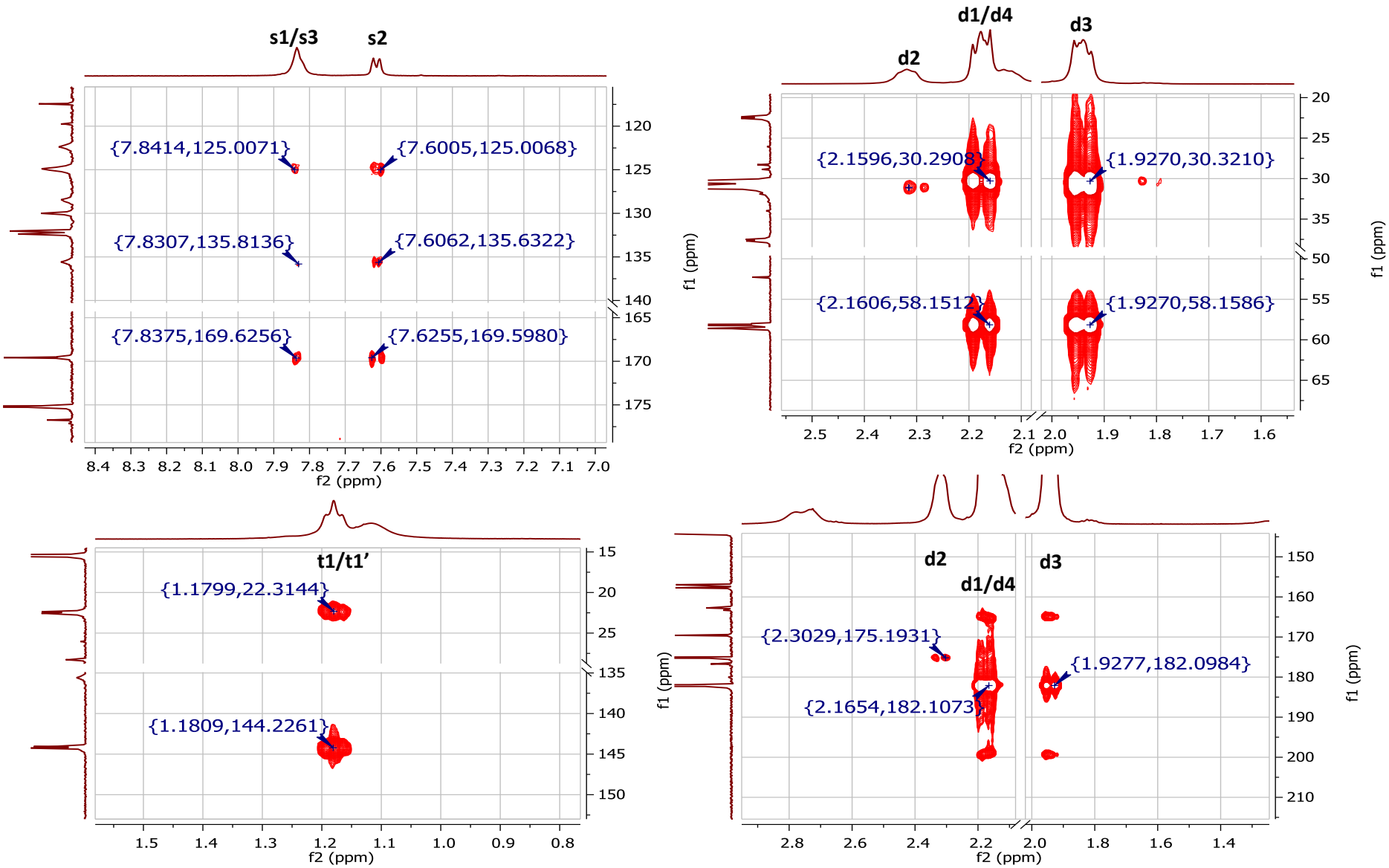

Supplementary Figure 18 | Partial (^{1}H-^{13}C correlation, multiple bond) HMBC NMR spectra for receptor **2** (10 mM) in D_2O with 10 mM phosphate buffer (pH 7.4) at 298 K

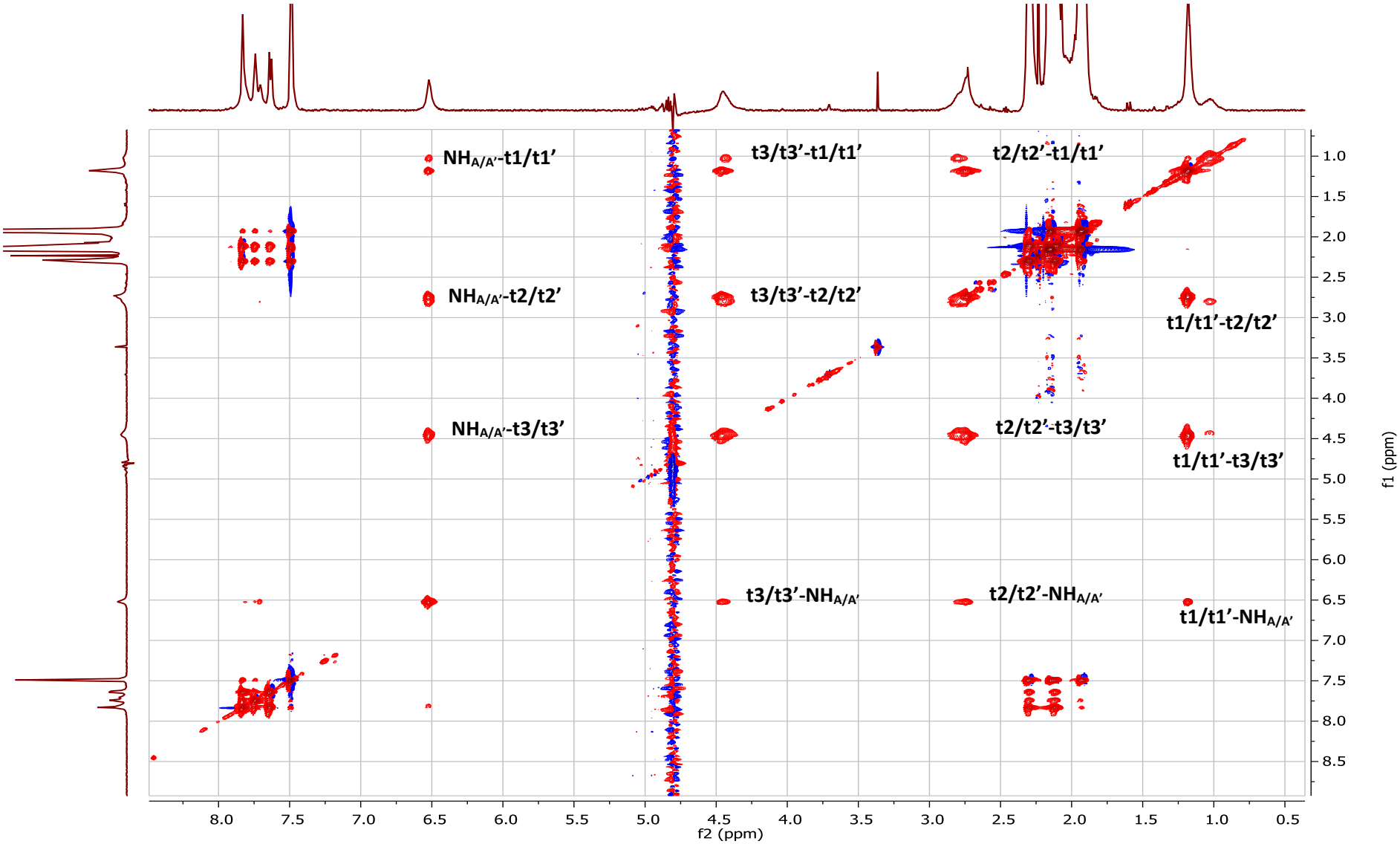

Supplementary Figure 19 | (^{1}H-^{1}H correlation, through space) NOESY NMR spectrum of receptor **2** (1 mM) in 9:1 H_2O/D_2O with 10 mM phosphate buffer (pH 7.4) at 298 K

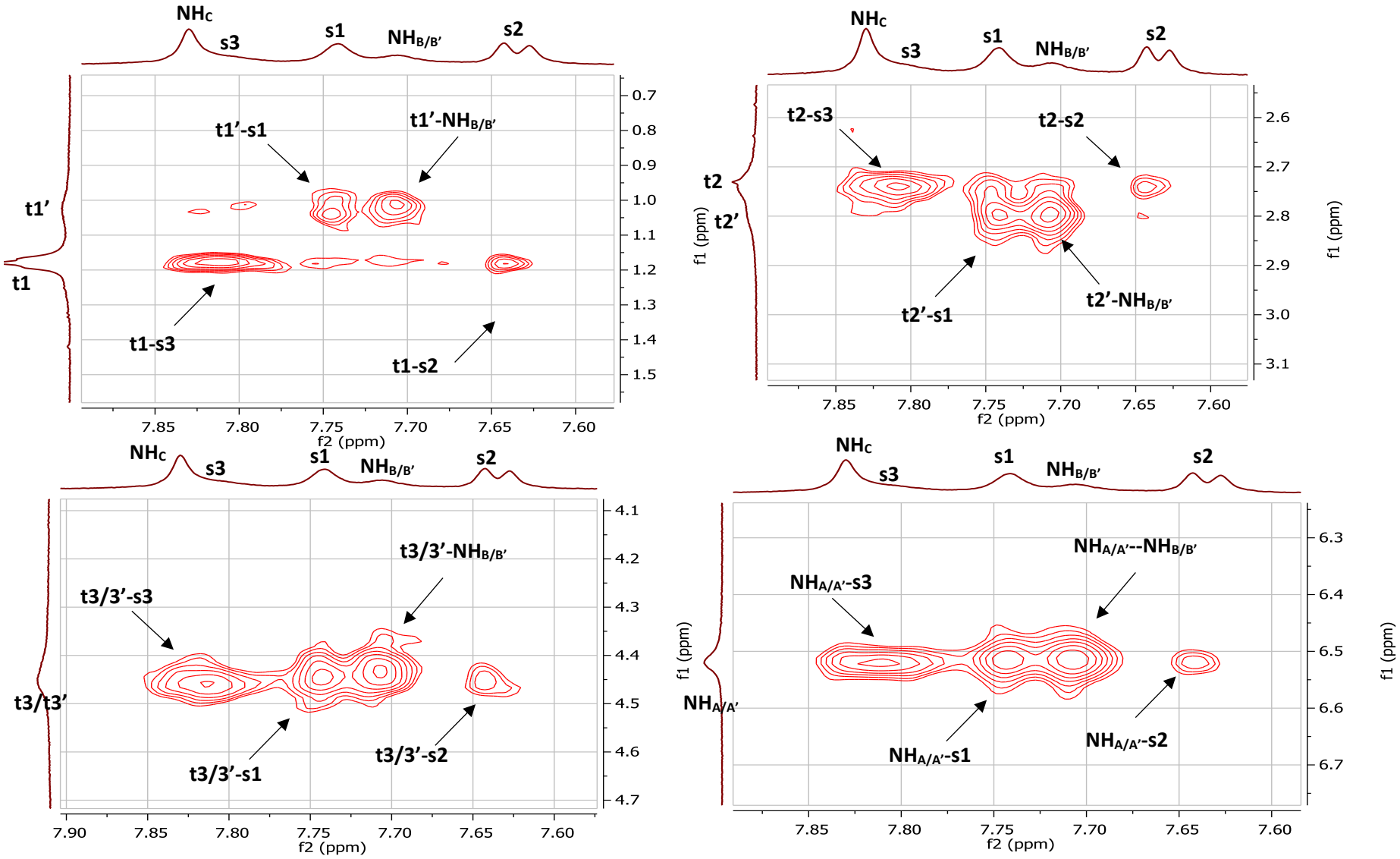

Supplementary Figure 20 | Partial (^{1}H-^{1}H correlation, through space) NOESY NMR spectra for receptor **2** (1 mM) in 9:1 H_2O/D_2O with 10 mM phosphate buffer (pH 7.4) at 298 K.

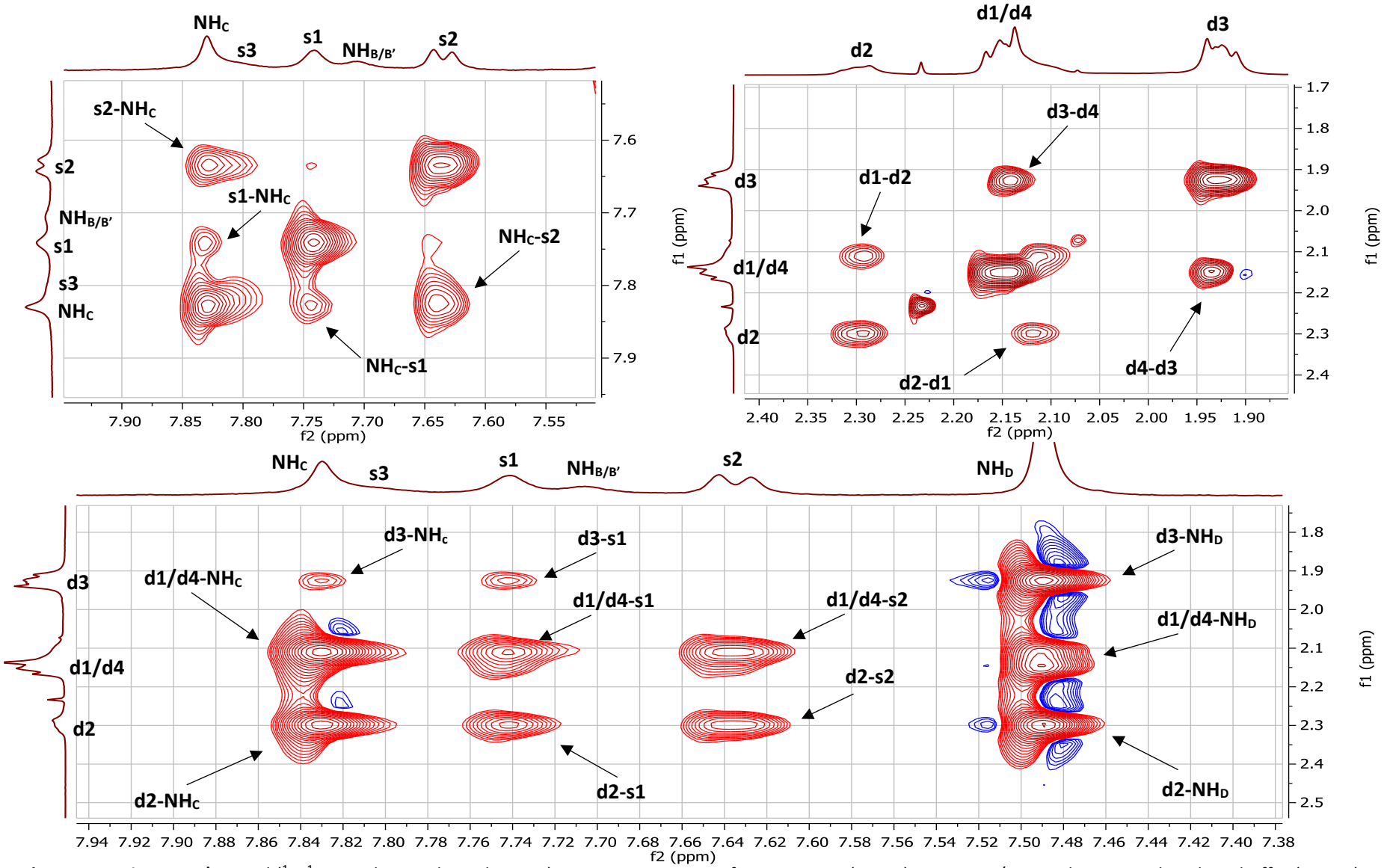

Supplementary Figure 21 | Partial (^{1}H-^{1}H correlation, through space) NOESY NMR spectra for receptor **2** (1 mM) in 9:1 H_2O/D_2O with 10 mM phosphate buffer (pH 7.4) at 298 K. Top left spectrum especially significant – NH_C correlates with s1 and s2, but NH_B does not correlate with s1 or s3. On the other hand, NH_B does correlate with t1', presumably an inward-directed ethyl group (see Supplementary Supplementary Figure **20**).

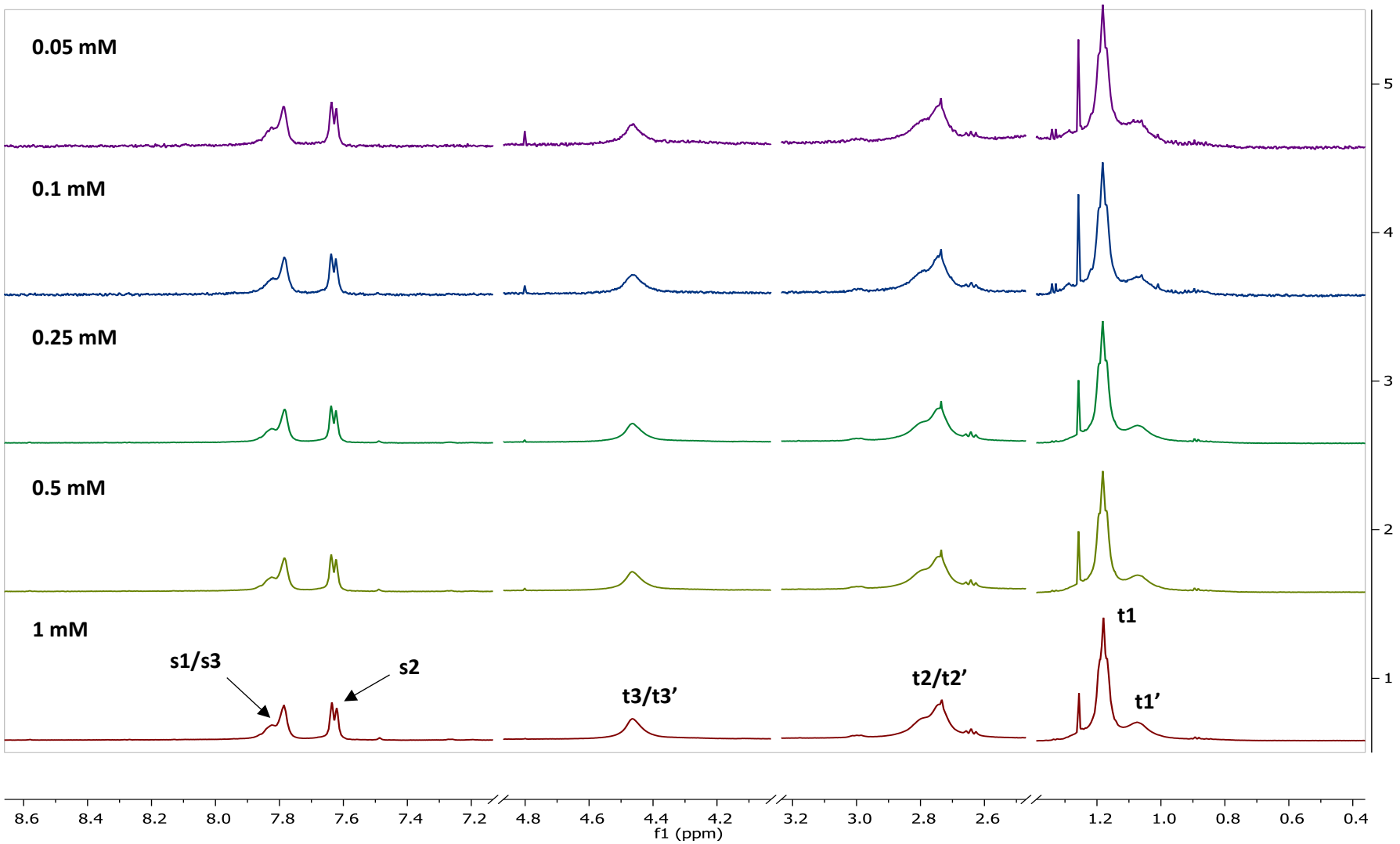

Supplementary Figure 22 | Partial ^{1}H NMR spectra showing receptor **2** at various concentrations in D_2O with 10 mM phosphate buffer (pH 7.4). No change in spectra across concentration range (1 mM – 0.05 mM) suggests receptor **2** is monomeric at these concentrations.

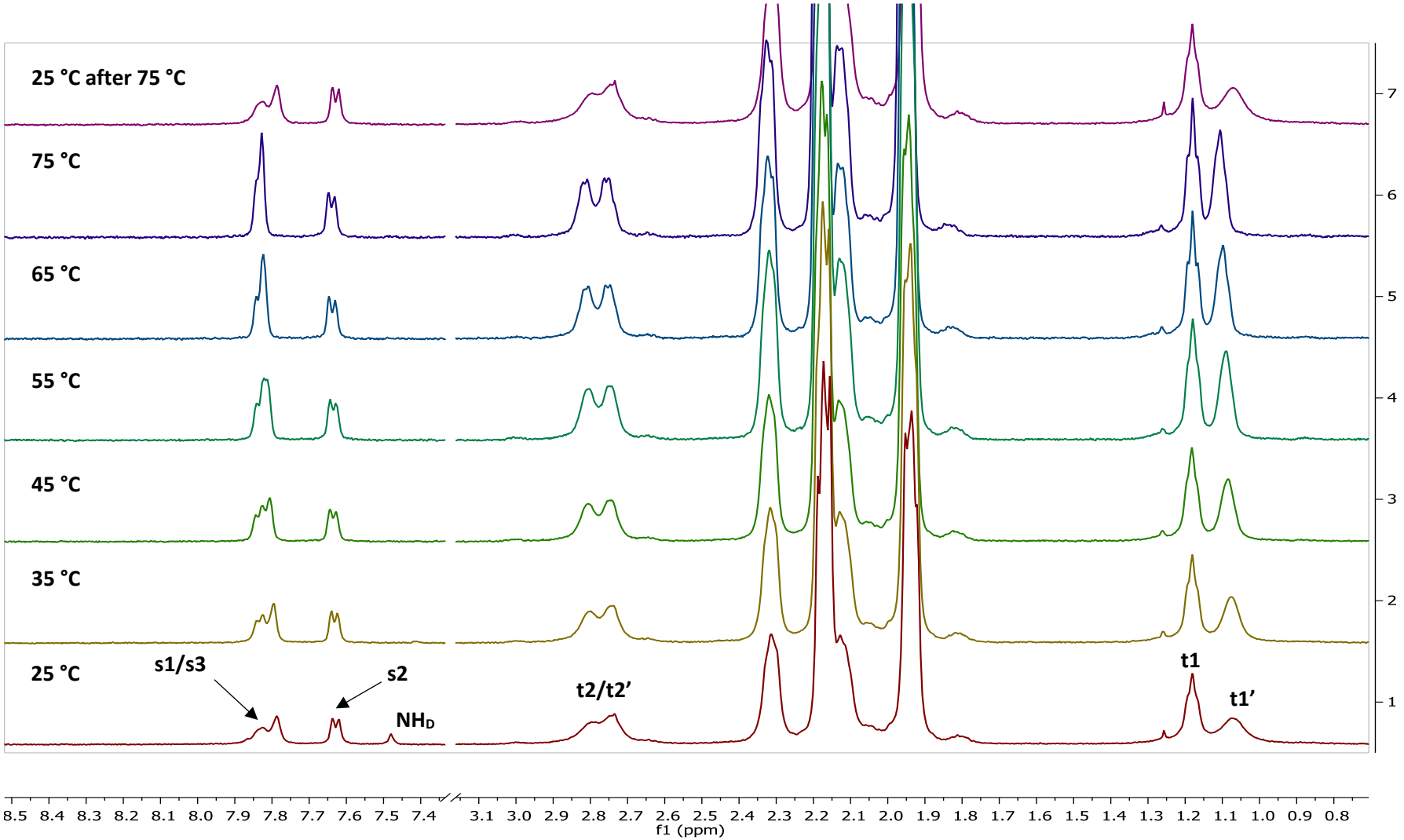

Supplementary Figure 23 | Partial ^{1}H NMR spectra showing receptor **2** at various temperatures in D_2O with 10 mM phosphate buffer (pH 7.4). Chemical shifts (δ, ppm) relative to proton t1 (1.18 ppm). Receptor signals sharpen upon heating, most notably t1/t1' and t2/t2' and s3. Signal for proton t3/t3' is omitted for clarity due to overlap with the residual solvent peak that varied in chemical shift upon heating. NH_D disappears over time due to deuterium exchange.

Stability and toxicity of receptor 2

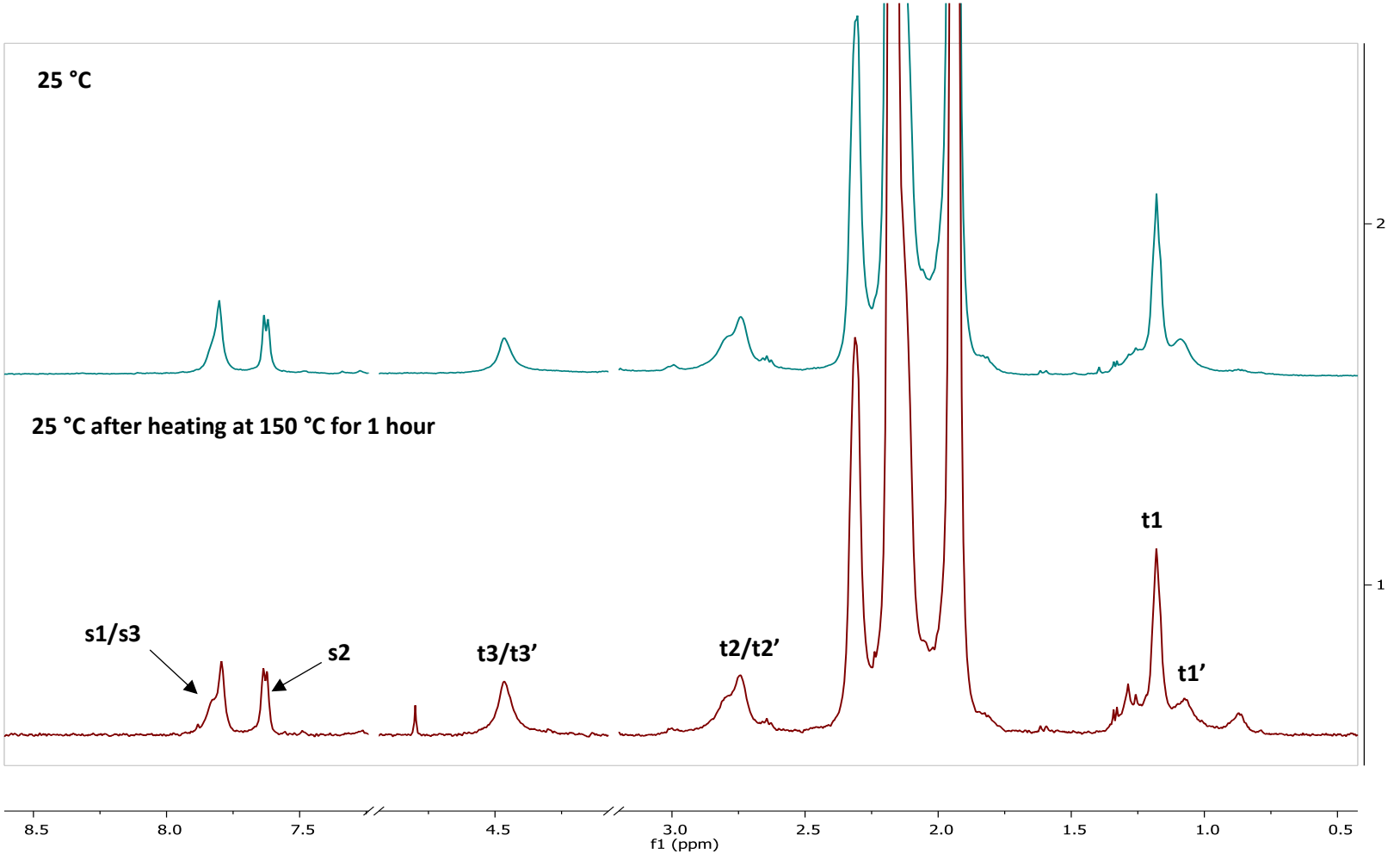

Supplementary Figure 24 | Partial ^{1}H NMR spectra showing receptor **2** (0.1 mM) at 25 °C (top) and receptor **2** (0.1 mM) 25 °C after heating at 150 °C for 1 hour in the solid state (bottom), showing no signs of decomposition. Both spectra recorded in D_2O with 10 mM phosphate buffer (pH 7.4).

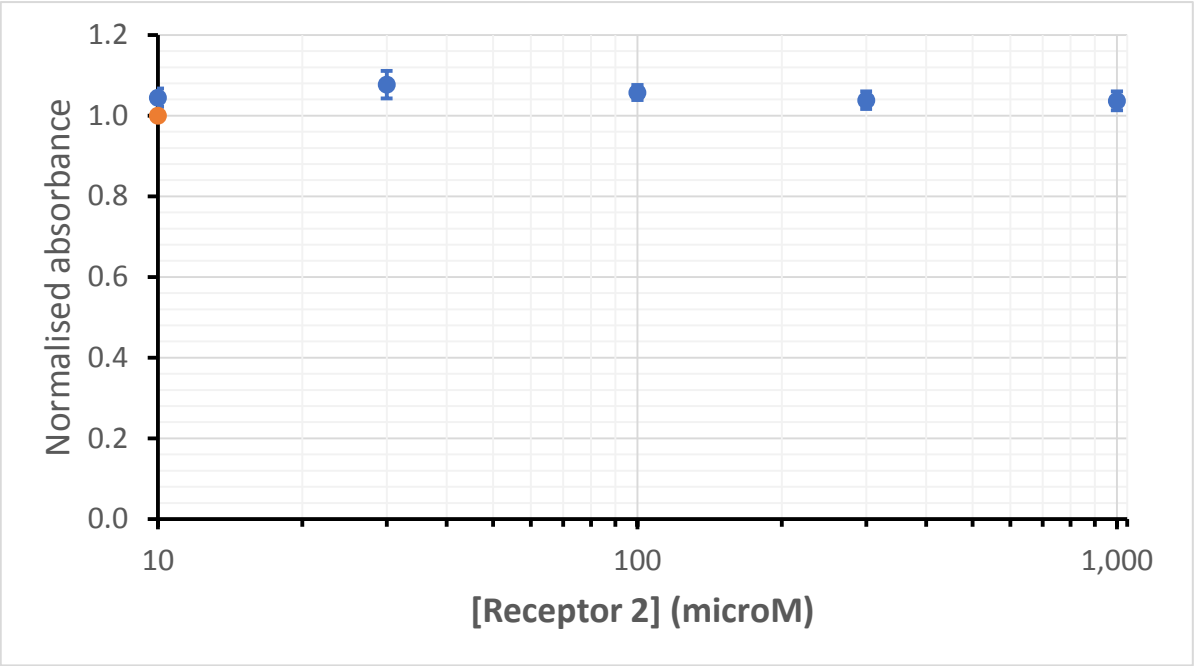

Supplementary Figure 25 | HeLa cells (H1HeLa (ATCC® CRL1958™)) were cultured in RPMI 1640 medium supplemented with 10% fetal calf serum, 100 U ml^{-1} penicillin and 100 microg ml^{-1} streptomycin (all from Life Technologies) at 37 °C in a humidified atmosphere of 5% CO_2. To test the cytotoxicity of receptor **2**, the cells were seeded in 96-well plates at densities of 2 x 10^4 cells/well and cultured for 48 h. Then, the indicated concentrations of receptor **2** (10 -1000 microM) were added to culture media and the cells incubated for 18 h. To assay cell viability, we used the XTT (sodium 2,3,-bis(2-methoxy-4-nitro-5-sulfophenyl)-5-[(phenylamino)-carbonyl]-2H-tetrazolium)) Cell Proliferation Assay Kit (ATCC) according to the manufacturers' instructions. The specific absorbance of test samples was measured using a Microplate Spectrophotometer (SpectraMax 190, Molecular Devices, Sunnyvale CA, USA). Cell viability is presented as specific absorbance values normalised to that of the control (culture media) (means ± SEM; with n individual wells of cells tested from 4 independent experiments. n = 20 (control), 27 (10 microM of receptor **2**), 24 (30 microM of receptor **2**) and 28 (100, 300 and 1000 microM of receptor **2**). There was no significant difference between the control (normal cultural medium, orange) and individual treatments for each of the concentrations of receptor **2** (blue) (with 95% confidence interval; P values vs. culture media: 10 microM of receptor **2**: 0.39; 30 microM of receptor **2**: 0.18; 100 microM of receptor **2**: 0.29; 300 microM of receptor **2**: 0.53; 1000 microM of receptor **2**: 0.52). Statistics were performed using Student's unpaired *t*-test, two-sided, with degrees of freedom of n-1). These data suggest that receptor **2** at concentrations as high as 1000 microM is without toxic effects.

2. Binding Studies

Methods and media

^{1}H NMR titrations. 1H-NMR titrations were performed on a Varian VNMRS 600 MHz spectrometer equipped with a ^{1}H observe cryogenically cooled probe. Solutions of saccharides in D_2O (99.9%) with 10 mM phosphate buffer (pH 7.4), containing receptor at a known concentration to be used in the experiment, were prepared and allowed to equilibrate overnight before use if necessary.[†] Aliquots were then added to an NMR tube containing a known concentration of receptor solution (typically 50 μM – 250 μM). The receptor concentration was therefore held constant while the carbohydrate concentration was increased. The NMR tube was shaken after each addition, manually centrifuged and the ^{1}H-NMR spectra acquired at 298 K.

If the receptor bound the saccharide slower than the NMR sample rate ("slow exchange"), the association constant K_a was determined by analysing the NMR integral of a peak assigned to the Host-Guest (HG) complex. The variable X was defined as the integral of an isolated resonance of the complex (typically in the aromatic region) divided by the integral of all the related resonances (typically the whole aromatic region). As X is proportional to the fraction of host in the bound state, the change in X could be plotted as a function of the guest concentration[‡] to give a curve which could be fitted to a 1:1 binding model to yield K_a. Mathematically, the fitting process is essentially identical to that employed for binding with fast exchange, except that the integral of a peak due to the HG complex replaces the averaged chemical shift of a peak due to bound + unbound receptor. The calculation was performed using a non-linear least squares curve-fitting programme implemented within Excel. The programme yields binding constants K_a and limiting X (X_{lim}) as output. K_a values are partially listed in Figure 4 (main paper) and in full in Supplementary Supplementary Table **5** below. An estimated error (standard deviation) for K_a was obtained from individual data points by assuming the determined K_a

[†] Required for reducing sugars with anomeric-OH.

[‡] In the case of reducing sugars, the total concentration (sum of two anomers) was used for the calculations. We have previously shown that the mixture of anomers should behave like a single substrate, with an apparent K_a value between that of the two anomers, provided the guest is in large excess throughout the titration. See: Ferrand, Y. *et al.* A synthetic lectin for O-linked beta-N-acetylglucosamine. *Angew. Chem., Int. Ed.* **48**, 1775-1779 (2009). The affinities reported here are thus composite values with contributions from both anomers. For the case of glucose, where the above proviso may not apply, see discussion below (P S45).

and X_{lim} and then These errors are reported in Supplementary Supplementary Table **5** and are typically well below 10%.

Receptor **2** bound three substrates in slow exchange: D-glucose, methyl β-D-glucoside, and D-cellobiose. Several substrates were also bound in fast exchange and values for K_a were determined using standard fitting procedures. In cases where the receptor bound the saccharide at similar or slightly faster rates than the NMR sample rate ("intermediate exchange", e.g. D-glucuronic acid), the binding constants could not be estimated due to broadening of receptor spectra. Spectra from the NMR titrations, and analysis curves where relevant, are included among Supplementary Supplementary Figure **26** – Supplementary Supplementary Figure **62** below. Commentary on individual cases is given in the figure captions.

Isothermal Titration Microcalorimetry (ITC) titrations. Isothermal Titration MicroCalorimetry (ITC) experiments were performed on a MicroCal iTC200 or MicroCal VP-ITC microcalorimeter. ITC experiments were carried out at 298 K. Saccharide solutions were prepared in HPLC-grade water with 10 mM phosphate buffer solution (pH 7.4) and allowed to equilibrate overnight if necessary. The sample cell was charged with a known concentration of receptor solution in HPLC-grade water with 10 mM phosphate buffer solution at pH 7.4 (typically 50 μM – 200 μM). Then, aliquots (typically 1.0 μL for the MicroCal iTC200, or 7.5 μL for the MicroCal VP-ITC) of carbohydrate solution were added and the evolution of heat was followed as a function of time. Heats of dilution were measured by injecting the same carbohydrate solution into HPLC-grade water with 10 mM phosphate buffer solution at pH 7.4, using identical conditions. For every addition, the heat of dilution was subtracted from the heat of binding using MicroCal software (MicroCal iTC_{200} Analysis Add-On Software Package (v7.20) for ORIGIN 7.0). This gave an XY matrix of heat vs. total guest concentration.[‡] This matrix was then imported into a specially written Excel programme to fit the data to a 1:1 binding model to give a K_a. ΔG can be derived from K_a and thus ΔS can be derived from ΔH and ΔG using common thermodynamic equations. The fitting procedure also yields errors in K_a as in the case of NMR described above. This method consistently produced more accurate fits than fitting the data to an S-curve, as in the MicroCal software (S-curves are typically not observed for binding constants below ~10^4 - 10^5 M^{-1}). Although fits produced using the supplied MicroCal software were generally similar to those calculated using the Excel programme, they also consistently overestimated the K_a by approximately 10% when compared to the equivalent NMR data. It was found that better corroboration of the ITC data with the equivalent NMR data was achieved using the Excel programme.

ITC outputs for heat of dilution of substrates and the corresponding binding experiments, as well as analysis curves, are included among Supplementary Supplementary Figure **28** – Supplementary Supplementary Figure **75**. An overview of the binding data, including thermodynamic quantities and errors is given in Supplementary Supplementary Table **5** below. It is relevant to estimate the minimum K_a which could have been measured by this technique. While this cannot be determined with certainty as binding events do not always generate a thermal signature, it is notable that for fructose (K_a = 60 M^{-1}, Supplementary Supplementary Figure **58**) and cellobiose (K_a = 30 M^{-1}, Supplementary Supplementary Figure **60**) differences between binding titrations and blank runs are clearly observable. In contrast, for the substrates grouped on the right hand side of Fig. 4 ("binding minimal/undetectable"), the blanks and binding titrations are almost identical. It therefore seems likely that quite weak binding (probably ≥30 M^{-1}, perhaps as low as 10 M^{-1}) could have been detected. On this basis, the selectivity of **2** for glucose over the "non-binding" molecules is probably ≥1000:1.

Preparation of biological media. Cell culture media were obtained from ThermoFisher Scientific and human serum from Sigma-Aldrich, and were aliquoted into 10 mL batches in a specially designed sterile fume hood. The cell culture media and human serum were passed through a membrane (10k MWCO) and then buffered with 10 mM phosphate buffer (pH 7.4). These batches were then used immediately for ITC binding studies to avoid contamination. The two varieties of cell culture media used were: Dulbecco's Modified Eagle Medium (DMEM, no glucose, cat. no. 11966025) and Leibovitz's L-15 Medium (no glucose, cat. no. 11415049). The Human Serum used originates from male AB clotted whole blood (cat. no. H6914). Formulations for both cell culture media, phosphate buffered saline (PBS) and the DMEM salt control media are listed below in Supplementary

Supplementary **Table 1** - Supplementary Supplementary Table **4**.

Removal of D-glucose from human serum. The concentration of initial D-glucose present in the human serum was measured to be 6.2 mM using a YSI 2300 STAT Plus Glucose and L-Lactate analyser. The D-glucose was oxidised to the D-glucono-δ-lactone (which then hydrolysed to gluconic acid in solution at pH 7.4) using a combination of enzymes: glucose oxidase and catalase. After oxidation, the concentration of D-glucose in the human serum was measured to be 0-0.005 mM (using the YSI 2300 STAT Plus). The procedure for the oxidation of D-glucose in the serum is as follows: A solution of enzymes (20 mL) consisting of glucose oxidase (10,000 U) and catalase (300,000 U) was prepared and then dialysed (500 MWCO) to remove low MW contaminants (notably glycerol). 0.2 mL of this enzyme

solution was added to human serum (10 mL) at 25-30 °C. The mixture was stirred at 25-30 °C while air was bubbled through the suspension for 2 hours. The mixture was then cooled to room temperature and passed through a membrane (10k MWCO) to give a colourless solution, which was used immediately for the corresponding binding studies.

Supplementary Table 1 | Formulation for phosphate buffered saline (PBS).

Component	**Concentration (mM)**
Sodium Chloride (NaCl)	140
Potassium Chloride (KCl)	2.7
Disodium phosphate (Na_2HPO_4)	10
Monopotassium phosphate (KH_2PO_4)	1.8

Supplementary Table 2 | Formulation for DMEM salt control

Component	**Concentration (mM)**
Calcium Chloride ($CaCl_2$) (anhyd.)	1.8
Ferric Nitrate ($Fe(NO_3)_3.9H_2O$)	2.50×10^{-4}
Magnesium Sulfate ($MgSO_4$) (anhyd.)	0.81
Potassium Chloride (KCl)	5.3
Sodium Bicarbonate ($NaHCO_3$)	44
Sodium Chloride (NaCl)	110
Sodium Phosphate monobasic (NaH_2PO_4-H_2O)	0.9

Supplementary Table 3 | Formulation for DMEM cell culture medium used, as described by the manufacturer.

Component	Concentration (mM)
Glycine	0.4
L-Arginine hydrochloride	0.4
L-Cystine 2HCl	0.2
L-Glutamine	4.0
L-Histidine hydrochloride-H_2O	0.2
L-Isoleucine	0.8
L-Leucine	0.8
L-Lysine hydrochloride	0.8
L-Methionine	0.2
L-Phenylalanine	0.4
L-Serine	0.4
L-Threonine	0.8
L-Tryptophan	0.078
L-Tyrosine disodium salt dihydrate	0.4
L-Valine	0.8
Choline chloride	0.029
D-Calcium pantothenate	0.0084
Folic Acid	0.0091
Niacinamide	0.033
Pyridoxine hydrochloride	0.019
Riboflavin	0.0011
Thiamine hydrochloride	0.012
i-Inositol	0.04
Calcium Chloride ($CaCl_2$) (anhyd.)	1.8
Ferric Nitrate ($Fe(NO_3)_3.9H_2O$)	2.50×10^{-4}
Magnesium Sulfate ($MgSO_4$) (anhyd.)	0.81
Potassium Chloride (KCl)	5.3
Sodium Bicarbonate ($NaHCO_3$)	44
Sodium Chloride (NaCl)	110
Sodium Phosphate monobasic (NaH_2PO_4-H_2O)	0.91
Phenol Red	0.040

Supplementary Table 4 | Formulation for Leibovitz's L-15 cell culture medium used, as described by the manufacturer.

Component	**Concentration (mM)**
Glycine	2.7
L-Alanine	2.5
L-Arginine	2.9
L-Asparagine	1.9
L-Cysteine	1.0
L-Glutamine	2.1
L-Histidine	1.6
L-Isoleucine	1.9
L-Leucine	0.95
L-Lysine	0.51
L-Methionine	0.50
L-Phenylalanine	0.76
L-Serine	1.9
L-Threonine	2.5
L-Tryptophan	0.098
L-Tyrosine	1.6
L-Valine	0.85
Choline chloride	0.0071
D-Calcium pantothenate	0.0021
Folic Acid	0.0023
Niacinamide	0.0082
Pyridoxine hydrochloride	0.0049
Riboflavin 5'-phosphate Na	2.0×10^{-4}
Thiamine monophosphate	0.0022
i-Inositol	0.011
Calcium Chloride ($CaCl_2$) (anhyd.)	1.3
Magnesium Chloride (anhydrous)	0.99
Magnesium Sulfate ($MgSO_4$) (anhyd.)	0.81
Potassium Chloride (KCl)	5.3
Potassium Phosphate monobasic (KH_2PO_4)	0.44
Sodium Chloride (NaCl)	140
Sodium Phosphate dibasic (Na_2HPO_4) anhydrous	1.3
D-Galactose	5.0
Phenol Red	0.027
Sodium Pyruvate	5.0

Summary of binding results (K_a)

Supplementary Table 5 | Summary of binding results for receptor **2** with various substrates at 298 K.

Substrate (medium)	Determined by NMR K_a (M^{-1})	Determined by ITC (kJ mol^{-1})			
		K_a (M^{-1})	ΔG	ΔH	TΔS
D-Glucose	18,600 ± 2.6%	18,200 ± 2.1%[a]	-24.3[a]	-23.0[a]	1.3[a]
D-Glucose pH 6 (PBS)	-	17,800 ± 3.8%	-24.3	-10.6	13.7
D-Glucose pH 7 (PBS)	-	17,300 ± 5.5%	-24.2	-10.9	13.3
D-Glucose pH 8 (PBS)	-	18,300 ± 1.8%	-24.3	-10.9	13.4
D-Glucose (human serum)	-	11,300 ± 2.4%	-23.1	-18.3	4.9
D-Glucose (DMEM cell culture)	-	5640 ± 2.1%	-21.4	-21.1	0.3
D-Glucose (DMEM salt control)	-	5160 ± 5.9%	-21.2	-21.0	0.2
D-Glucose (Leibovitz's L-15)	-	5210 ± 8.6%	-21.2	-17.4	3.8
Methyl β-D-Glucoside	7520 ± 5.5%	7890 ± 16%	-22.2	-13.4	11.1
D-Glucuronic Acid	n.d.[b]	5340 ± 3.5%	-21.3	-34.7	-13.4
D-Xylose	n.d.[b]	5800 ± 3.0%	-21.5	-20.0	1.5
2-Deoxy-D-Glucose	n.d.[b]	725 ± 5.7%	-16.3	-12.1	4.3
D-Galactose	132 ± 10%	182 ± 2.3%	-12.9	-12.5	0.4
D-Mannose	140 ± 1.3%	143 ± 1.1%	-12.3	-14.7	-2.4
D-Ribose	267 ± 3.8%	216 ± 1.9%	-13.3	-28.8	-15.5
D-Fructose	51 ± 5.5%	60 ± 2.7%	-10.6	-33.6	-23.4
D-Cellobiose	31 ± 9.0%	30 ± 16%	-8.5	-38.5	-30.0
Mannitol		0			
D-Gluconate[c]	0[d]	0			
Methyl α-D-Glucoside	0[d]	0			
N-Acetyl-D-glucosamine		0			
D-Maltose		0			
L-Fucose		0			
Ascorbic Acid		0			
Uracil (PBS)		0			
Uric Acid (PBS)		0			
Cytosine		0			
Adenosine		0			
L-Phenylalanine		0			
L-Tryptophan		0			
Paracetamol		0			

All solutions at pH 7.4 in 10 mM phosphate buffer solution unless otherwise stated. Errors reported as standard deviations of calculated K_a values. [a] Average of 9 independent measurements, see Supplementary Table 6 and discussion. [b] Not determined due to broadened signals. [c] Prepared by dissolution of D-glucono-δ-lactone in 10 mM phosphate buffer, pH 7.4. After 4 h ^{1}H NMR indicated that the lactone had hydrolysed to give the gluconate. [d] NMR binding study attempted. Signal broadening could be observed at high substrate concentrations, but binding could not be quantified.

Binding data and analyses

Glucose 10

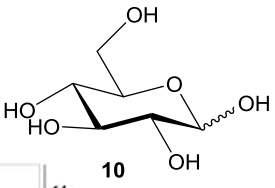

10

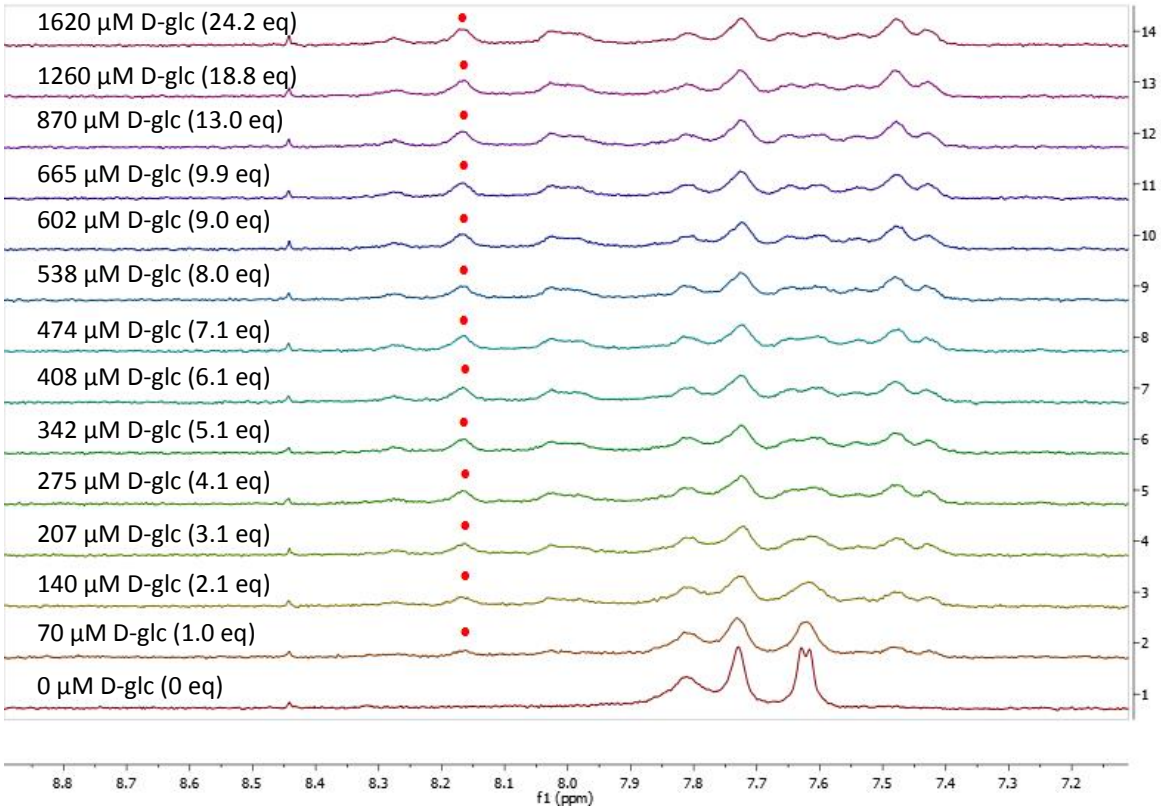

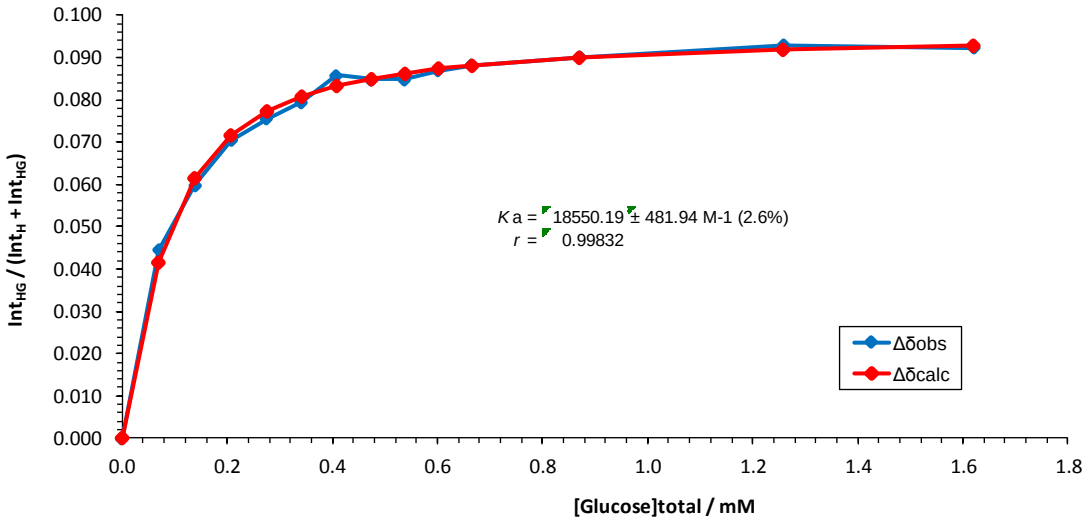

Supplementary Figure 26 | Partial ^{1}H NMR spectra (top) and binding analysis curve (bottom) for receptor **2** (67 µM) titrated with a combined solution of D-glucose **10** (11.8 mM) and receptor **2** (67 µM), in D_2O with 10 mM phosphate buffer (pH 7.4) at 298 K. Spectra imply binding with slow exchange on NMR timescale. Integrations of the peak at 8.19 ppm (denoted with •) versus the region 8.35-7.39 ppm were plotted against D-glucose concentration (mM). The calculated values for the integrals are overlaid with the observed values, giving K_a = 18,550 ± 482 M^{-1} (2.6%). Limiting Integration = 10.8, X_{lim} = 0.093. The experiment was performed 6 times with similar results.

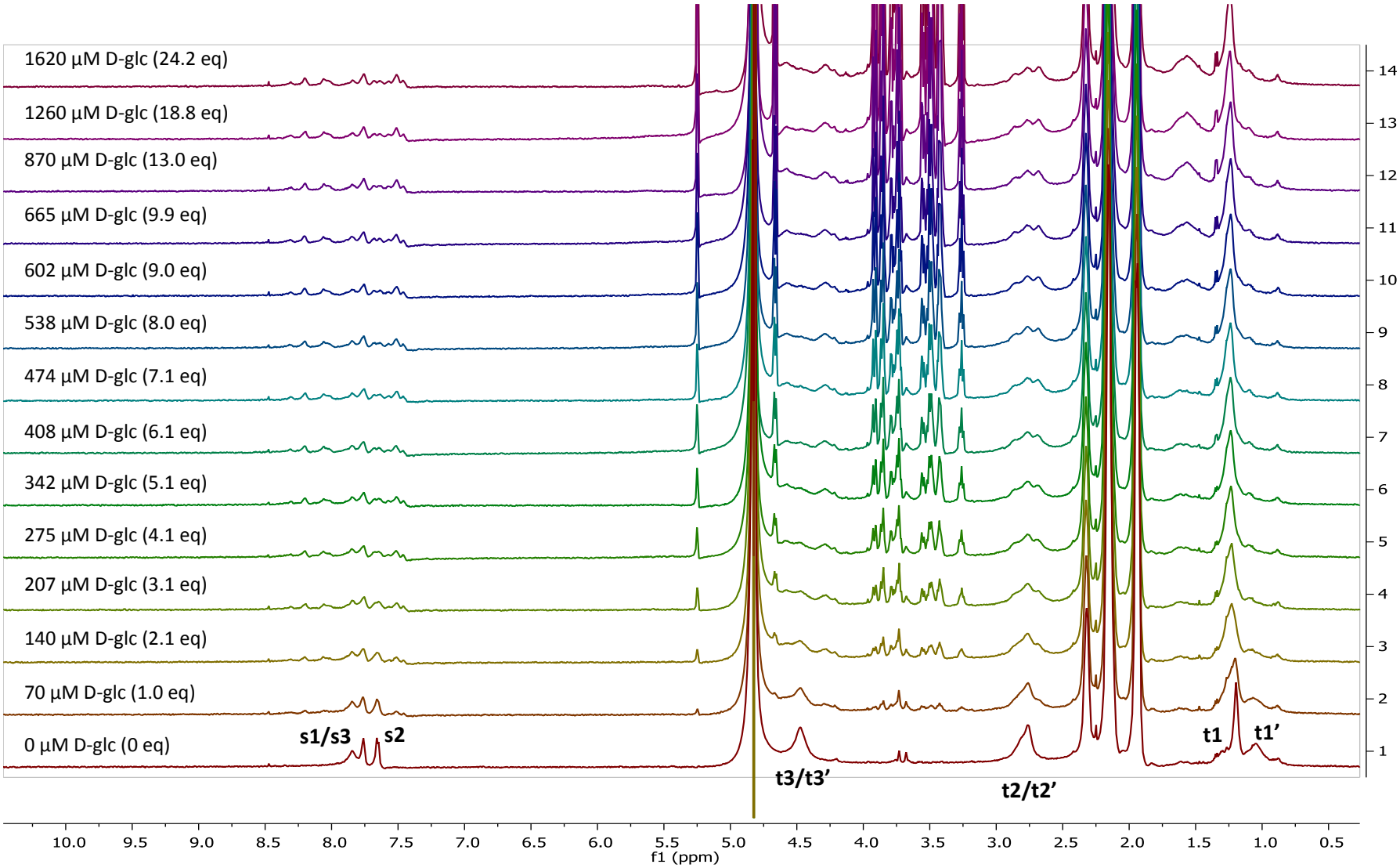

Supplementary Figure 27 | ^{1}H NMR spectra for receptor **2** (67 µM) titrated with a combined solution of D-glucose **10** (11.8 mM) and receptor **2** (67 µM), in D_2O with 10 mM phosphate buffer (pH 7.4) at 298 K.

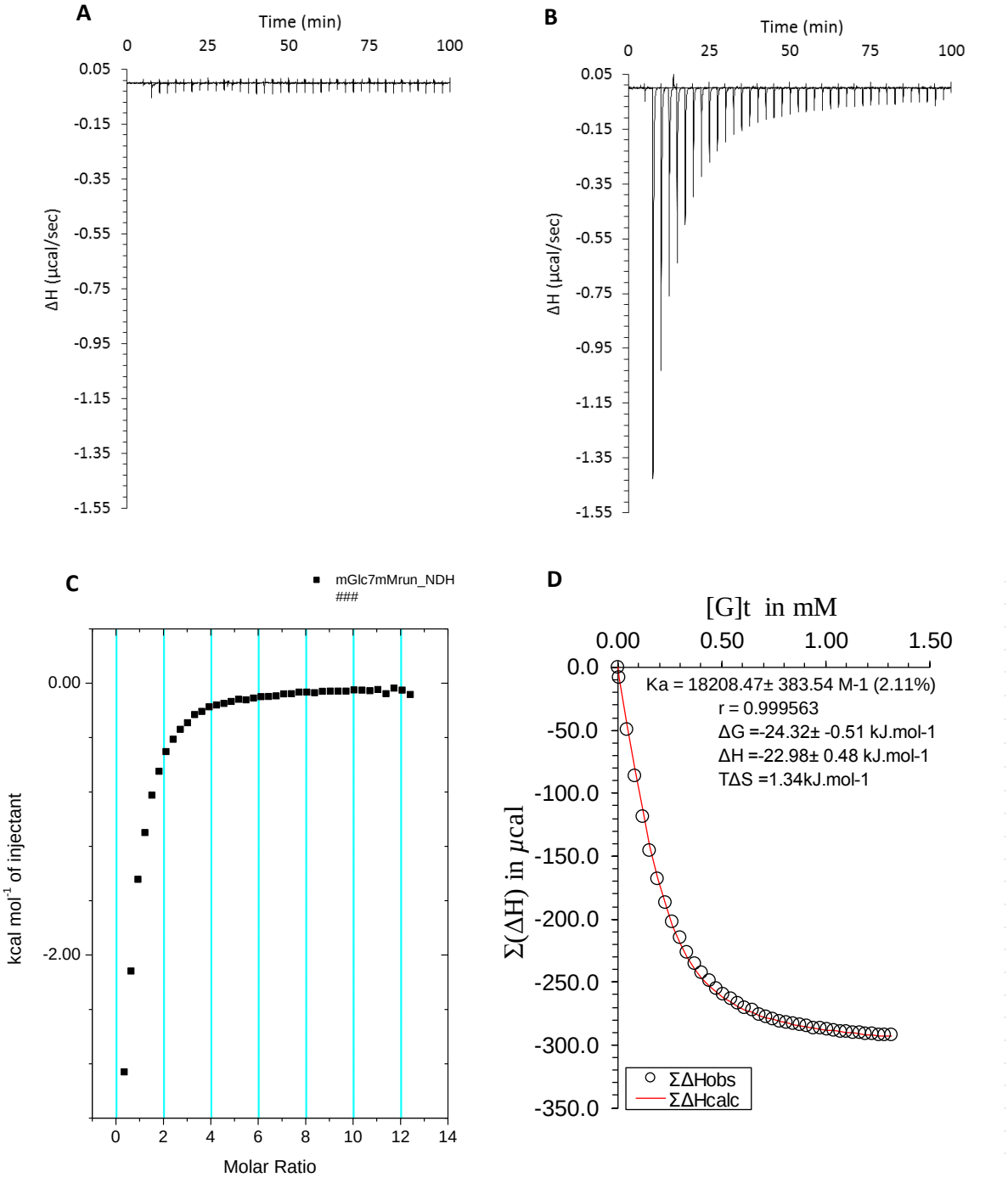

Supplementary Figure 28 | ITC binding results for receptor **2** (0.24 mM) titrated with D-glucose **10** (7.5 mM) in 10 mM phosphate buffer solution (pH 7.4), in which: A) shows the blank run (addition of sugar into water); B) shows the titration (sugar into receptor **2**); C) shows the plotted change in enthalpy vs molar ratio and D) shows the fit calculated using an Excel spreadsheet (K_a = 18,200 ± 383 M^{-1}). This experiment was repeated several times to ensure consistency, see discussion below and Supplementary Table 6.

Consistency of ITC results. We have found that routine ITC analyses tend to give consistent values for K_a (and ΔG) but that values for ΔH and ΔS are more variable. In the case of receptor **2** + glucose we were especially concerned to obtain accurate results, so that the titration was performed repeatedly on two different instruments. A few outliers were excluded, and the remaining results are shown in Supplementary Table 6. Averaging these data gives ΔG = -24.3, ΔH = -23 and TΔS = 1.3 kJ mol^{-1}, as indicated in Supplementary Table 5 and the main paper.

Supplementary Table 6 | ITC binding results for receptor **2** with D-glucose **10** in water (pH 7.4, 10 mM phosphate buffer solution) at 298 K.

Receptor (2) (μM)	**D-glucose (1) (mM)**	**K_a (M^{-1})**	**ΔG (kJ mol^{-1})**	**ΔH (kJ mol^{-1})**	**TΔS (kJ mol^{-1})**
52	3	19,200	-24.5	-24.7	-0.2
52	3	17,200	-24.2	-23.8	0.43
52	3	20,600	-24.6	-25.9	-1.25
55	7.5	15,300	-23.9	-22.7	1.2
100	7.5	19,200	-24.4	-21.3	3.2
130	7.5	16,400	-24.0	-20.4	3.6
130	7.5	20,400	-24.6	-25.2	-0.6
240	7.5	18,200	-24.3	-23.0	1.3
300	7.5	17,900	-24.3	-20.2	4.0
Average		18,300	-24.3	-23.0	1.3

Role of glucose anomers. As discussed above,[‡] the binding constants from both NMR and ITC experiments were calculated using the total concentration of glucose (sum of two anomers). Provided the guest is in large excess throughout the titration, the signal should vary as if just one substrate is present, analysis yielding a composite K_a with contributions from both anomers. Although the assumption of [guest] >> [host] holds for most substrates in this (and earlier) work, it is challenged for **2** + glucose because of the unusually high affinity. It does, however, hold approximately true for the titrations performed at the lowest concentrations of **2** (e.g. 52 μM, see Supplementary Table 6 above). As the apparent K_a is not concentration-dependent (Supplementary Table 6), it seems that in practice glucose is behaving like the less strongly-bound substrates. The K_a values measured for glucose are therefore taken to be composites encompassing both anomers, comparable to those for other reducing sugars.

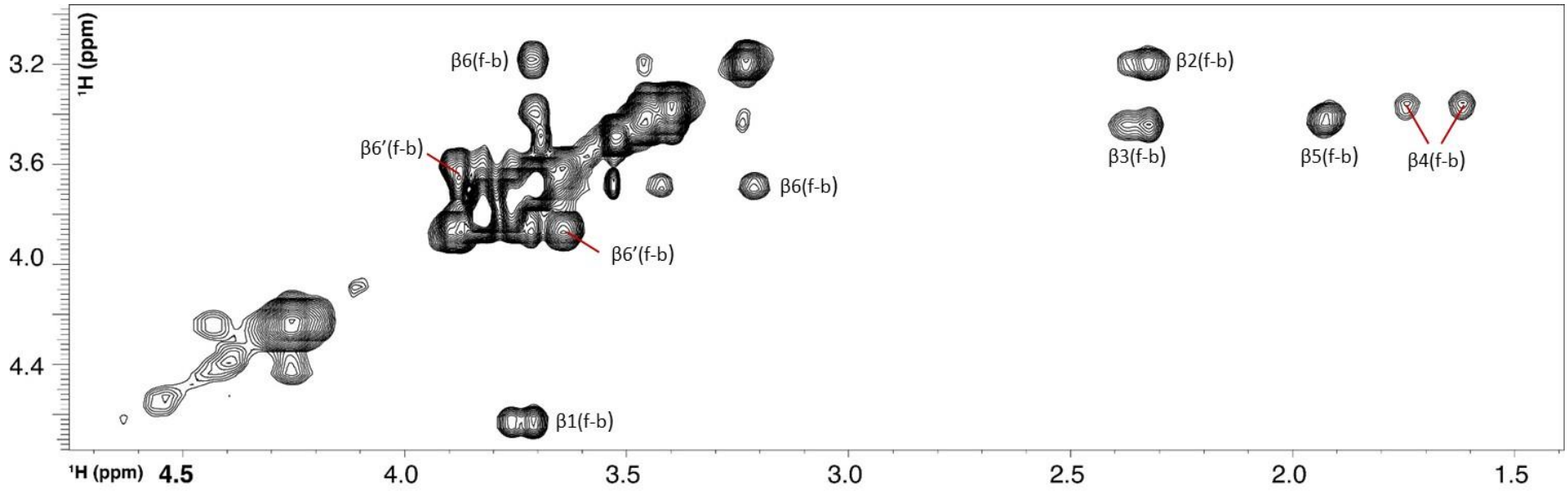

Supplementary Figure 29 | Partial ^{1}H-^{1}H NMR ROESY spectrum of receptor **2** (2 mM) with D-glucose **10** (5 mM, 2.5 equivalents) in D_2O at 298 K (see also Fig. 3c). Chemical exchange peaks are observed between the D-glucose bound to the receptor (whose signals appear more upfield) and free D-glucose. These exchange signals are labelled accordingly (i.e. β2(f-b) indicates chemical exchange between free ("f") and bound ("b") β-D-glucose for the proton at position 2). Exchange peaks are observed for only the β anomer under these conditions (mixing time of 100 ms). For protons β1/2/3/4 two signals can be observed, attributed to the two non-equivalent orientations within the binding site. Exchange peaks for the α anomer were observed at much longer mixing times (>500 ms). Quantification of the selectivity of **2** for the α and β anomers could not be achieved using this method, however determination of selectivity was achieved using ^{1}H-^{13}C HSQC (see Supplementary Supplementary Figure **30** below). Comparison of the chemical shifts between the free protons for D-glucose allowed assignment of the ^{1}H NMR chemical shifts for the bound forms of β-D-glucose, which are listed in Supplementary Table 7 below.

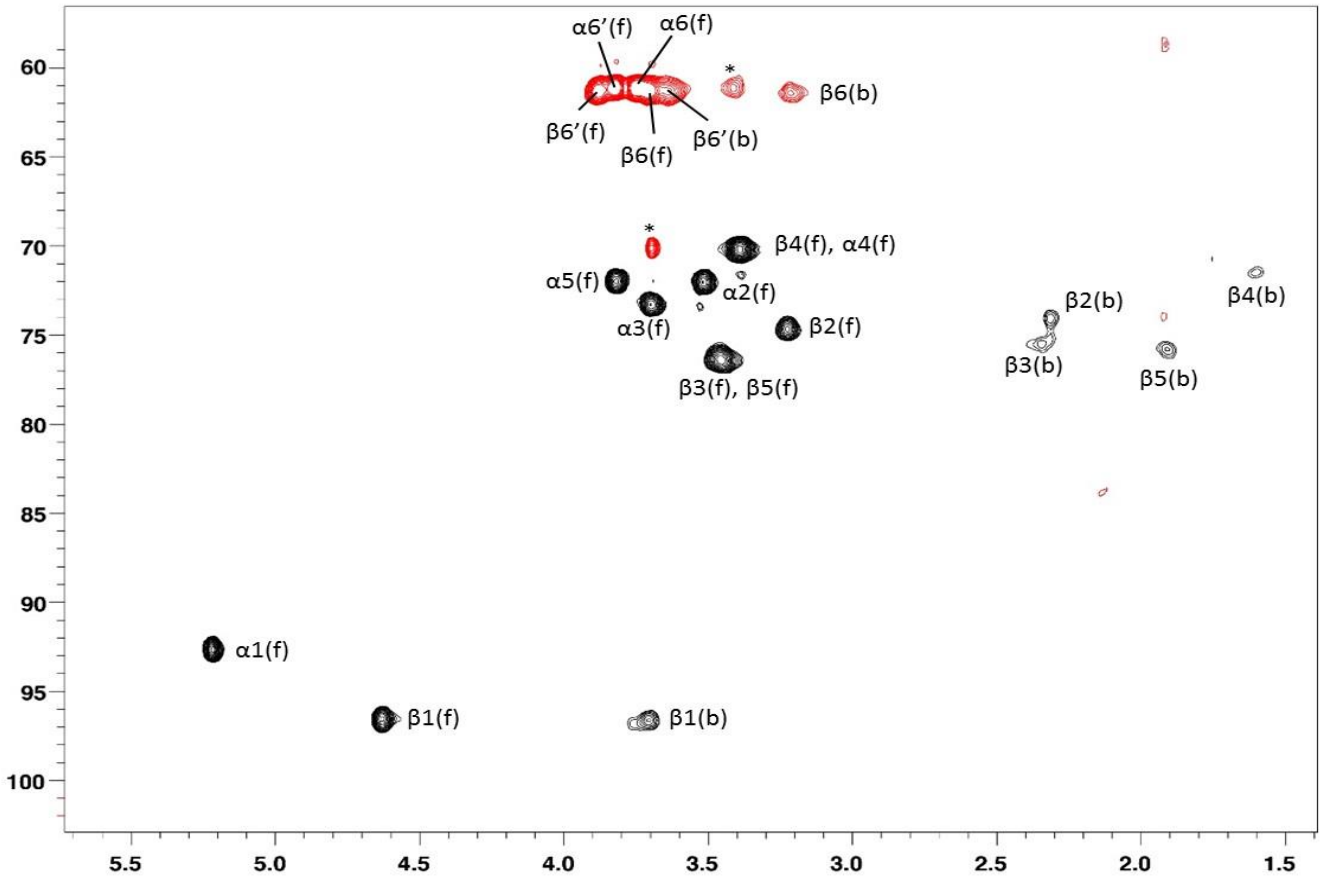

Supplementary Figure 30 | Partial (^{1}H-^{13}C correlation, one bond) HSQC NMR spectrum of receptor **2** (2 mM) with D-glucose **10** (5 mM, 2.5 equivalents) in D_2O at 298 K. NMR signals for D-glucose bound to the receptor (whose signals appear more upfield in the ^{1}H (f1) dimension, horizontal axis) and free glucose in solution. These signals for "free" and "bound" states are shown in black for CH protons and red for CH_2 protons, and are labelled accordingly (i.e. β2(f) indicates free β-D-glucose and β2(b) indicates the bound form for the proton at position 2). NMR signals corresponding to bound D-glucose are observed for the β anomer only, indicating an expected preference for binding the β anomer. The ratio of intensity of signals for bound β-D-glucose and baseline noise is measured as 6:1 (signal:noise). Assuming the bound signals for the α anomer are at most the same intensity as the baseline noise, then it can be assumed the selectivity for β and α-D-glucose is also at least 6:1 (β:α) but could potentially be higher.

Supplementary Table 7 | Chemical shifts (δ in ppm) of β-D-glucose **10** unbound and bound to receptor **2**. Values obtained in D_2O/H_2O (1:9) at 298 K. The values for difference in chemical shift (Δδ) upon complexation of glucose with receptor **2** are also given, indicating how shielded the CH protons of the carbon skeleton become when bound to the receptor.

β-D-glucose chemical shifts (δ, ppm)

H	Unbound	Bound to **2**	Δδ on binding to **2**
1	4.63	3.72	-0.91
2	3.23	2.34	-0.89
3	3.47	2.37	-1.10
4	3.39	1.63[a], 1.74[b]	-1.76, -1.65
5	3.45	1.94	-1.51
6	3.71	3.23	-0.48
6’	3.88	3.64	-0.24

[a] Stronger signal, presumably corresponding to the major orientation within the binding site. [b] Weaker signal, presumably corresponding to the minor orientation.

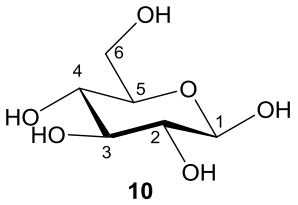

10

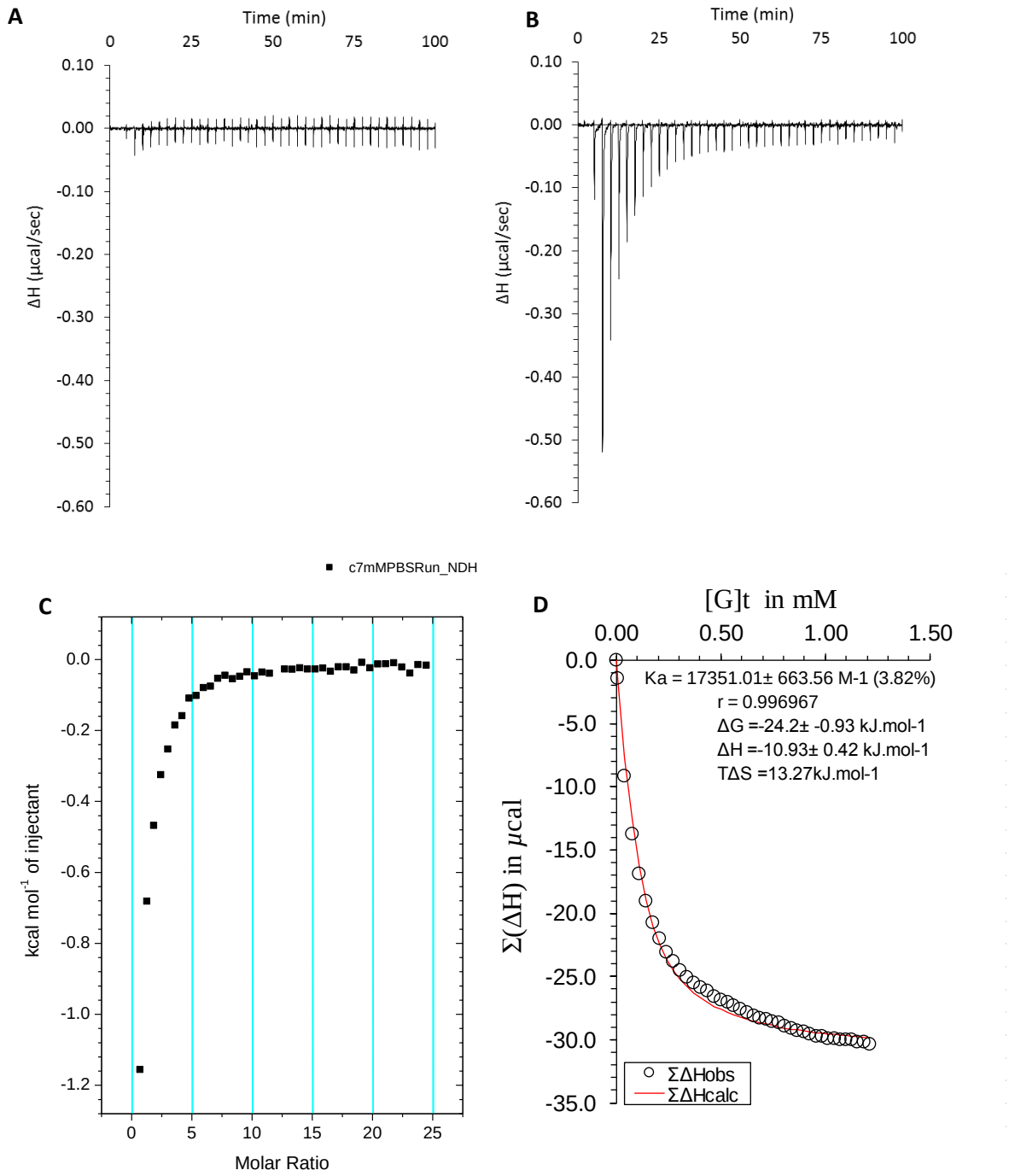

Supplementary Figure 31 | ITC binding results for receptor **2** (0.06 mM) titrated with D-glucose **10** (7 mM) in 10 mM phosphate buffered saline solution (pH 7), in which: A) shows the blank run (addition of sugar into water); B) shows the titration (sugar into receptor **2**); C) shows the plotted change in enthalpy vs molar ratio; and D) shows the fit calculated using an Excel spreadsheet (K_a = 17,351 ± 663 M^{-1}). The experiment was performed once.

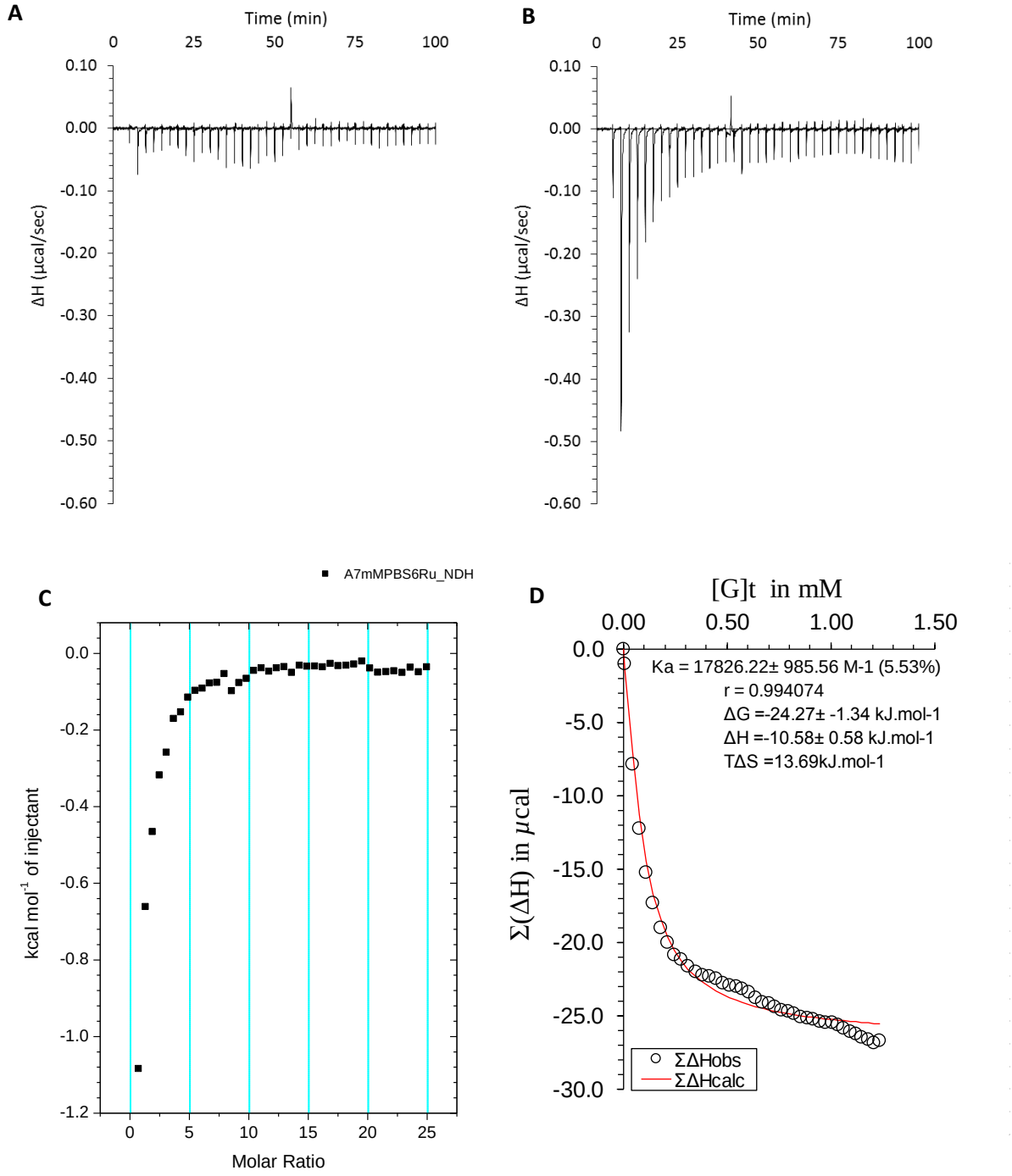

Supplementary Figure 32 | ITC binding results for receptor **2** (0.06 mM) titrated with D-glucose **10** (7 mM) in 10 mM phosphate buffered saline solution (PBS, pH 6), in which: A) shows the blank run (addition of sugar into water); B) shows the titration (sugar into receptor **2**); C) shows the plotted change in enthalpy vs molar ratio; and D) shows the fit calculated using an Excel spreadsheet (K_a = 17,826 ± 985 M^{-1}). The experiment was performed once.

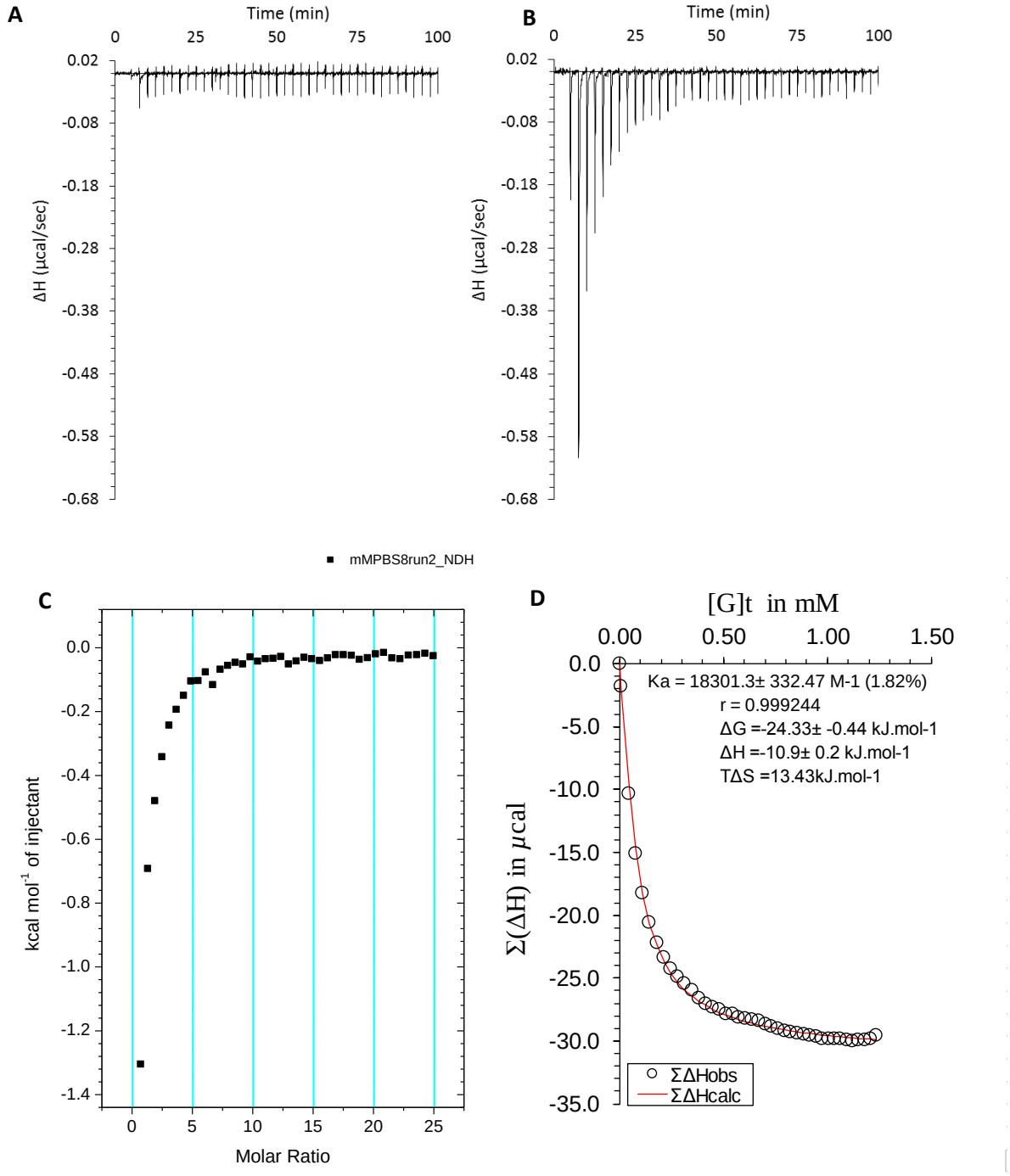

Supplementary Figure 33 | ITC binding results for receptor **2** (0.06 mM) titrated with D-glucose **10** (7 mM) in 10 mM phosphate buffered saline solution (pH 8), in which: A) shows the blank run (addition of sugar into water); B) shows the titration (sugar into receptor **2**); C) shows the plotted change in enthalpy vs molar ratio; and D) shows the fit calculated using an Excel spreadsheet (K_a = 18,301 ± 332 M^{-1}). The experiment was performed once.

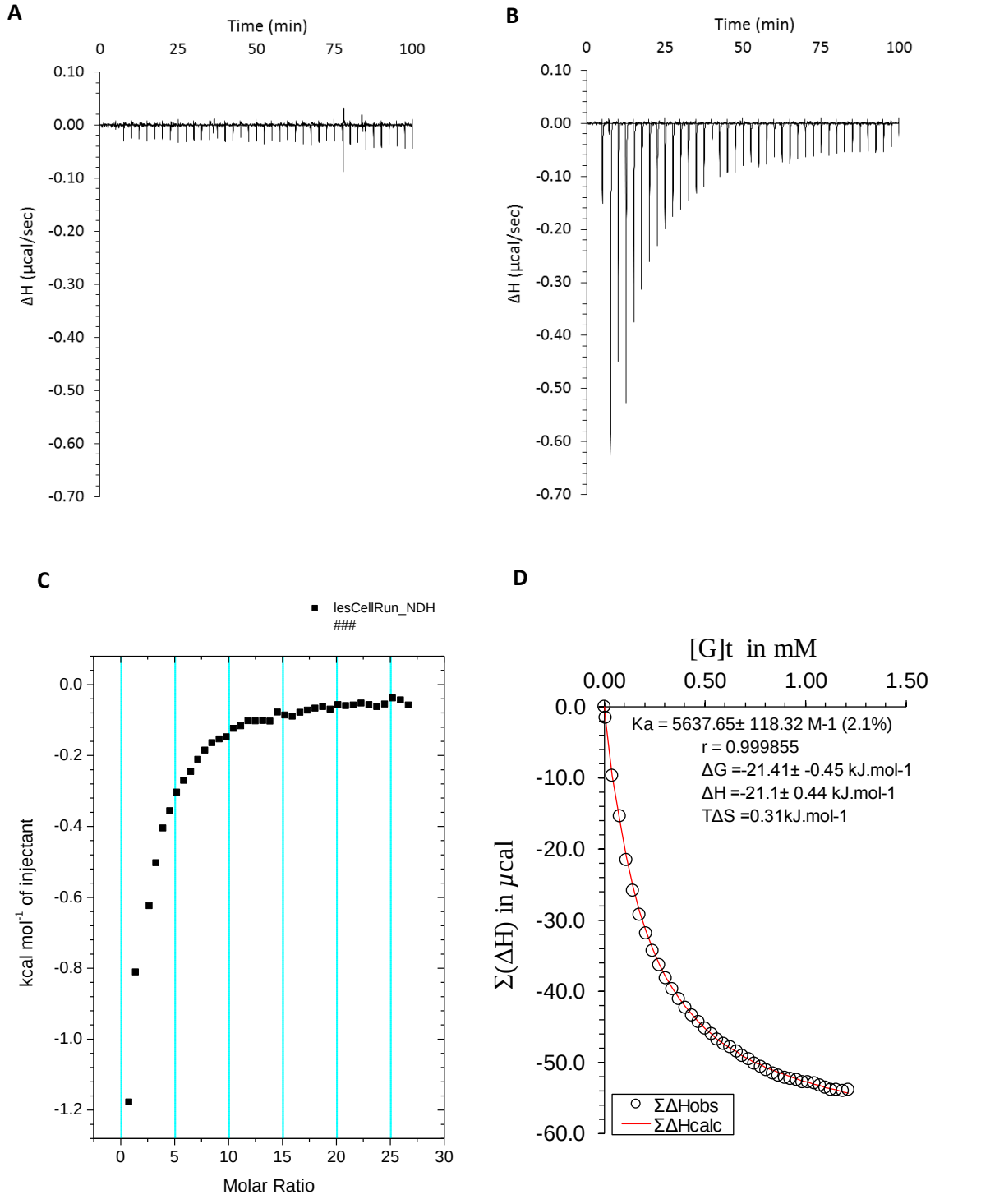

Supplementary Figure 34 | ITC binding results for receptor **2** (0.06 mM) titrated with D-glucose **10** (7 mM) in DMEM Cell Culture Medium (no glucose, 10k MWCO, 90% v/v) and 10 mM phosphate buffer solution (pH 7.4), in which: A) shows the blank run (addition of sugar into medium); B) shows the titration (sugar into receptor **2**); C) shows the plotted change in enthalpy vs molar ratio; and D) shows the fit calculated using an Excel spreadsheet (K_a = 5637 ± 118 M^{-1}). The experiment was performed once.

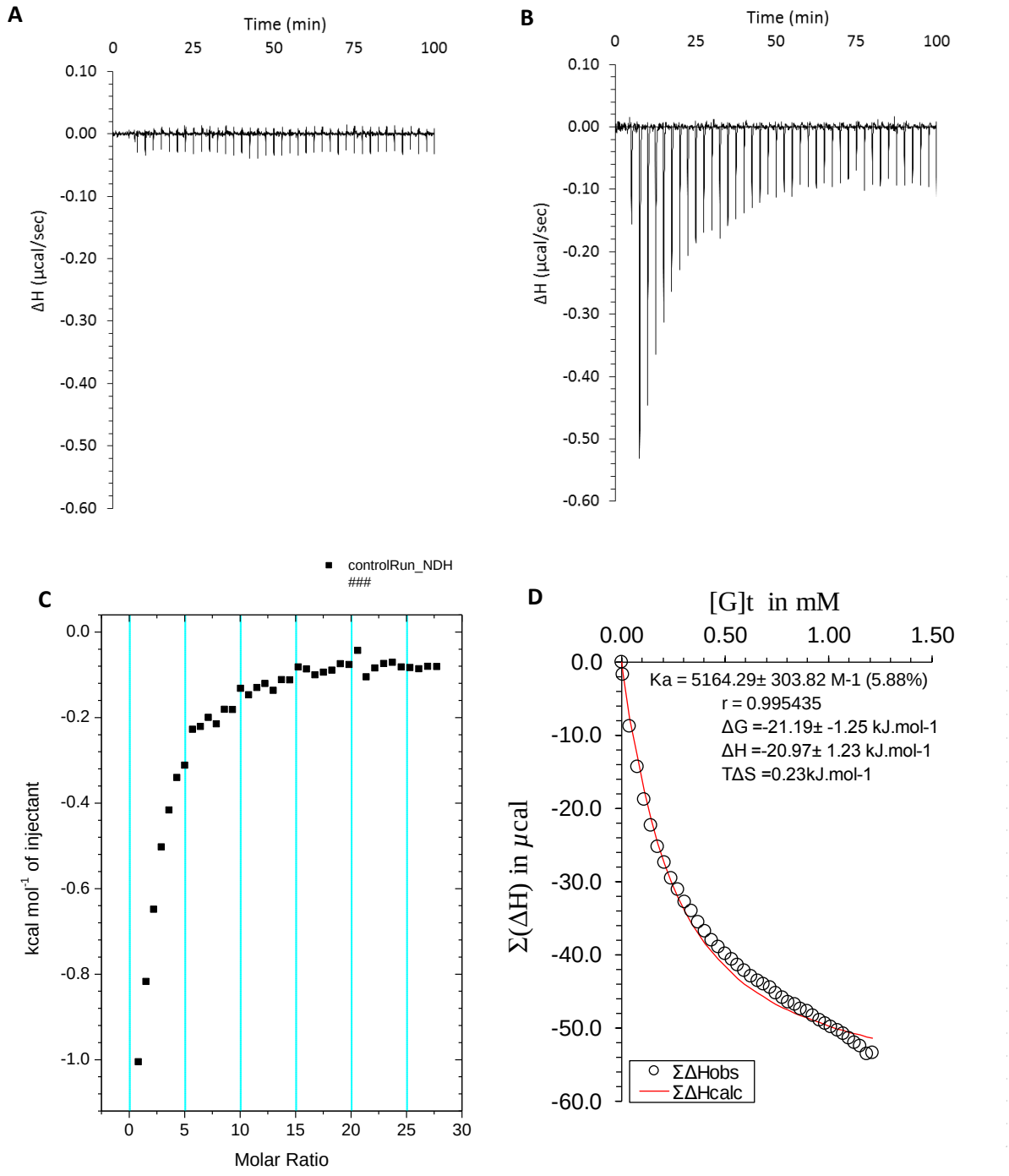

Supplementary Figure 35 | ITC binding results for receptor **2** (0.06 mM) titrated with D-glucose **10** (7 mM) in DMEM salt control medium with 10 mM phosphate buffer solution (pH 7.4), in which: A) shows the blank run (addition of substrate into medium); B) shows the titration (substrate into receptor **2**); C) shows the plotted change in enthalpy vs molar ratio; and D) shows the fit calculated using an Excel spreadsheet (K_a = 5164 ± 303 M^{-1}). The experiment was performed 2 times with similar results.

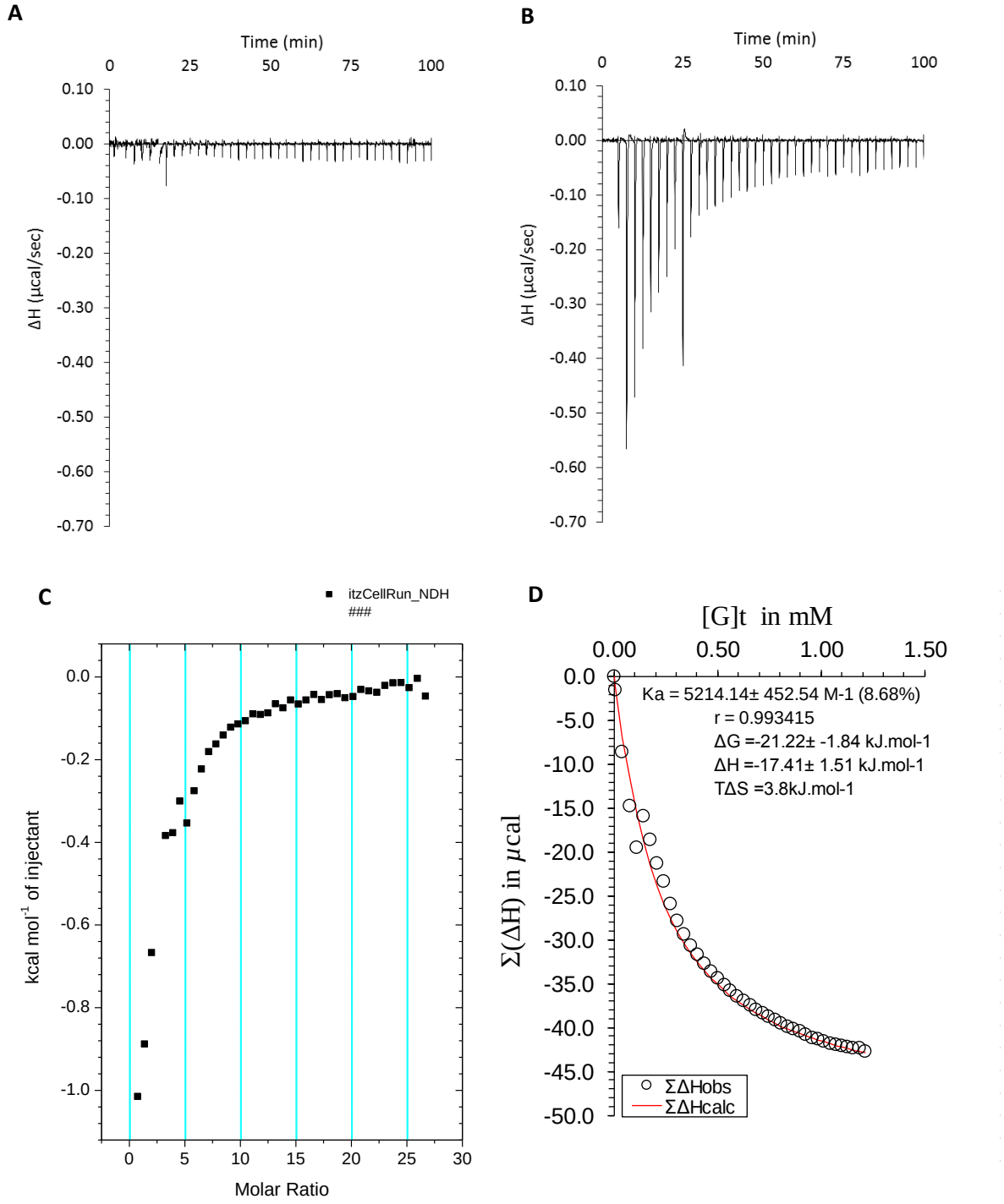

Supplementary Figure 36 | ITC binding results for receptor **2** (0.06 mM) titrated with D-glucose **10** (7 mM) in Leibovitz's L-15 Cell Culture Medium (no glucose, 10k MWCO, 90% v/v) and 10 mM phosphate buffer solution (pH 7.4), in which: A) shows the blank run (addition of sugar into medium); B) shows the titration (sugar into receptor **2**); C) shows the plotted change in enthalpy vs molar ratio; and D) shows the fit calculated using an Excel spreadsheet (K_a = 5214 ± 452 M^{-1}). The experiment was performed once.

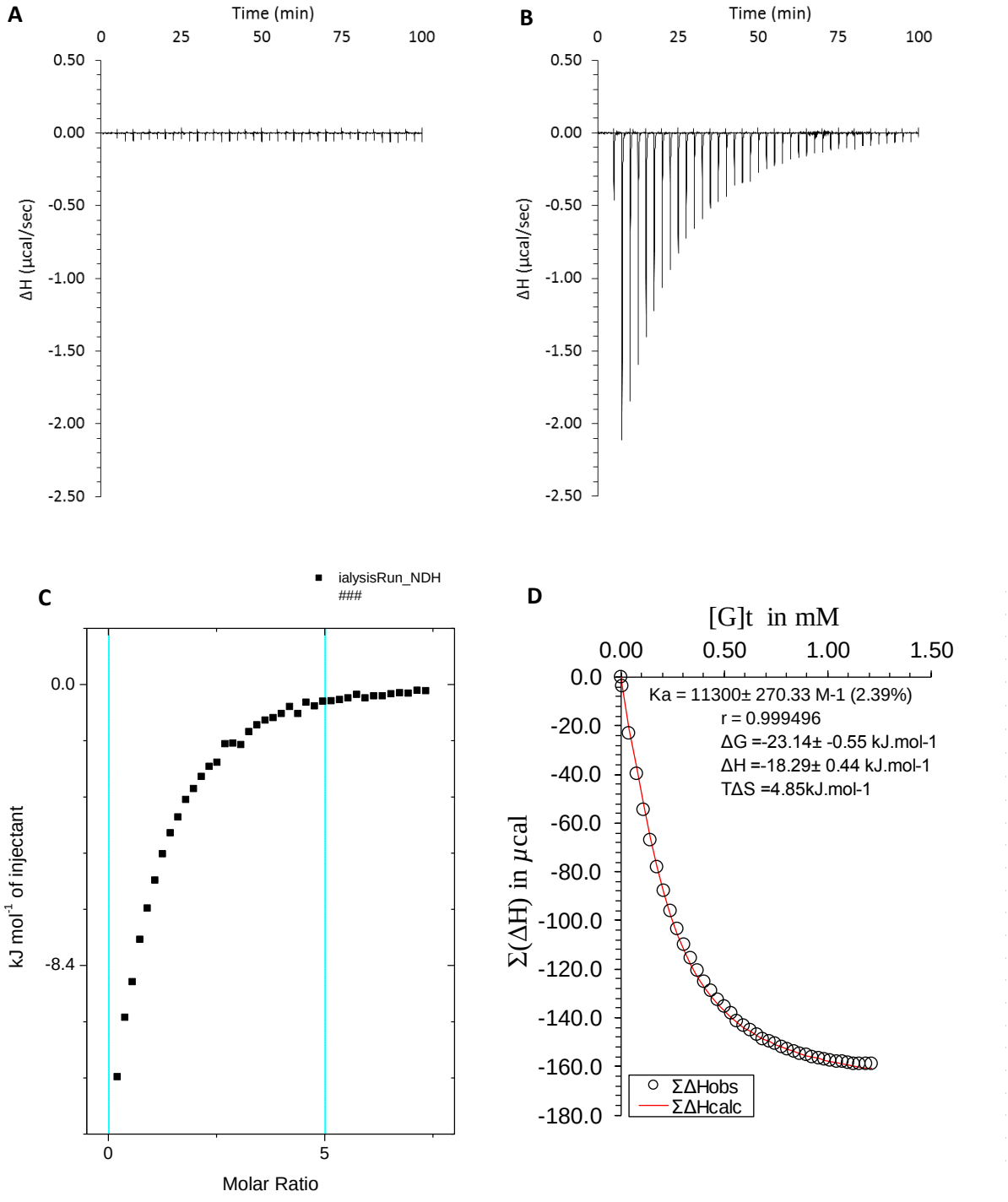

Supplementary Figure 37 shows the ITC binding results for receptor **2** (0.2 mM) titrated with D-glucose **10** (7 mM) in human serum (90% v/v, no glucose) with 10 mM phosphate buffer (pH 7.4) in which: A) shows the blank run (addition of substrate into medium); B) shows the titration (substrate into receptor **2**); C) shows the plotted change in enthalpy vs molar ratio; and D) shows the fit calculated using an Excel spreadsheet (K_a = 11,300 ± 270 M^{-1}). The experiment was performed once.

Methyl β-D-glucoside 11

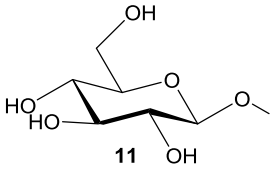

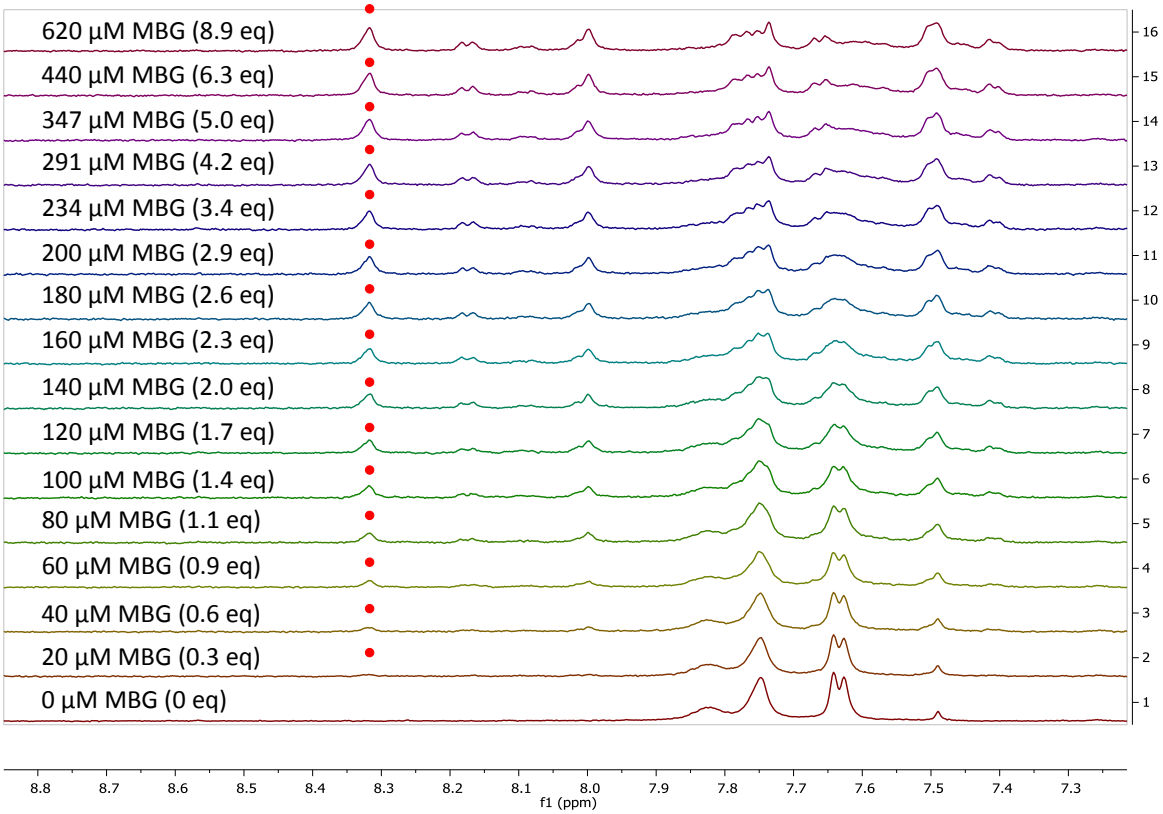

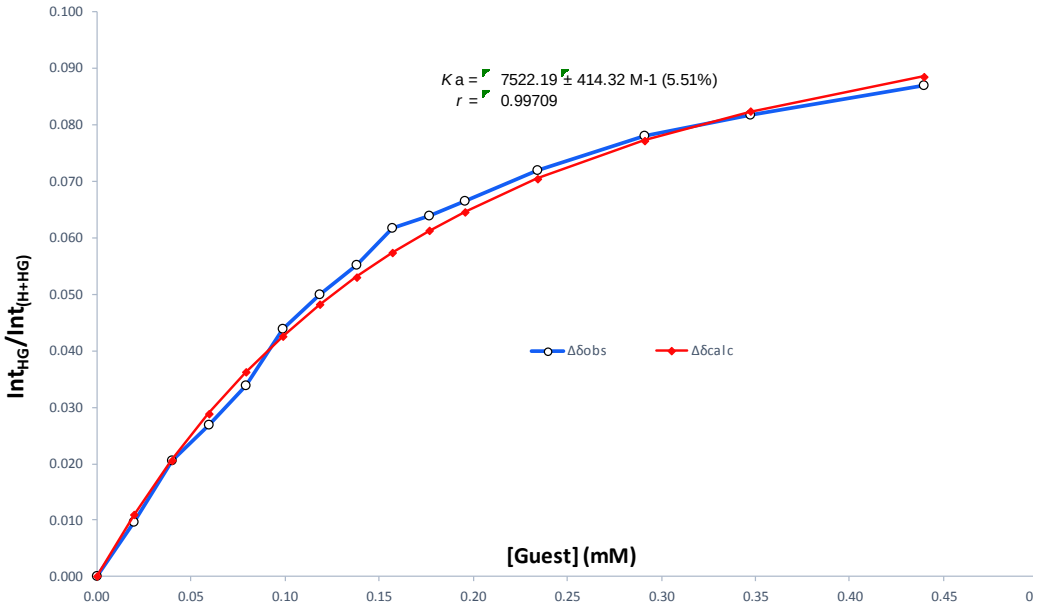

Supplementary Figure 38 | ^{1}H NMR spectra (top) and binding analysis curve (bottom) for receptor **2** (0.07 mM) titrated with a combined solution of methyl β-D-glucoside **11** (10 mM) and receptor **2** (0.07 mM), in D_2O with 10 mM phosphate buffer (pH 7.4) at 298 K. Spectra imply binding with slow exchange on NMR timescale. Integrations of peak at 8.31 ppm (denoted with •) versus region 8.36-7.36 ppm were plotted against guest concentration (mM). The calculated values for the integrals are overlaid with the observed values, giving K_a = 7522 ± 414 M^{-1} (5.51%). Limiting integration = 11.5, X_{lim} = 0.09. The experiment was performed 3 times with similar results.

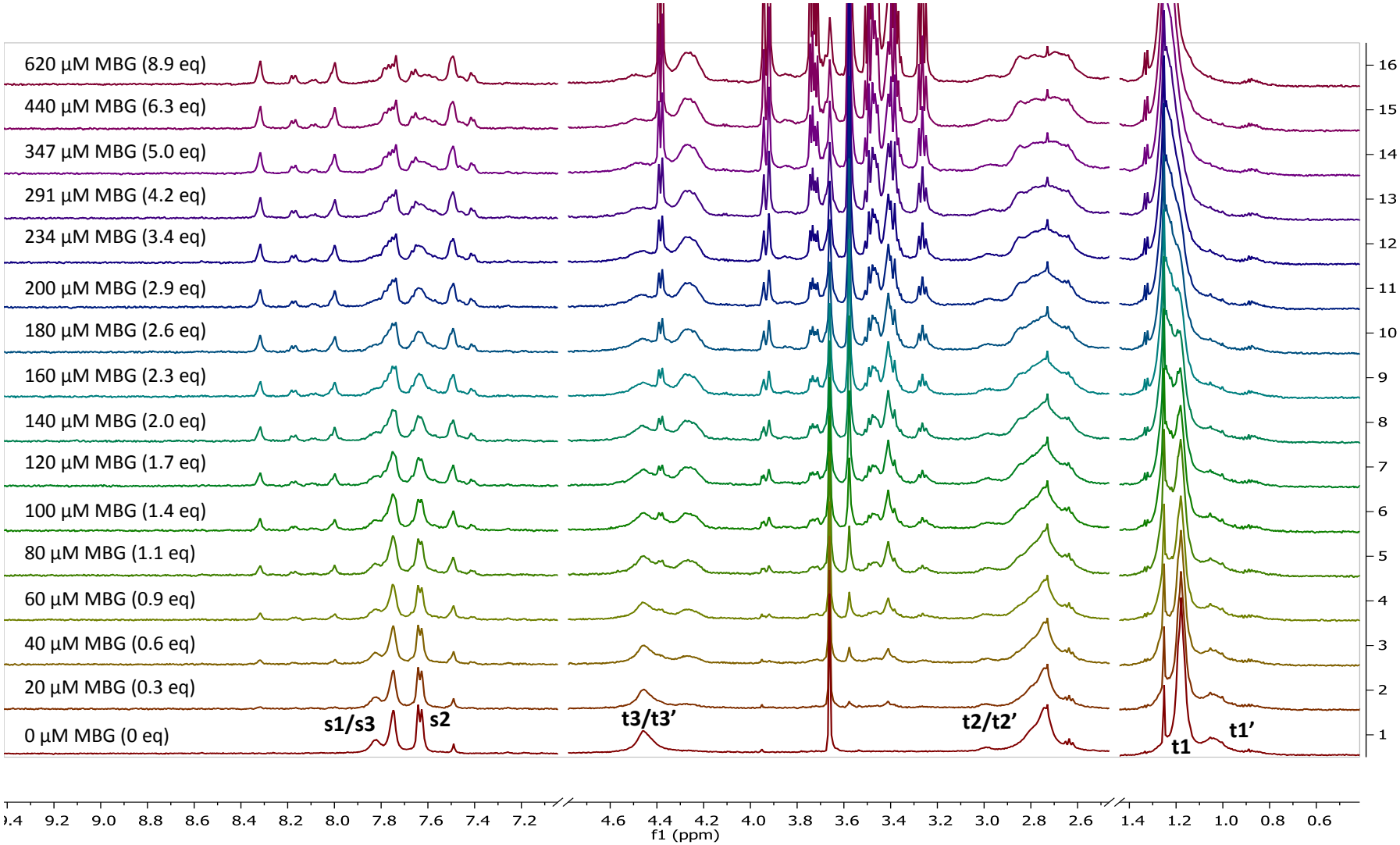

Supplementary Figure 39 ^{1}H NMR spectra for receptor **2** (0.07 mM) titrated with a combined solution of methyl β-D-glucoside **11** (10 mM) and receptor **2** (0.07 mM), in D_2O with 10 mM phosphate buffer (pH 7.4) at 298 K

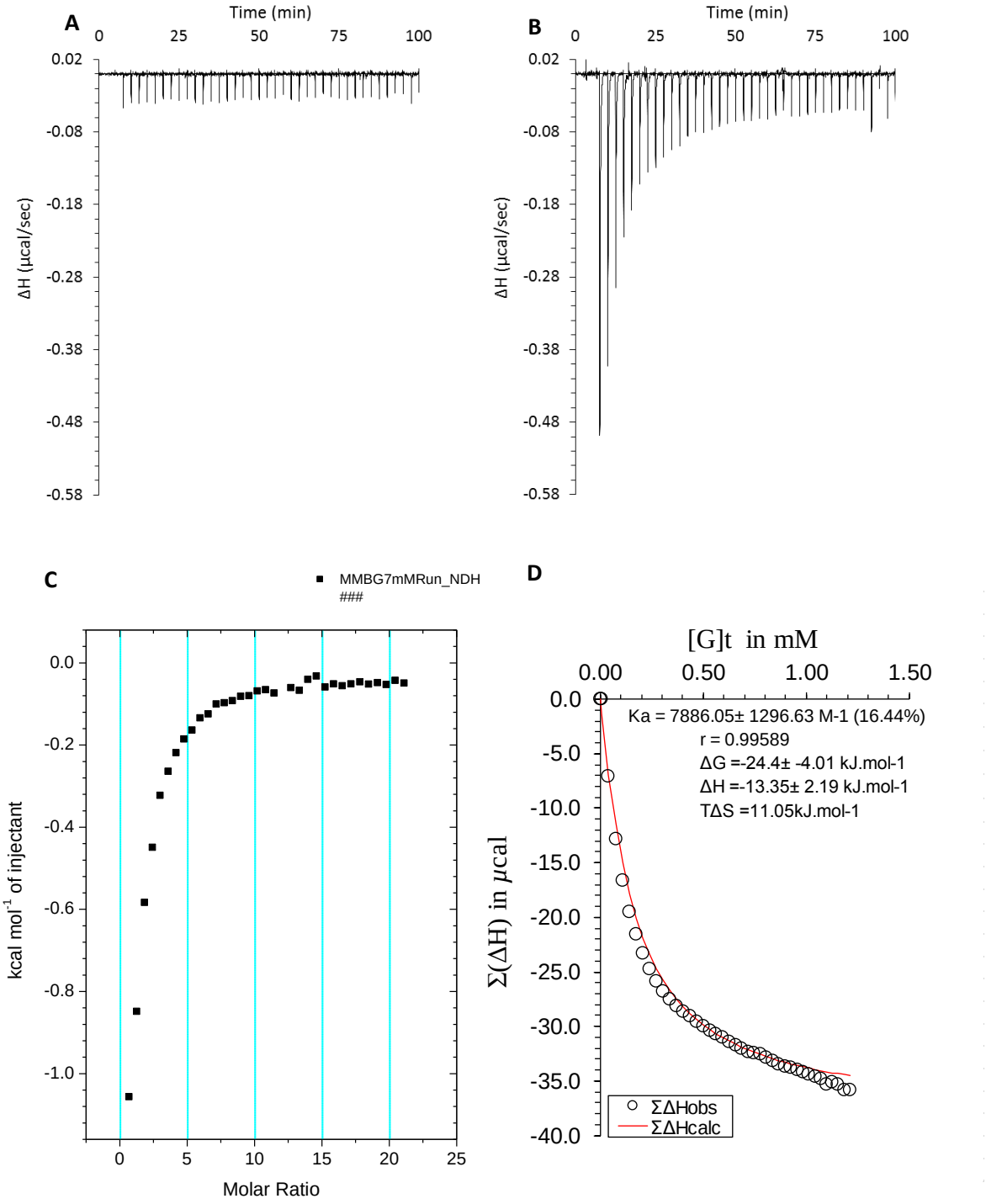

Supplementary Figure 40 | ITC binding results for receptor **2** (0.06 mM) titrated with methyl β-D-glucoside **11** (7 mM) in 10 mM phosphate buffer solution (pH 7.4), in which: A) shows the blank run (addition of sugar into water); B) shows the titration (sugar into receptor **2**); C) shows the plotted change in enthalpy vs molar ratio; and D) shows the fit calculated using an Excel spreadsheet (K_a = 7886 ± 1296 M^{-1}). The experiment was performed once.

D-Glucuronic acid 12

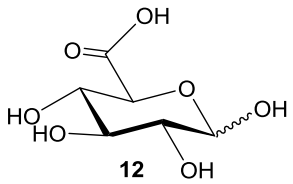

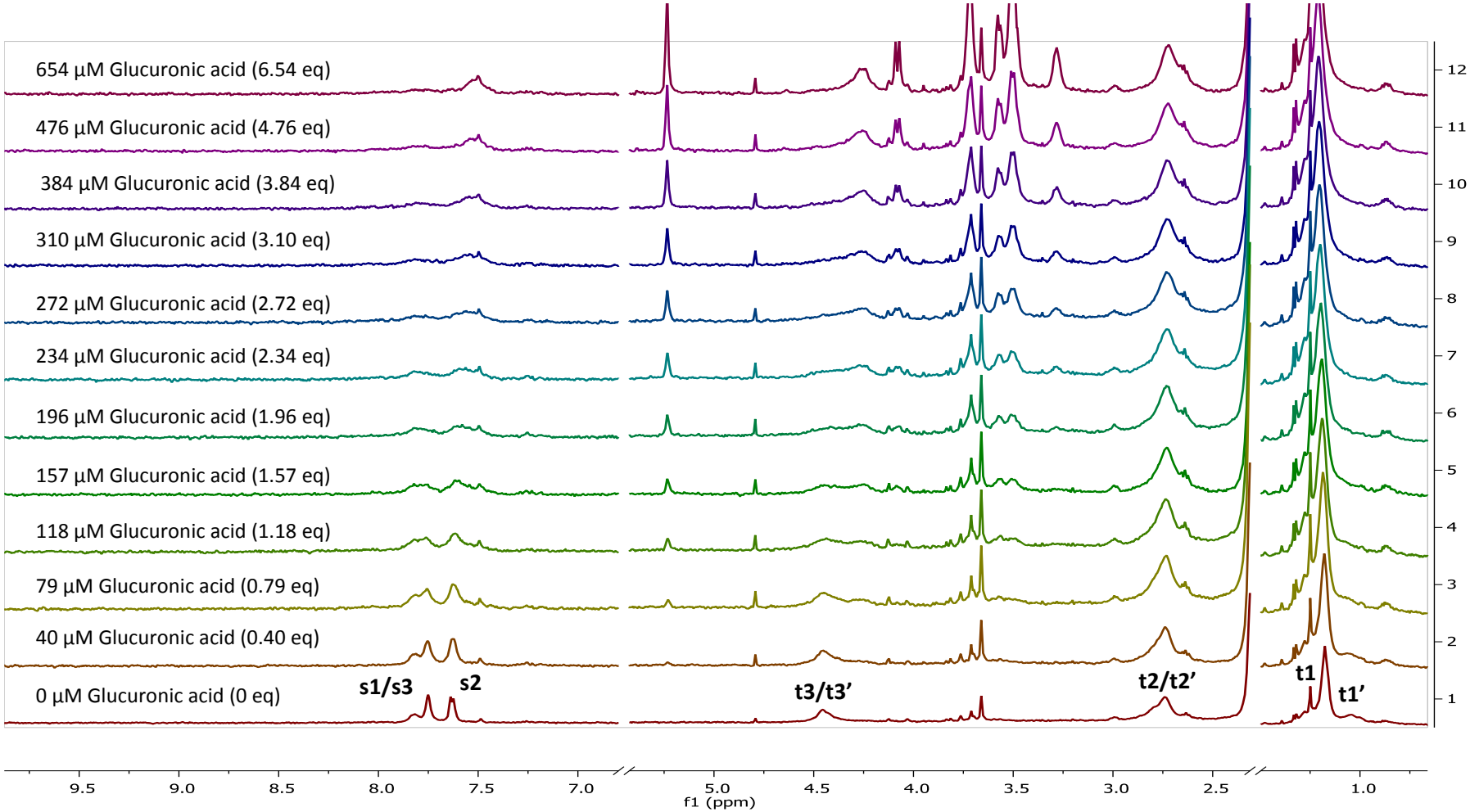

Supplementary Figure 41 | Partial ^{1}H NMR spectra for receptor **2** (0.1 mM) titrated with a combined solution of D-glucuronic acid **12** (10 mM) and receptor **2** (0.1 mM), in D_2O with 10 mM phosphate buffer (pH 7.4) at 298 K. Spectra imply binding with intermediate rate of exchange (rate between fast and slow exchange rates between H and HG species) on NMR timescale. Due to severe broadening of peaks for receptor **2** upon addition of guest, no K_a was determinable. The experiment was performed once.

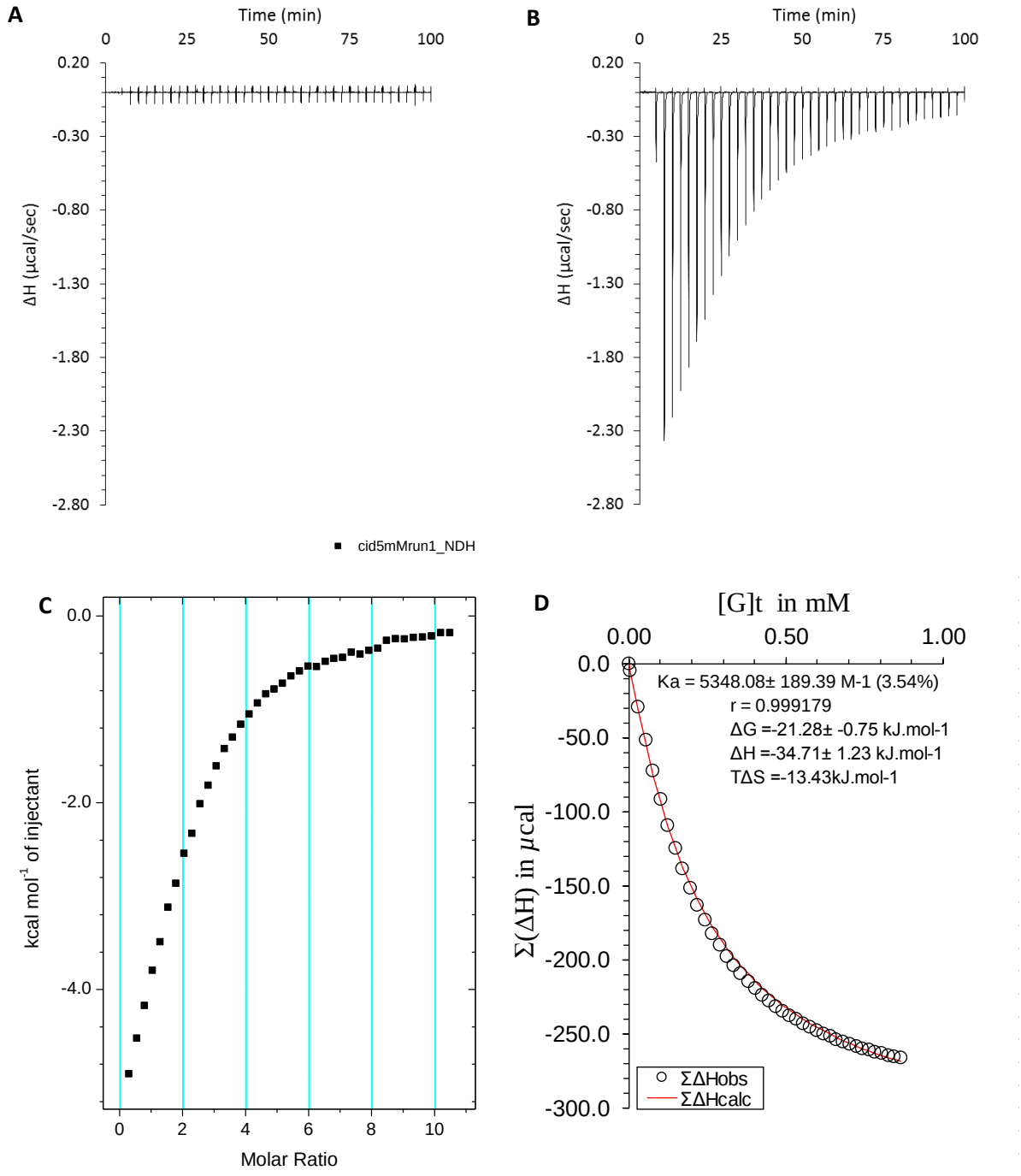

Supplementary Figure 42 | ITC binding results for receptor **2** (0.2 mM) titrated with D-glucuronic acid **12** (5 mM) in 10 mM phosphate buffer solution (pH 7.4) in which: A) shows the blank run (addition of substrate into medium); B) shows the titration (substrate into receptor **2**); C) shows the plotted change in enthalpy vs molar ratio; and D) shows the fit calculated using an Excel spreadsheet (K_a = 5348 ± 189 M^{-1}). The experiment was performed 3 times with similar results.

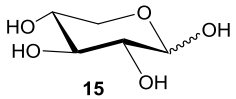

D-Xylose 13

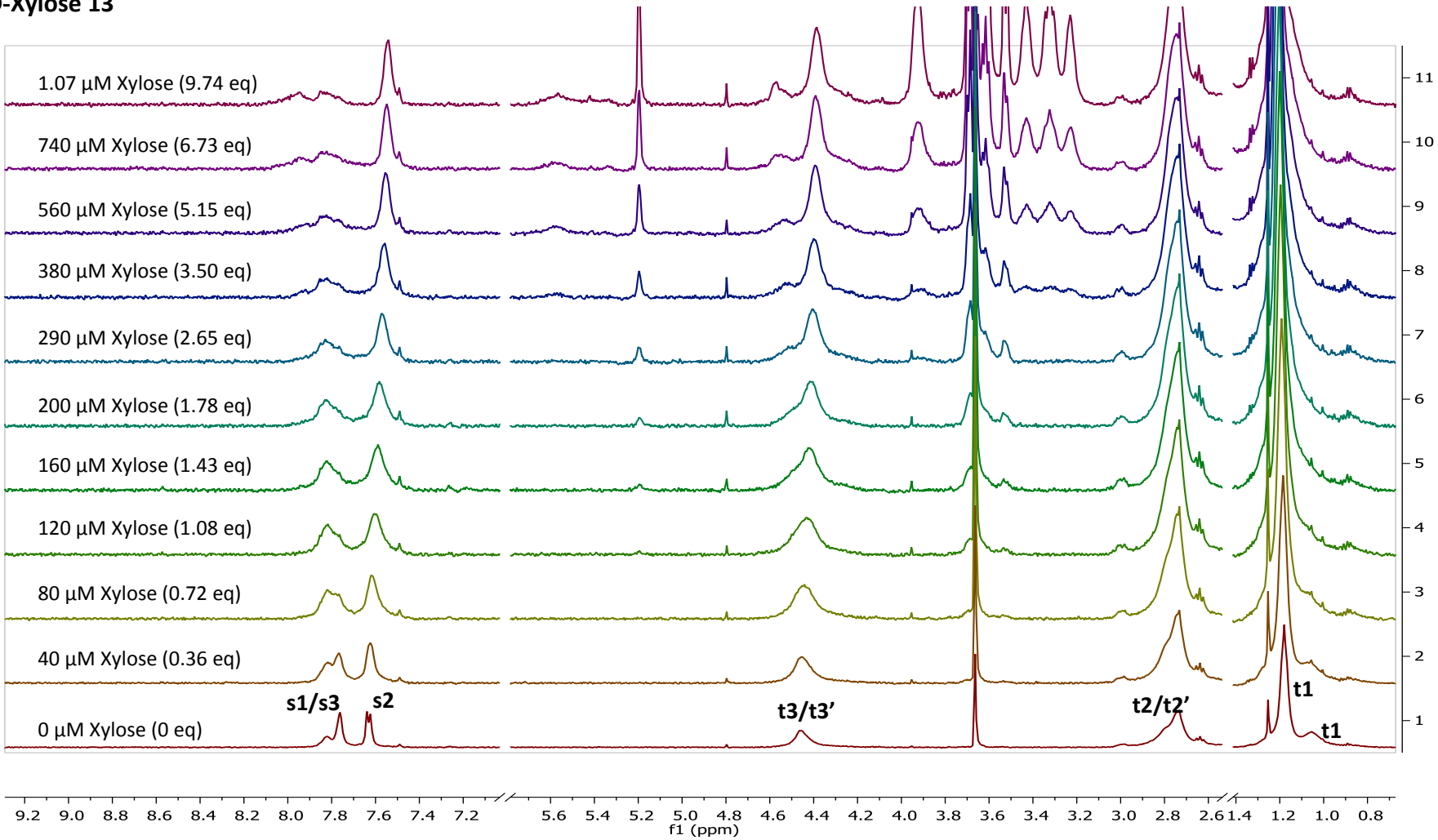

Supplementary Figure 43 | ^{1}H NMR spectra for receptor **2** (0.11 mM) titrated with a combined solution of D-xylose **13** (10 mM) and receptor **2** (0.11 mM), in D_2O with 10 mM phosphate buffer (pH 7.4) a t 298 K. Spectra imply binding with intermediate rate of exchange (rate between fast and slow exchange rates between H and HG species) on NMR timescale. Due to severe broadening of peaks for receptor **2** upon addition of guest, no K_a was determinable. The experiment was performed once.

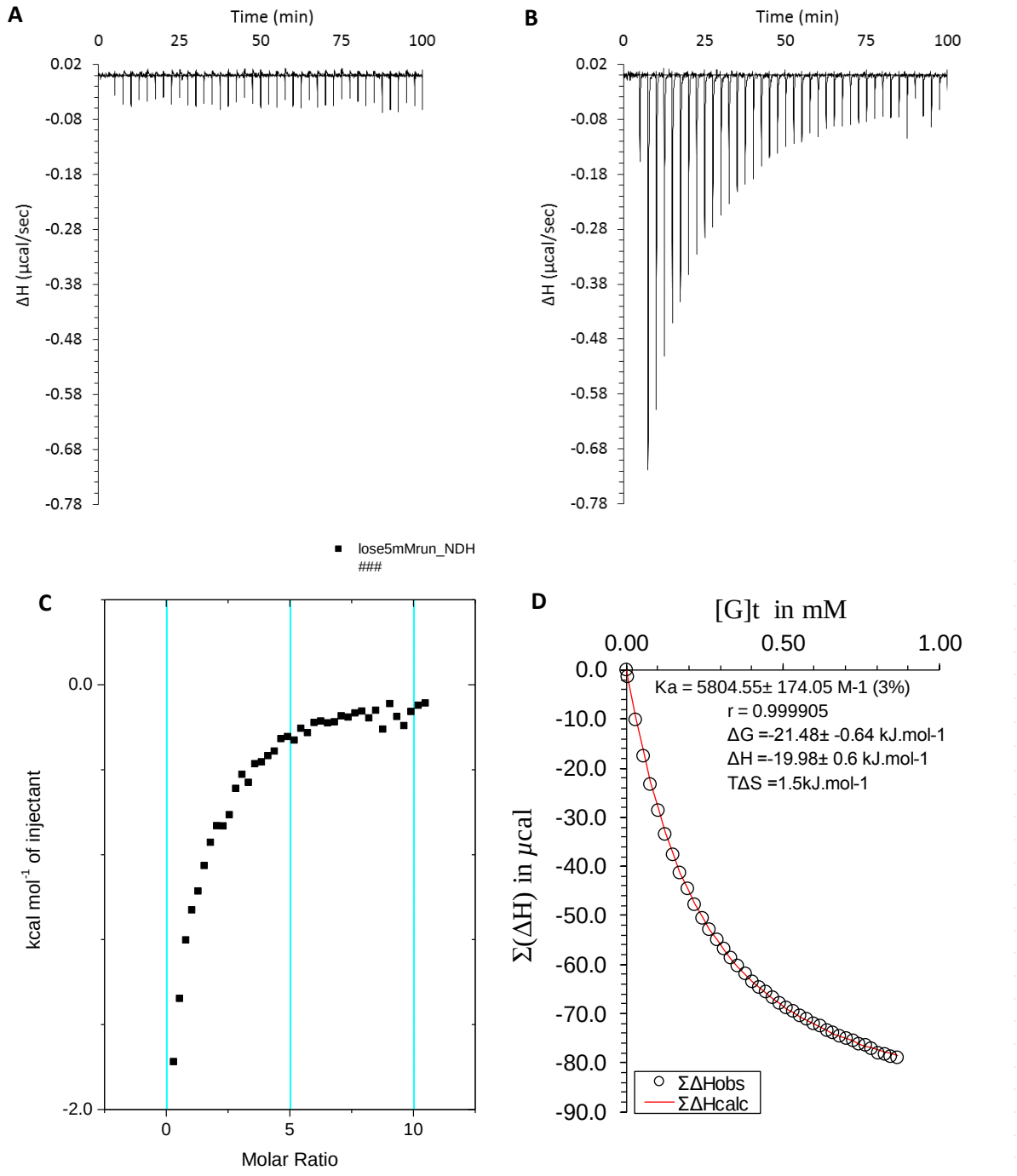

Supplementary Figure 44 | ITC binding results for receptor **2** (0.1 mM) titrated with D-xylose **13** (5 mM) in 10 mM phosphate buffer solution (pH 7.4) in which: A) shows the blank run (addition of substrate into medium); B) shows the titration (substrate into receptor **2**); C) shows the plotted change in enthalpy vs molar ratio; and D) shows the fit calculated using an Excel spreadsheet (K_a = 5804 ± 174 M^{-1}). The experiment was performed 2 times with similar results.

2-Deoxy-D-glucose 14

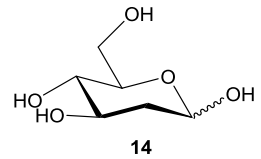

14

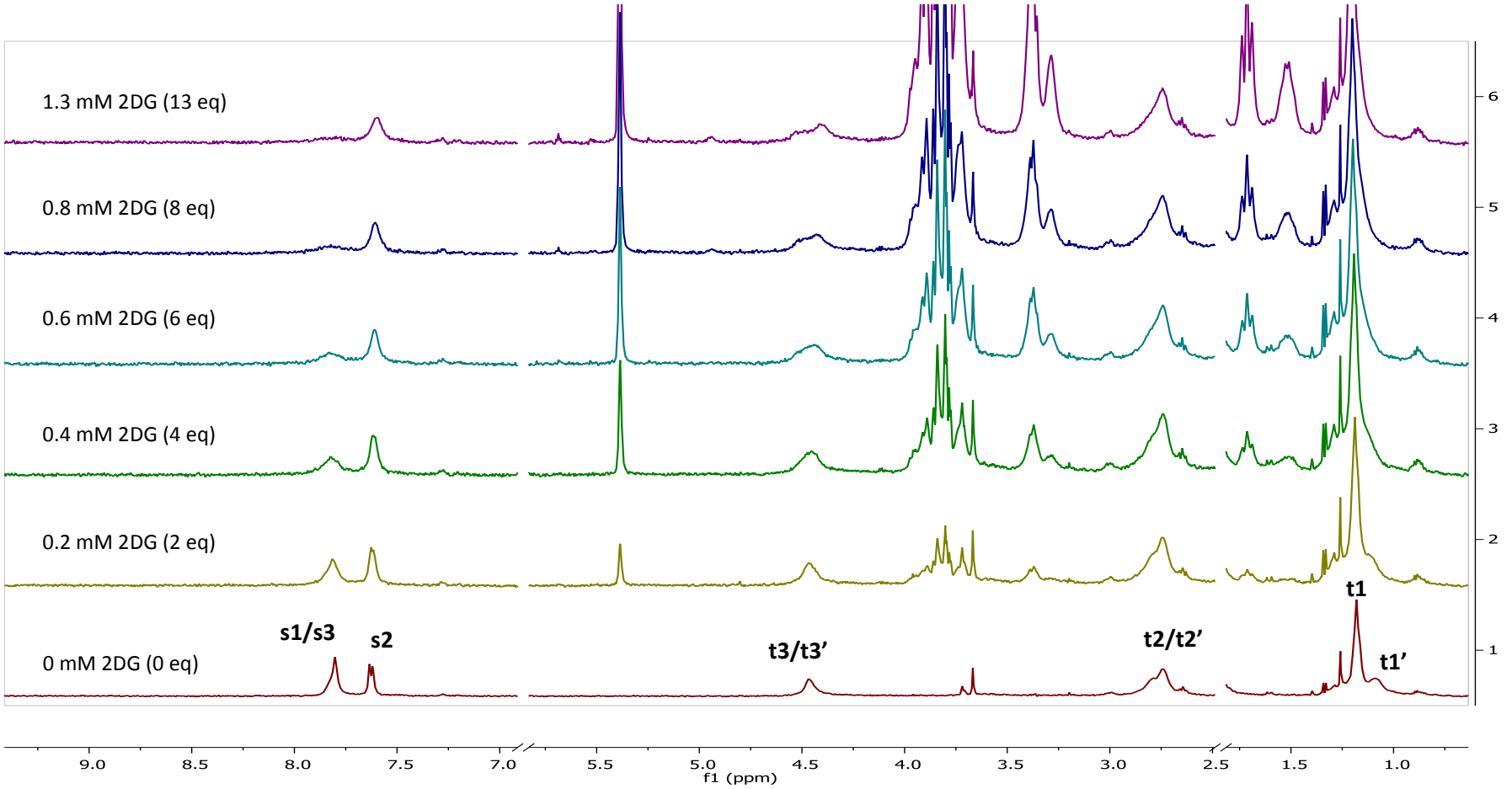

Supplementary Figure 45 | Partial ^{1}H NMR spectra for receptor **2** (0.1 mM) titrated with a combined solution of 2-deoxy-D-glucose **14** (50 mM) and receptor **2** (0.1 mM), in D_2O with 10 mM phosphate buffer (pH 7.4) at 298 K. Spectra imply binding with intermediate rate of exchange (rate between fast and slow exchange rates between H and HG species) on NMR timescale. Due to severe broadening of peaks for receptor **2** upon addition of guest, no K_a was determinable. The experiment was performed once.

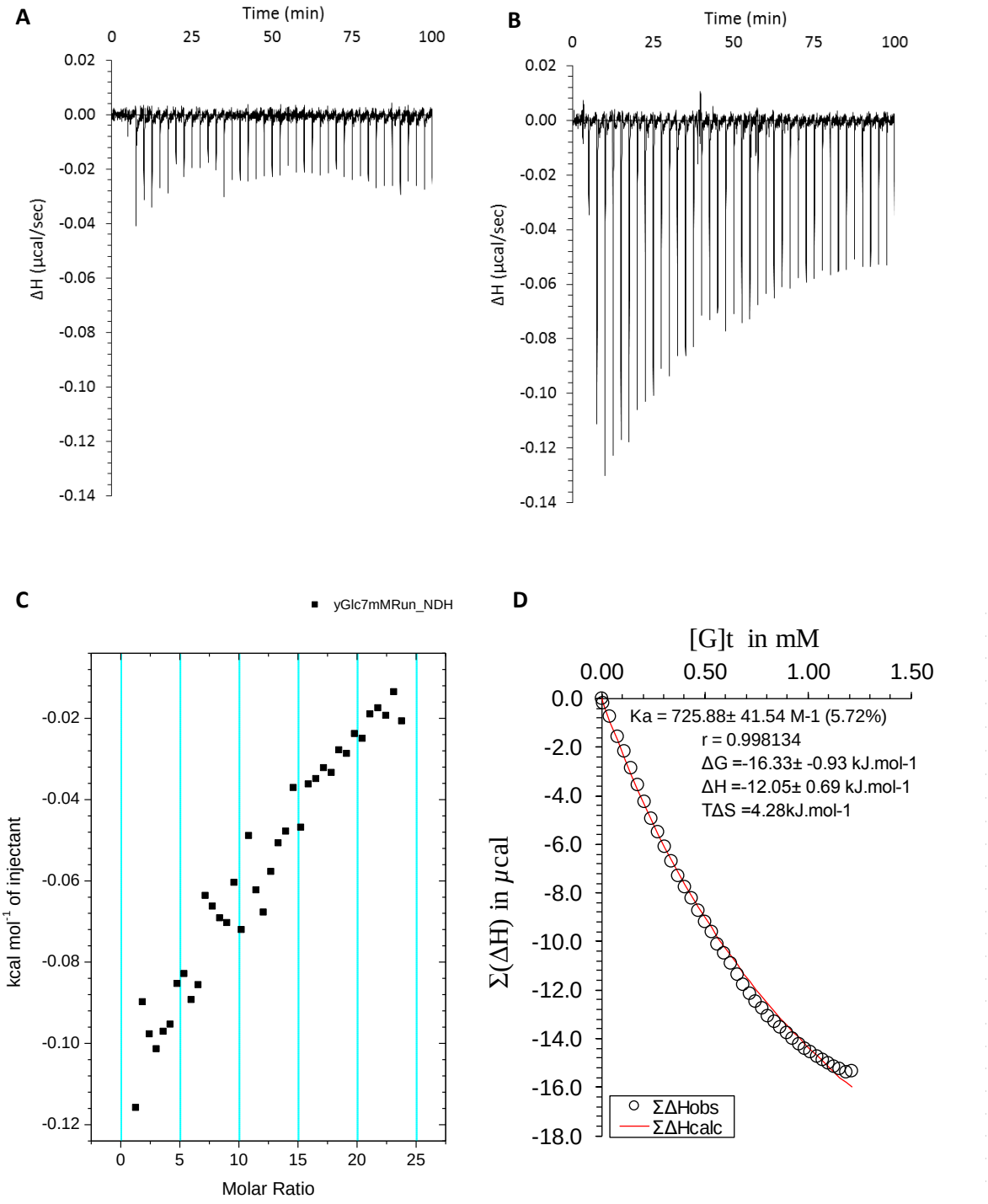

Supplementary Figure 46 | ITC binding results for receptor **2** (0.06 mM) titrated with 2-deoxy-D-glucose **14** (7 mM) in 10 mM phosphate buffer solution (pH 7.4), in which: A) shows the blank run (addition of sugar into water); B) shows the titration (sugar into receptor **2**); C) shows the plotted change in enthalpy vs molar ratio; and D) shows the fit calculated using an Excel spreadsheet (K_a = 725 ± 41 M^{-1}). The experiment was performed once.

D-Galactose 15

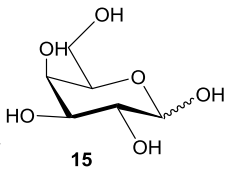

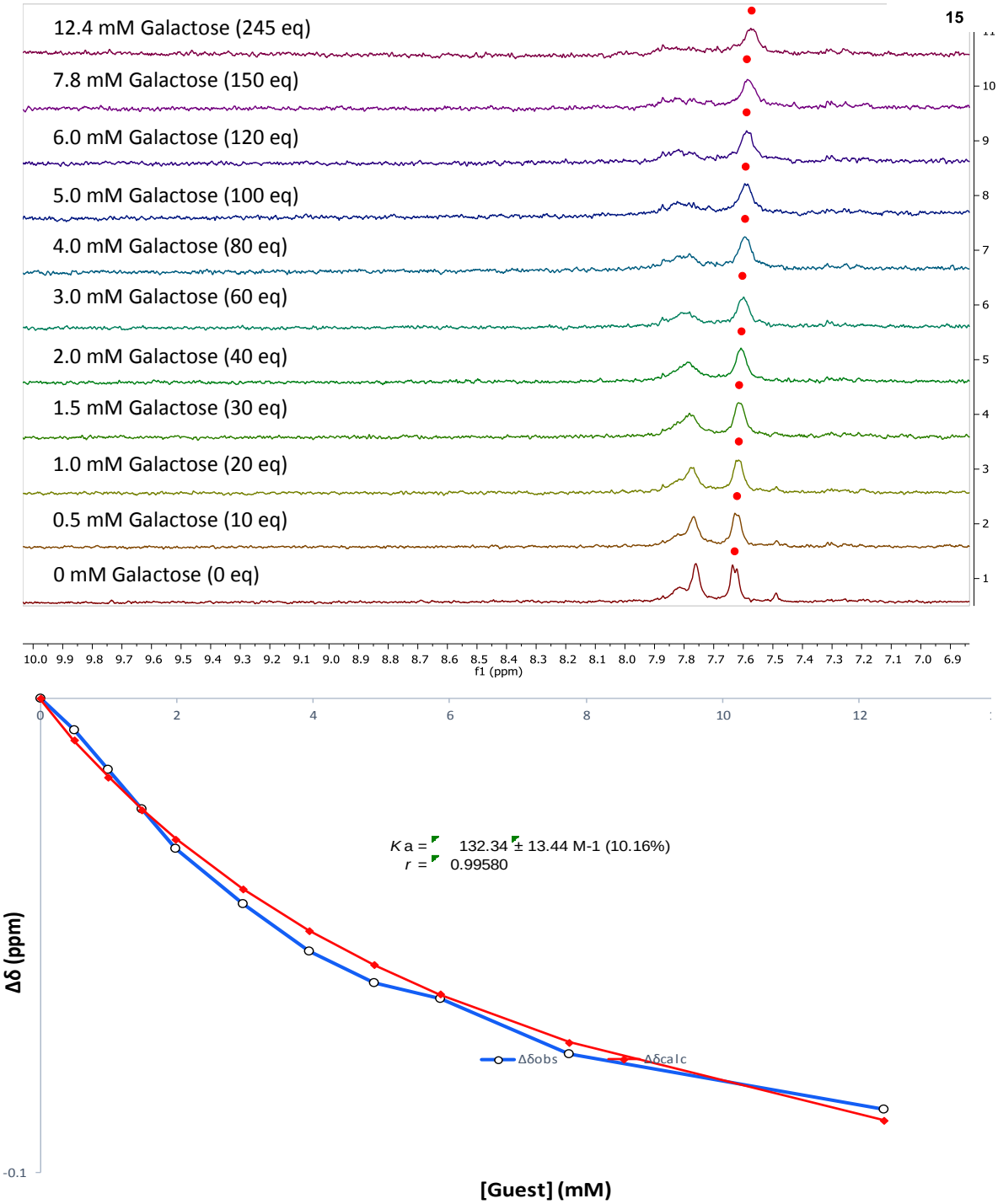

Supplementary Figure 47 | Partial ^{1}H NMR spectra (top) and binding analysis curve (bottom) for receptor **2** (0.05 mM) titrated with a combined solution of D-galactose **15** (250 mM) and receptor **2** (0.05 mM), in D_2O with 10 mM phosphate buffer (pH 7.4) at 298 K. Spectra imply binding with fast/intermediate exchange on NMR timescale. Changes in chemical shift (Δδ ppm) of peak at 7.63 ppm (denoted with •) were plotted against increasing guest concentration (mM). The calculated values for the Δδ are overlaid with the observed values giving K_a = 132 ± 13 M^{-1} (10.2%). Limiting Δδ = -0.053. The experiment was performed once.

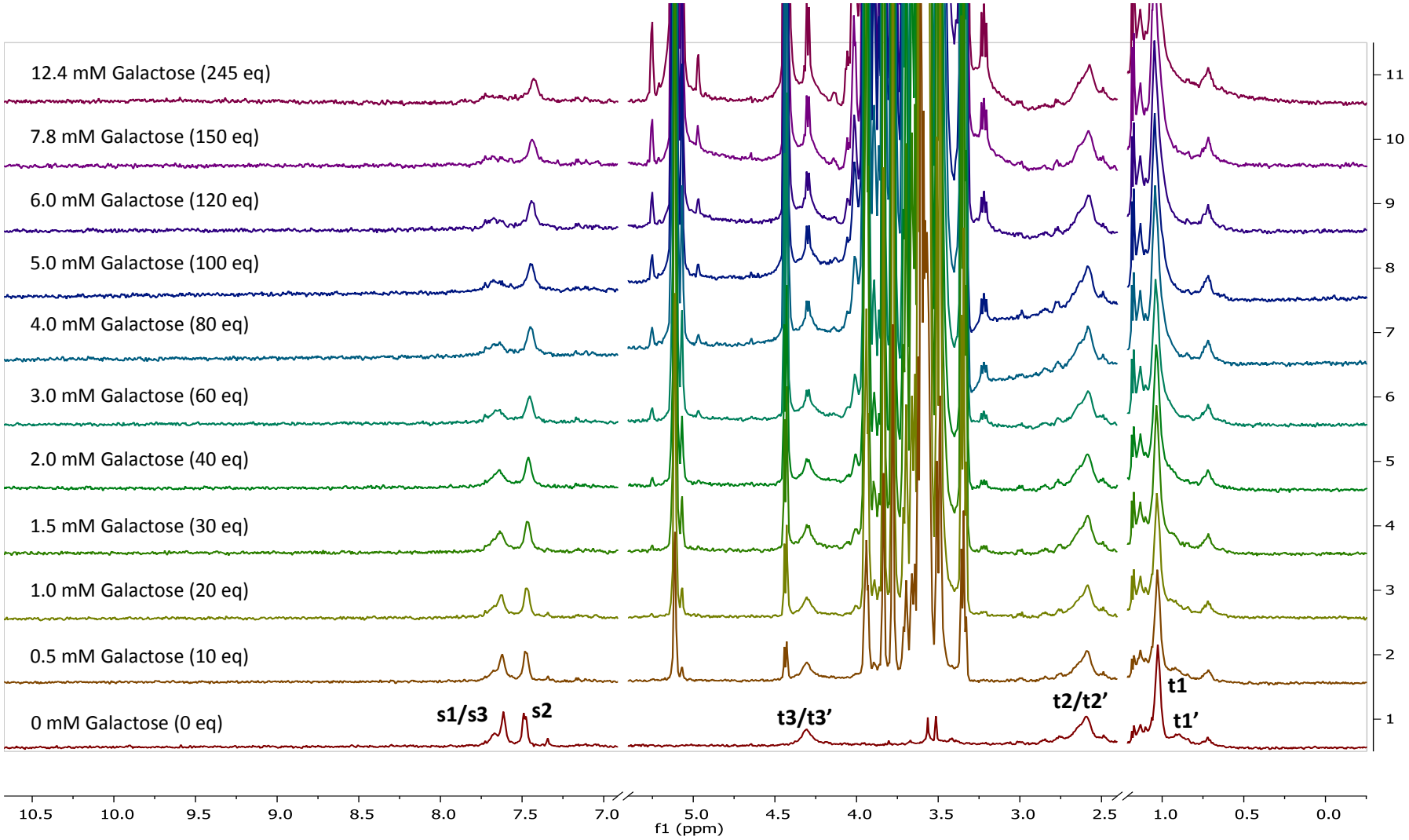

Supplementary Figure 48 | ^{1}H NMR spectra for receptor **2** (0.05 mM) titrated with a combined solution of D-galactose **15** (250 mM) and receptor **2** (0.05 mM), in D_2O with 10 mM phosphate buffer (pH 7.4) at 298 K

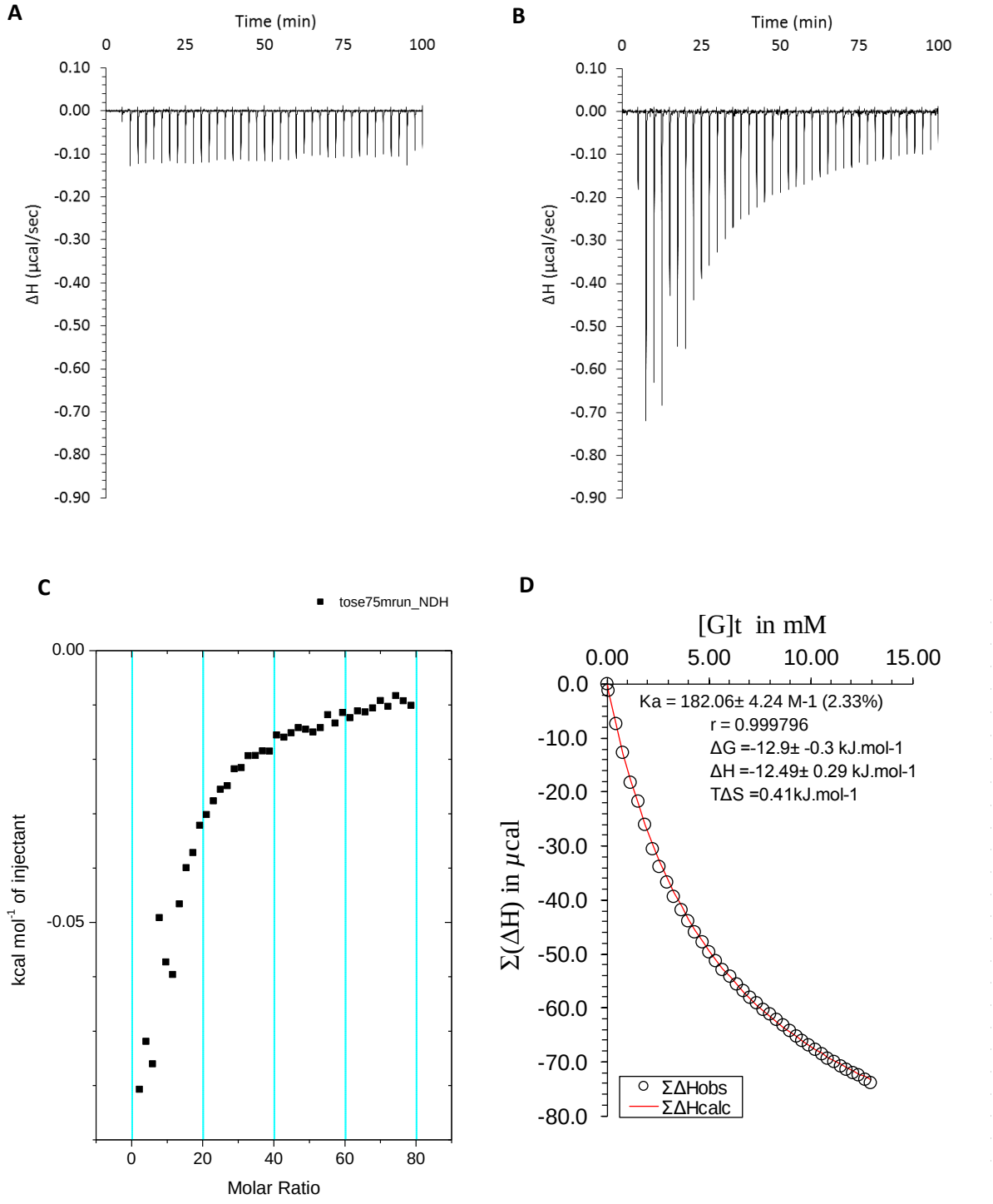

Supplementary Figure 49 | ITC binding results for receptor **2** (0.2 mM) titrated with D-galactose **15** (75 mM) in 10 mM phosphate buffer solution (pH 7.4) in which: A) shows the blank run (addition of substrate into medium); B) shows the titration (substrate into receptor **2**); C) shows the plotted change in enthalpy vs molar ratio; and D) shows the fit calculated using an Excel spreadsheet (K_a = 182 ± 4.2 M^{-1}). The experiment was performed 2 times with similar results.

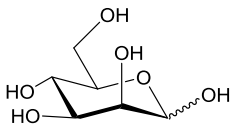

16

D-Mannose 16

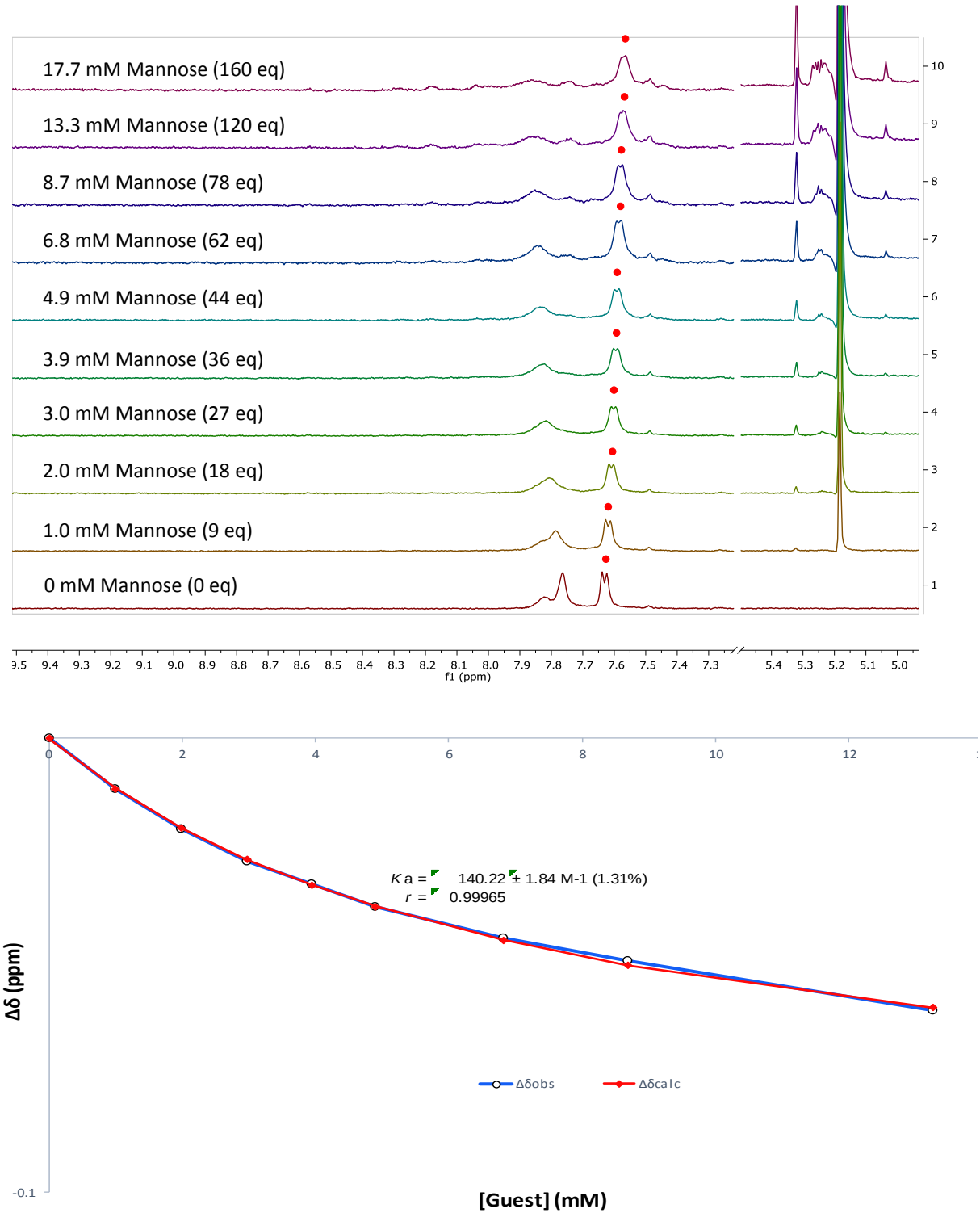

Supplementary Figure 50 | Partial ^{1}H NMR spectra (top) and binding analysis curve (bottom) for receptor **2** (0.11 mM) titrated with a combined solution of D-mannose **16** (250 mM) and receptor **2** (0.11 mM), in D_2O with 10 mM phosphate buffer (pH 7.4) at 298 K. Spectra imply binding with fast/intermediate exchange on NMR timescale. Changes in chemical shift (Δδ ppm) of peak at 7.63 ppm (denoted with •) were plotted against increasing guest concentration (mM). The calculated values for the Δδ are overlaid with the observed values giving K_a = 140 ± 2 M^{-1} (1.31%). Limiting Δδ = -0.060. The experiment was performed once.

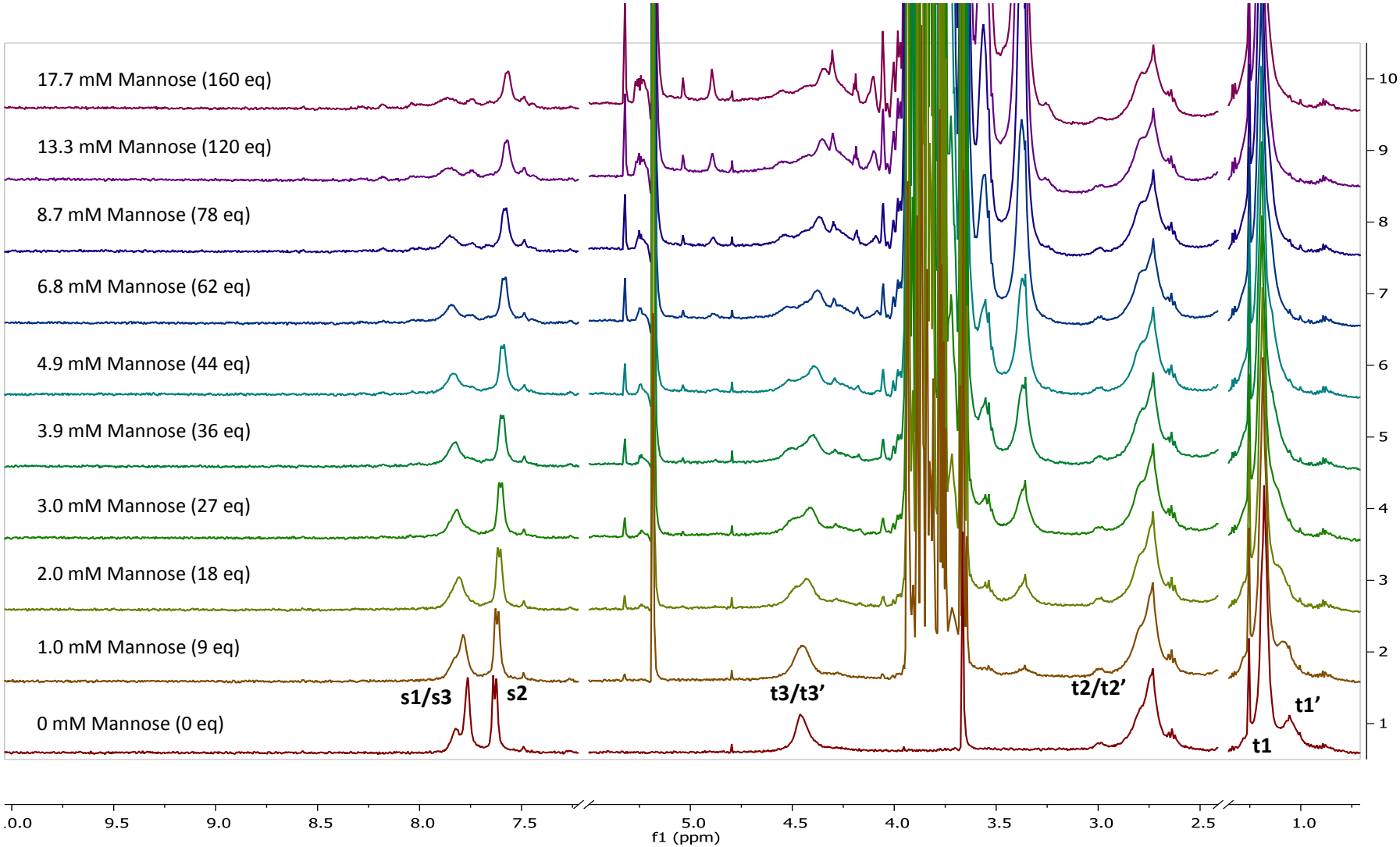

Supplementary Figure 51 | ^{1}H NMR spectra for receptor **2** (0.11 mM) titrated with a combined solution of D-mannose **16** (250 mM) and receptor **2** (0.11 mM), in D_2O with 10 mM phosphate buffer (pH 7.4) at 298 K

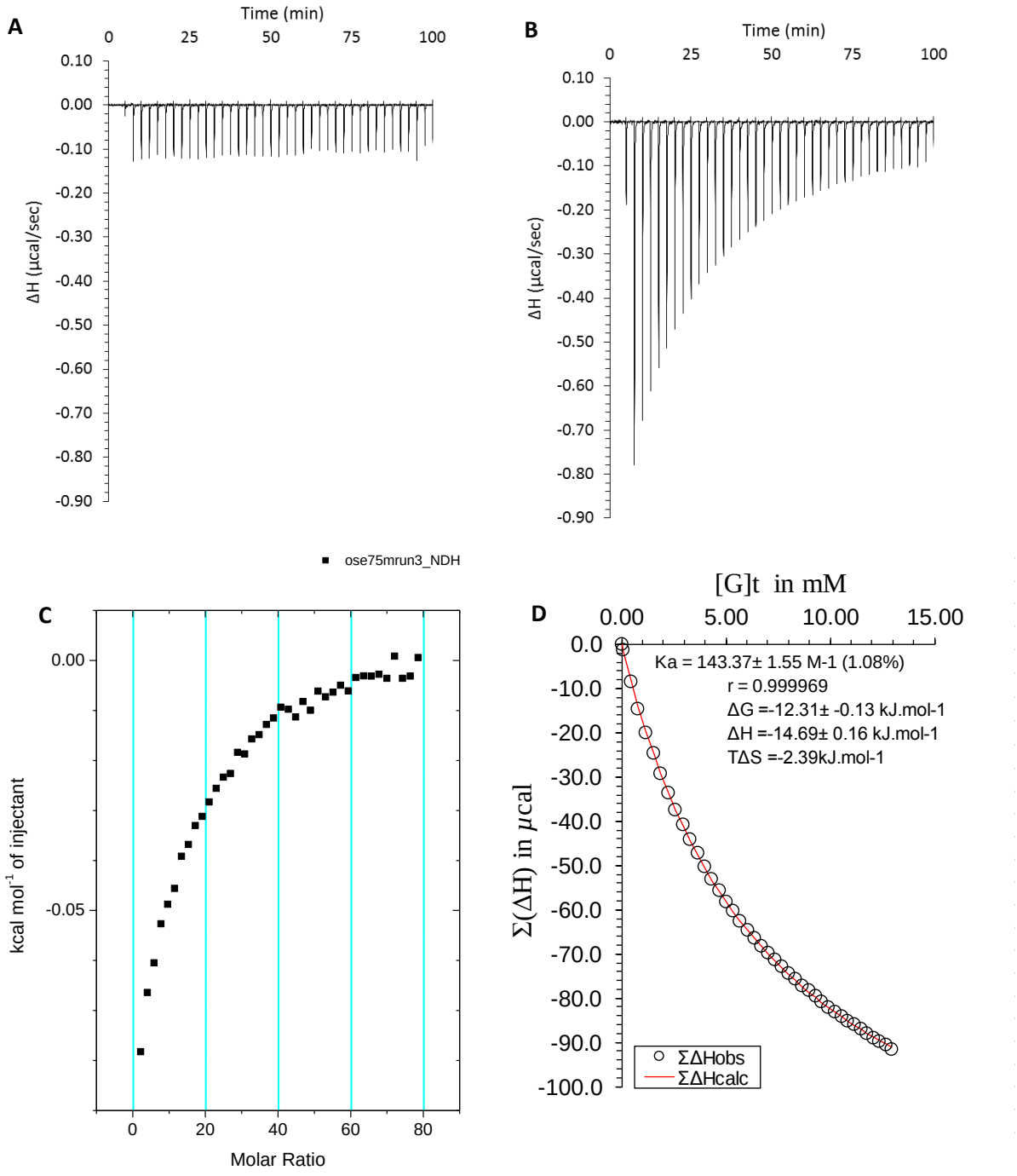

Supplementary Figure 52 | ITC binding results for receptor **2** (0.2 mM) titrated with D-mannose **16** (75 mM) in 10 mM phosphate buffer solution (pH 7.4) in which: A) shows the blank run (addition of substrate into medium); B) shows the titration (substrate into receptor **2**); C) shows the plotted change in enthalpy vs molar ratio; and D) shows the fit calculated using an Excel spreadsheet (K_a = 143 ± 1.5 M^{-1}). The experiment was performed 2 times with similar results.

D-Ribose 17

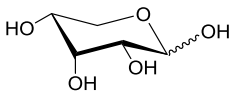

17

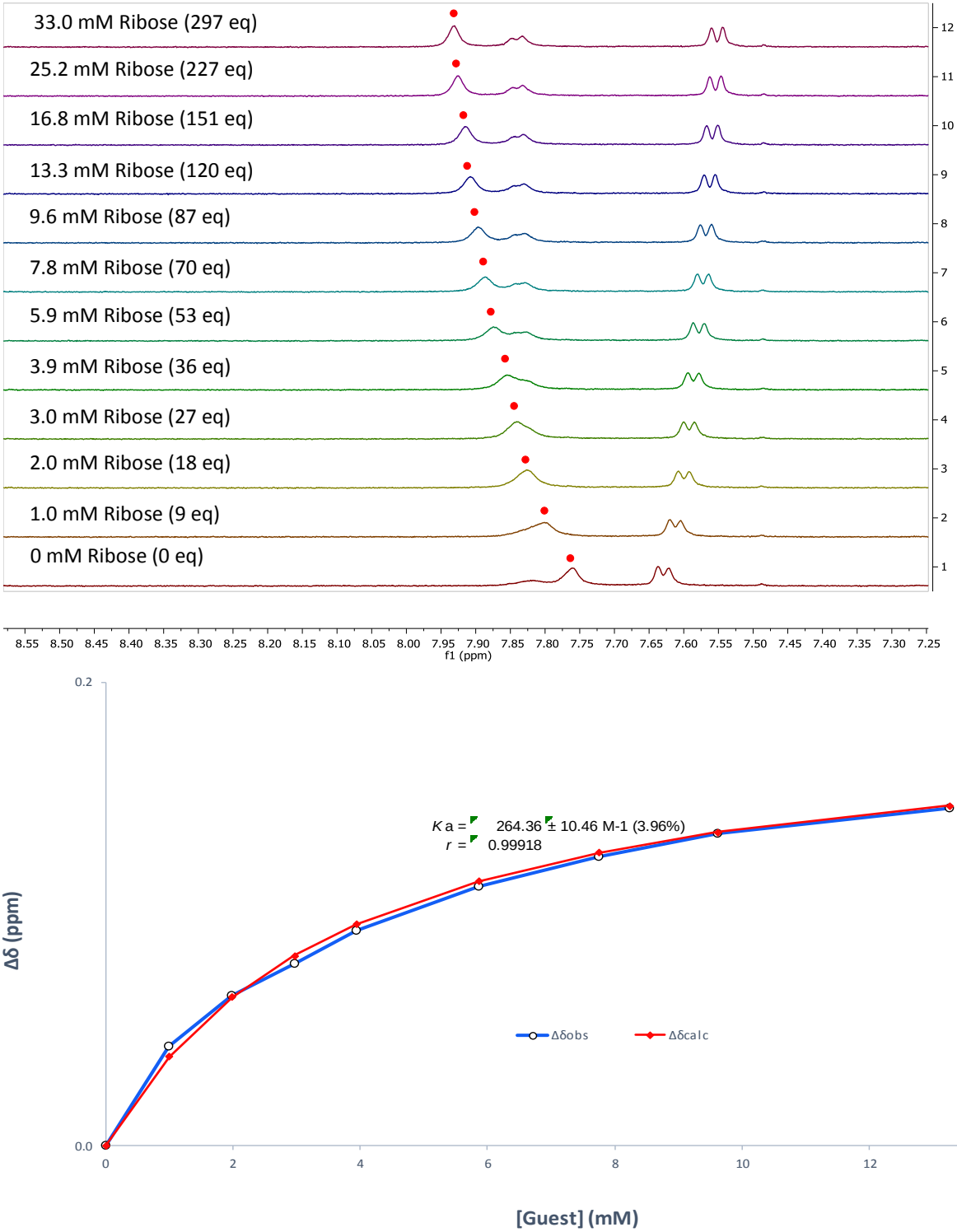

Supplementary Figure 53 | Partial ^{1}H NMR spectra (top) and binding analysis curve (bottom) for receptor **2** (0.11 mM) titrated with a combined solution of D-ribose **17** (250 mM) and receptor **2** (0.11 mM), in D_2O with 10 mM phosphate buffer (pH 7.4) at 298 K. Spectra imply binding with fast exchange on NMR timescale. Changes in chemical shift (Δδ ppm) of peak at 7.76 ppm (denoted with •) were plotted against increasing guest concentration (mM). The calculated values for the Δδ are overlaid with the observed values giving K_a = 264 ± 10 M^{-1} (3.96%). Limiting Δδ = -0.170. The experiment was performed once.

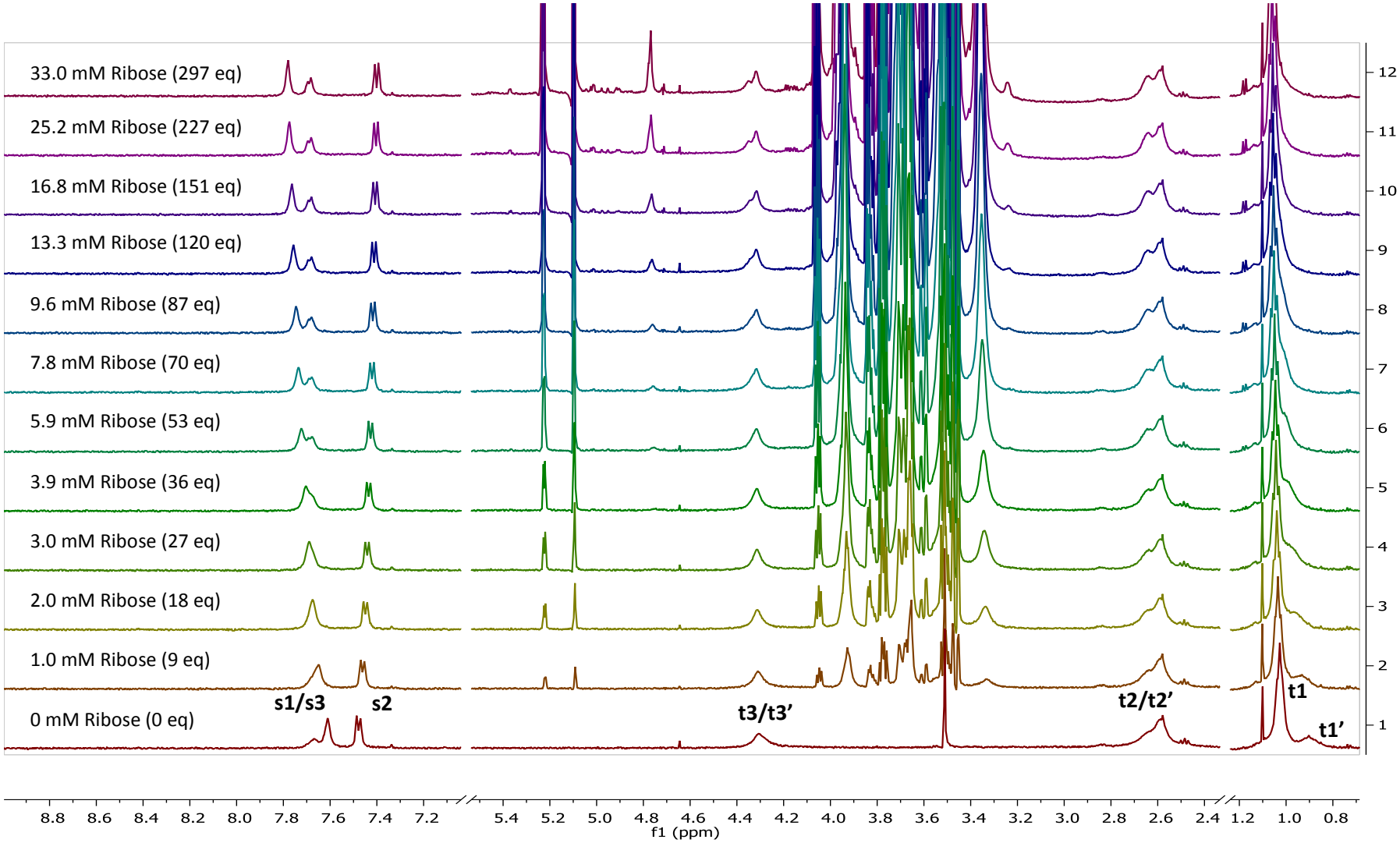

Supplementary Figure 54 | ^{1}H NMR spectra for receptor **2** (0.11 mM) titrated with a combined solution of D-ribose **17** (250 mM) and receptor **2** (0.11 mM), in D_2O with 10 mM phosphate buffer (pH 7.4) at 298 K

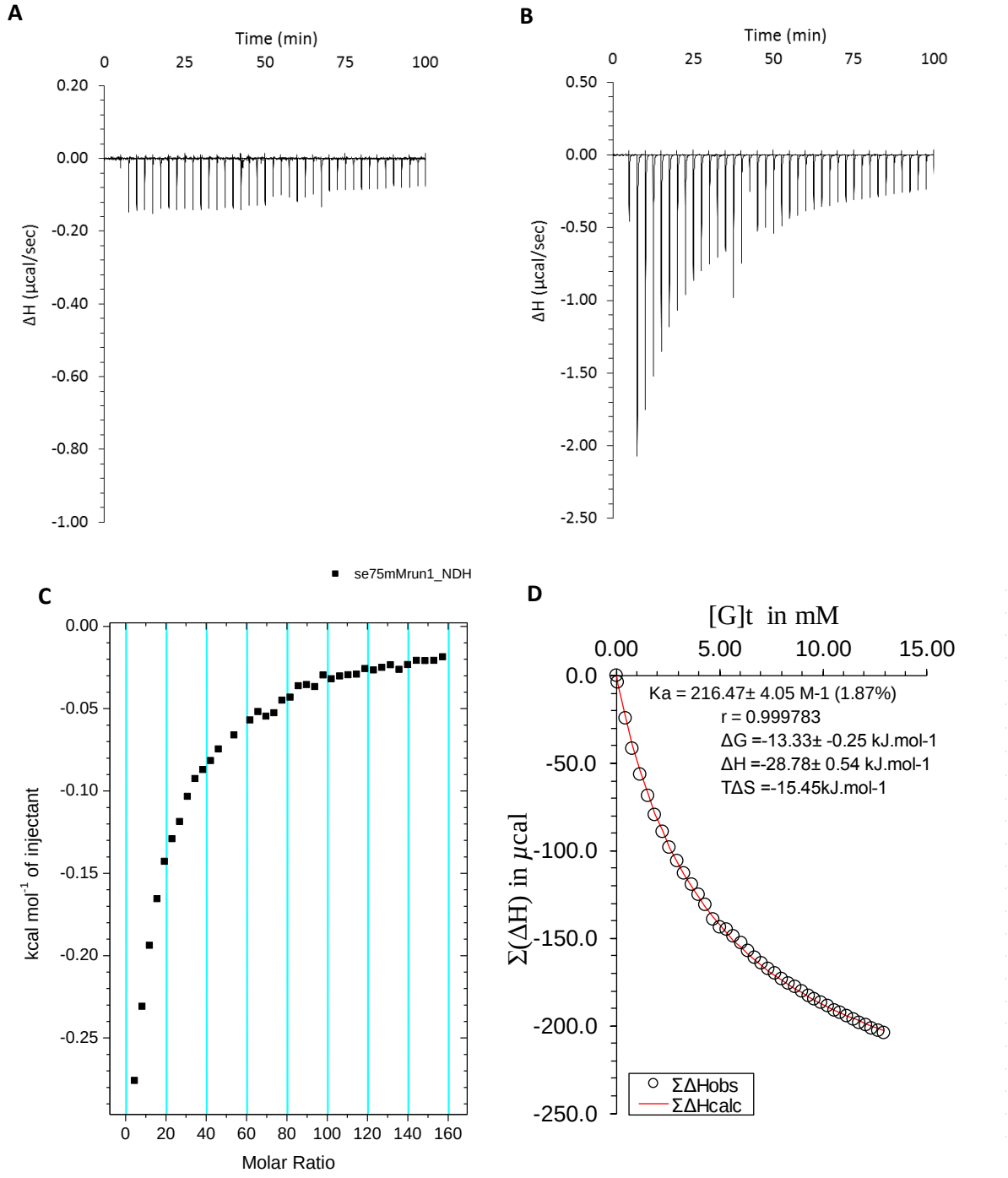

Supplementary Figure 55 | ITC binding results for receptor **2** (0.1 mM) titrated with D-ribose **17** (75 mM) in 10 mM phosphate buffer solution (pH 7.4) in which: A) shows the blank run (addition of substrate into medium); B) shows the titration (substrate into receptor **2**); C) shows the plotted change in enthalpy vs molar ratio; and D) shows the fit calculated using an Excel spreadsheet (K_a = 216.5 ± 4.1 M^{-1}). The experiment was performed once.

D-Fructose 18

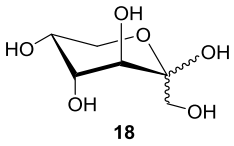

18

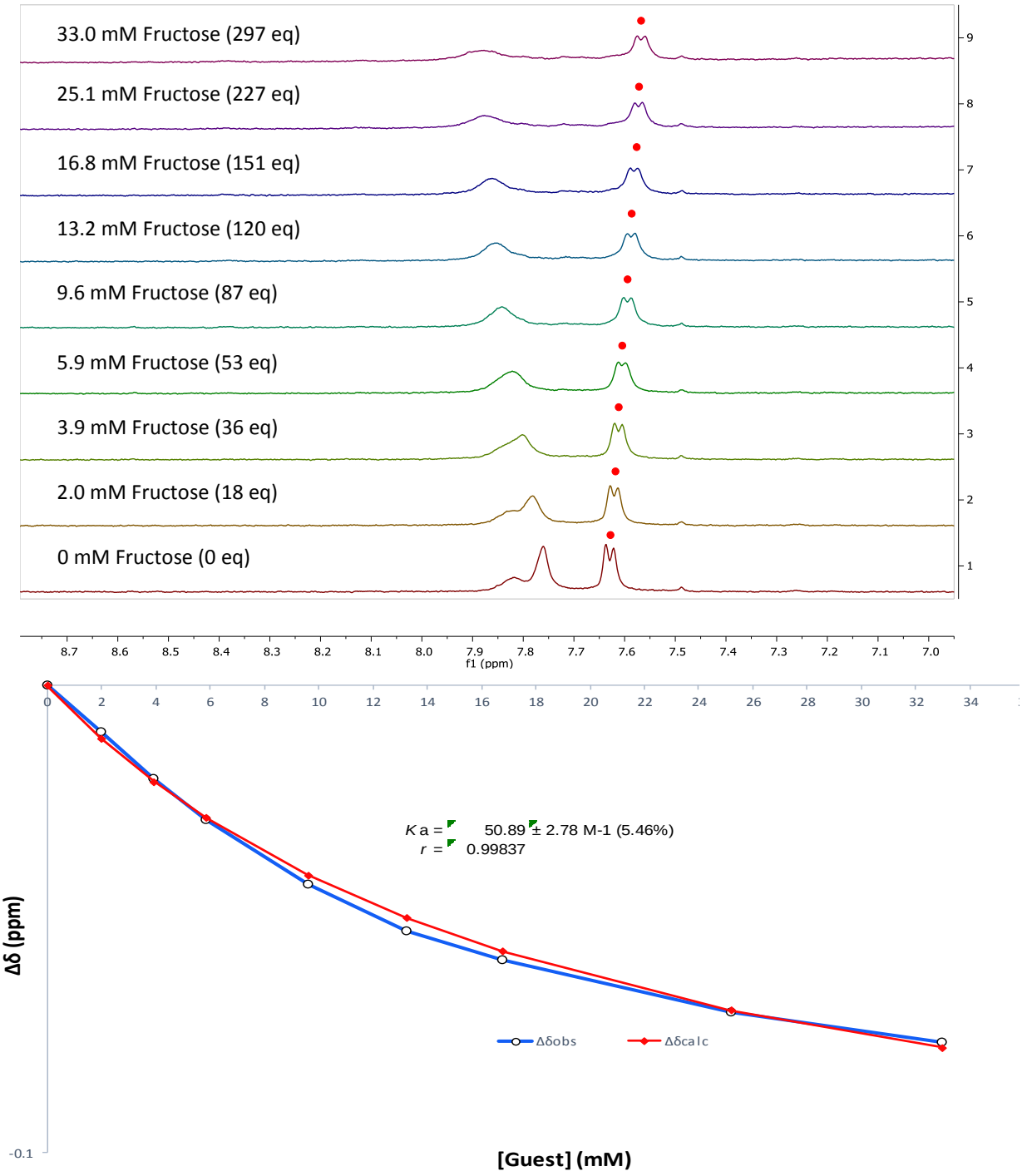

Supplementary Figure 56 | Partial ^{1}H NMR spectra (top) and binding analysis curve (bottom) for receptor **2** (0.11 mM) titrated with a combined solution of D-fructose **18** (250 mM) and receptor **2** (0.11 mM), in D_2O with 10 mM phosphate buffer (pH 7.4) at 298 K. Spectra imply binding with fast/intermediate exchange on NMR timescale. Changes in chemical shift (Δδ ppm) of peak at 7.63 ppm (denoted with •) were plotted against increasing guest concentration (mM). The calculated values for the Δδ are overlaid with the observed values giving K_a = 51 ± 3 M^{-1} (5.46%). Limiting Δδ = -0.061. The experiment was performed once.

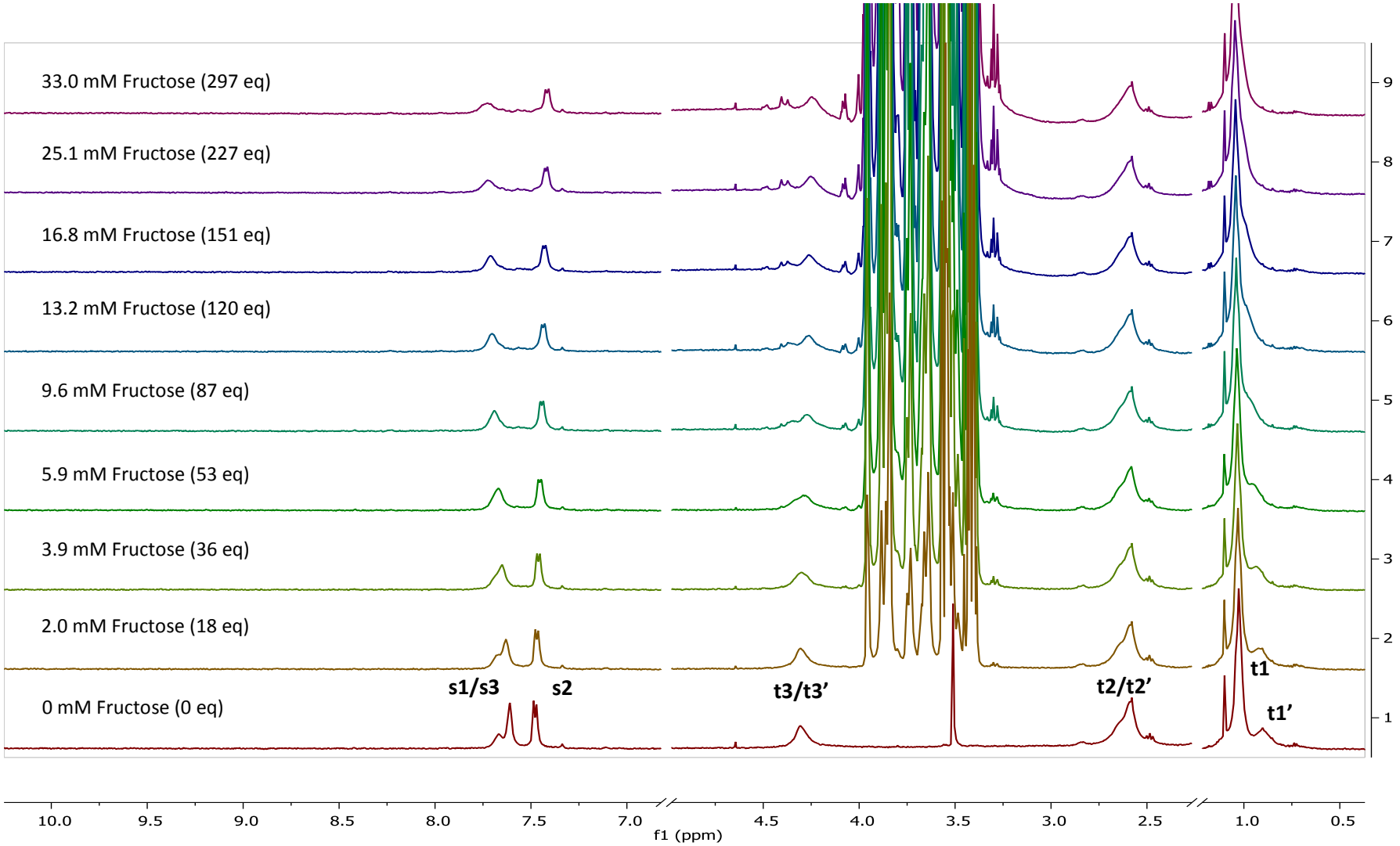

Supplementary Figure 57 | ^{1}H NMR spectra for receptor **2** (0.11 mM) titrated with a combined solution of D-fructose **18** (250 mM) and receptor **2** (0.11 mM), in D_2O with 10 mM phosphate buffer (pH 7.4) at 298 K

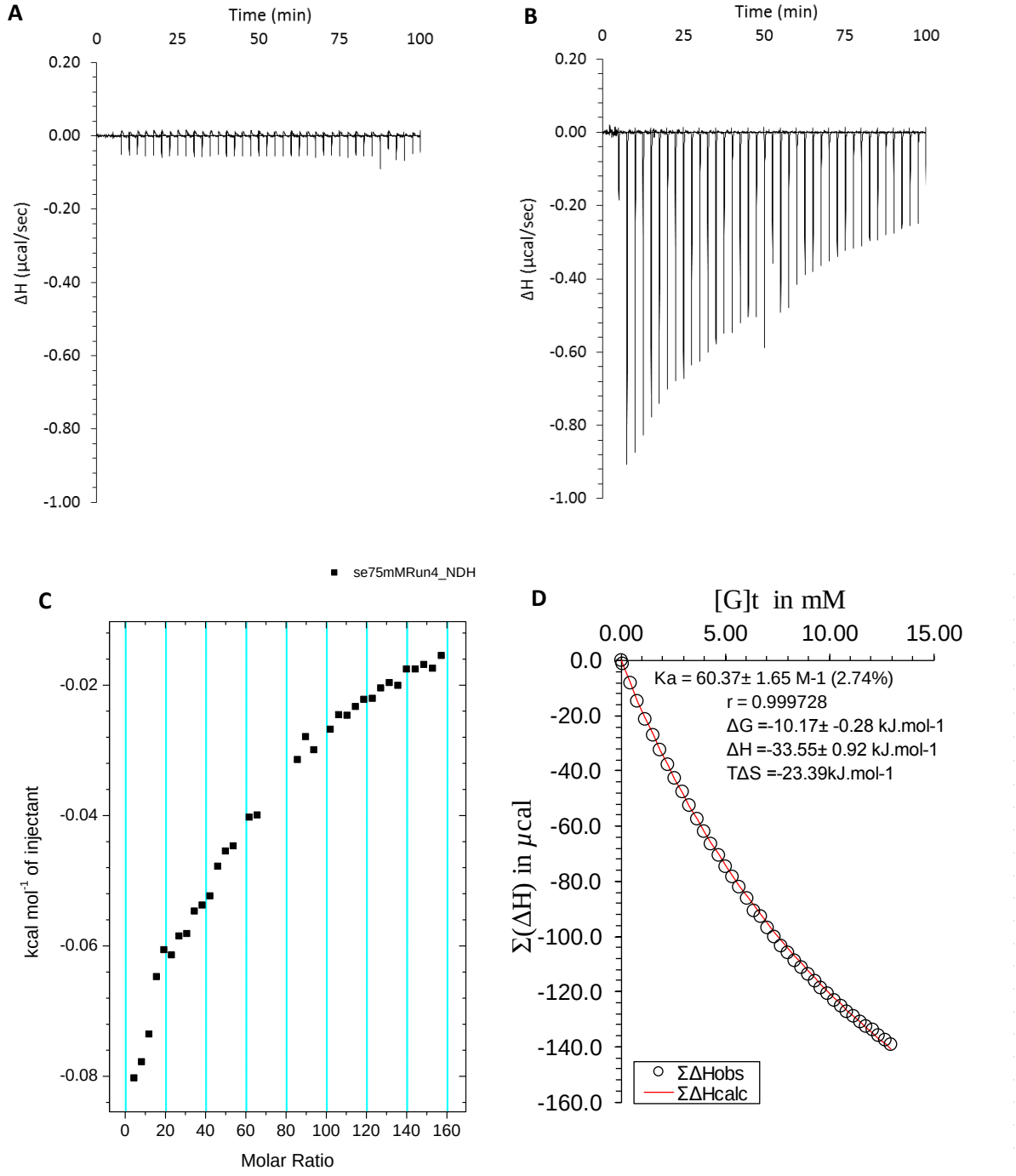

Supplementary Figure 58 | ITC binding results for receptor **2** (0.1 mM) titrated with D-fructose **18** (75 mM) in 10 mM phosphate buffer solution (pH 7.4) in which: A) shows the blank run (addition of substrate into medium); B) shows the titration (substrate into receptor **2**); C) shows the plotted change in enthalpy vs molar ratio; and D) shows the fit calculated using an Excel spreadsheet (K_a = 60.3 ± 1.6 M^{-1}). The experiment was performed 2 times with similar results.

D-Cellobiose 19

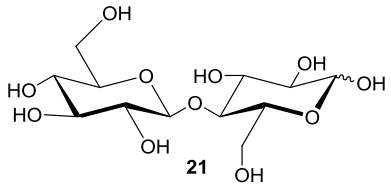

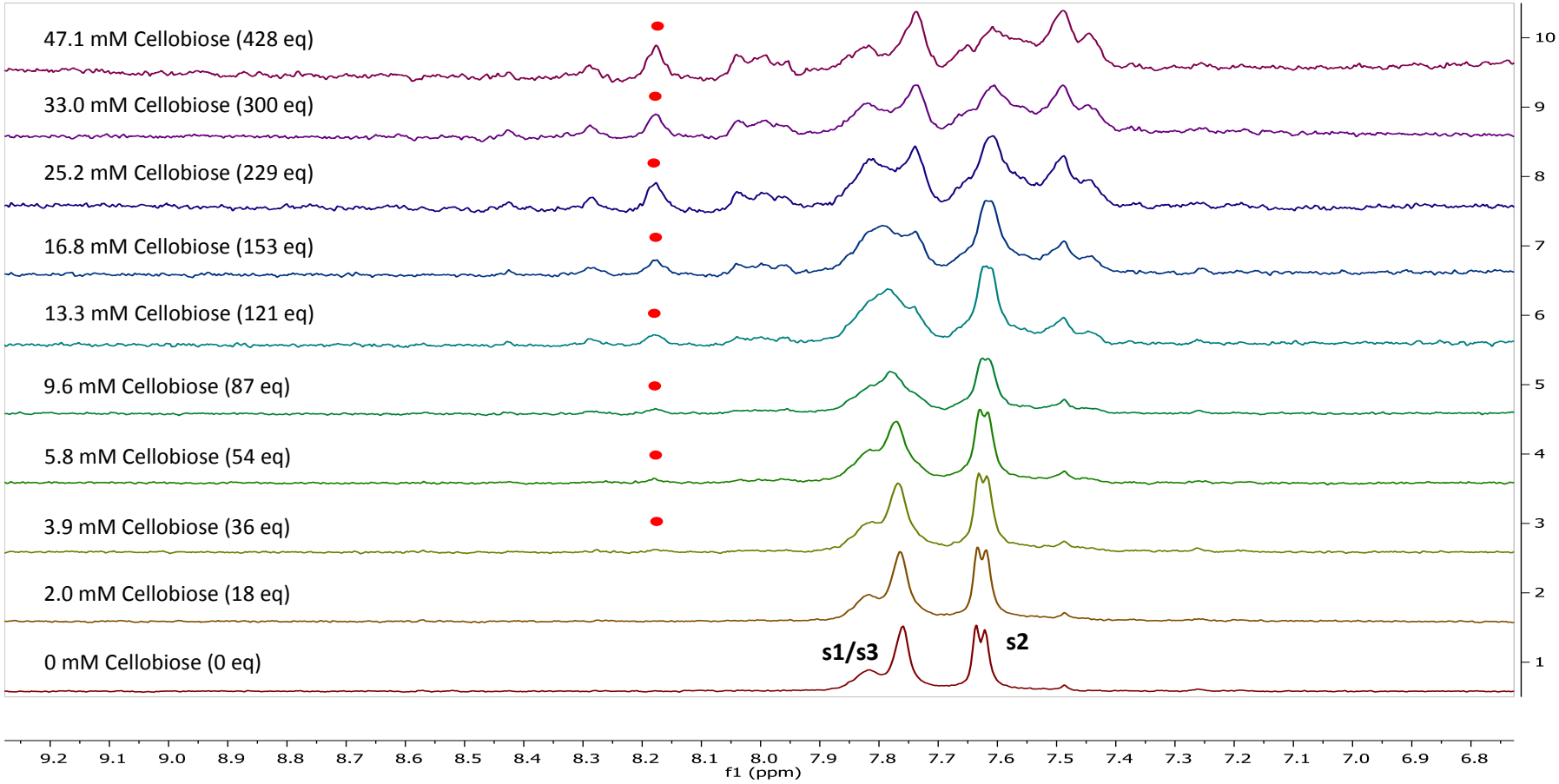

Supplementary Figure 59 | Partial ^{1}H NMR spectra for receptor **2** (0.11 mM) titrated with a combined solution of D-cellobiose **19** (250 mM) and receptor **2** (0.11 mM), in D_2O with 10 mM phosphate buffer (pH 7.4) at 298 K. Spectra imply binding with slow exchange on NMR timescale. Integrations of peak at 8.18 ppm (denoted with •) versus region 8.36-7.36 ppm were used to calculate the K_a (M^{-1}) at each point of addition (see Supplementary Table 7), an average of these calculated values gives K_a = 31 ± 2.66 (9%). The experiment was performed once.

Supplementary Table 8 | Calculated values for K_a when titrating cellobiose (250 mM) against receptor **2** (0.11 mM) in D_2O with 10 mM phosphate buffer (pH 7.4) at 298 K.

	Calculated K_a / M^{-1}
	29.0
	31.2
	29.4
	34.9
Average K_a / M^{-1}	31.1
Std Dev (Error)	2.66 (9%)

The integrals of the peak at δ 8.18 ppm (denoted with •, see Supplementary Supplementary Figure **59**) were measured relative to the region δ 8.36-7.36. These values were then compared to that at the end of the titration, when all receptor is assumed to be saturated with guest. Based on this assumption, K_a could be calculated from each point in the titration. An average K_a = 31.1 M^{-1} ± 2.66 (9%) was obtained in agreement with results obtained from ITC studies. Not all the spectra were used due to baseline distortions resulting from the large excess of guest present.

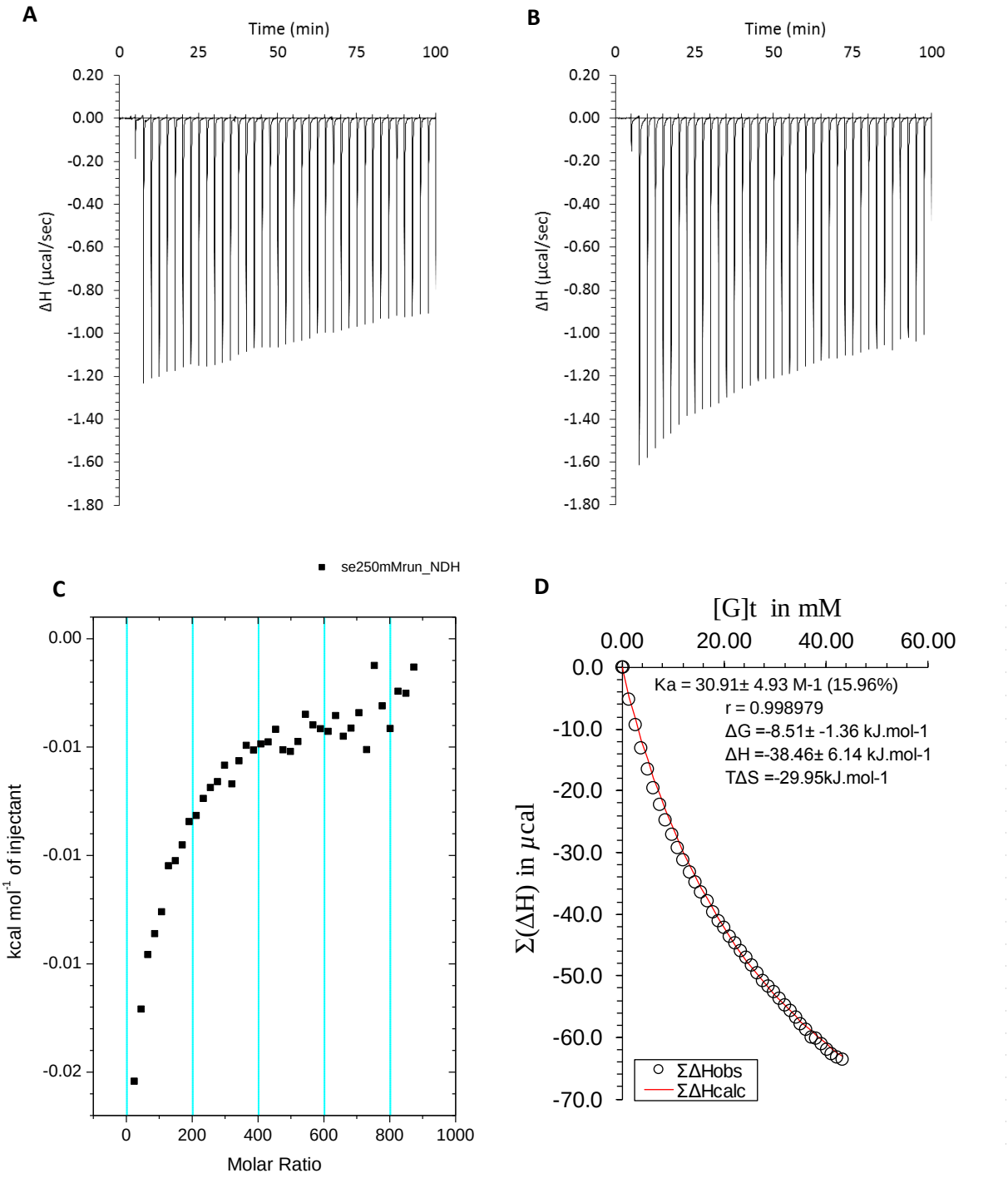

Supplementary Figure 60 | ITC binding results for receptor **2** (0.06 mM) titrated with D-cellobiose **19** (250 mM) in 10 mM phosphate buffer solution (pH 7.4) in which: A) shows the blank run (addition of substrate into medium); B) shows the titration (substrate into receptor **2**); C) shows the plotted change in enthalpy vs molar ratio; and D) shows the fit calculated using an Excel spreadsheet (K_a = 30.9 ± 4.9 M^{-1}). The experiment was performed once.

“Non-binding” substrates

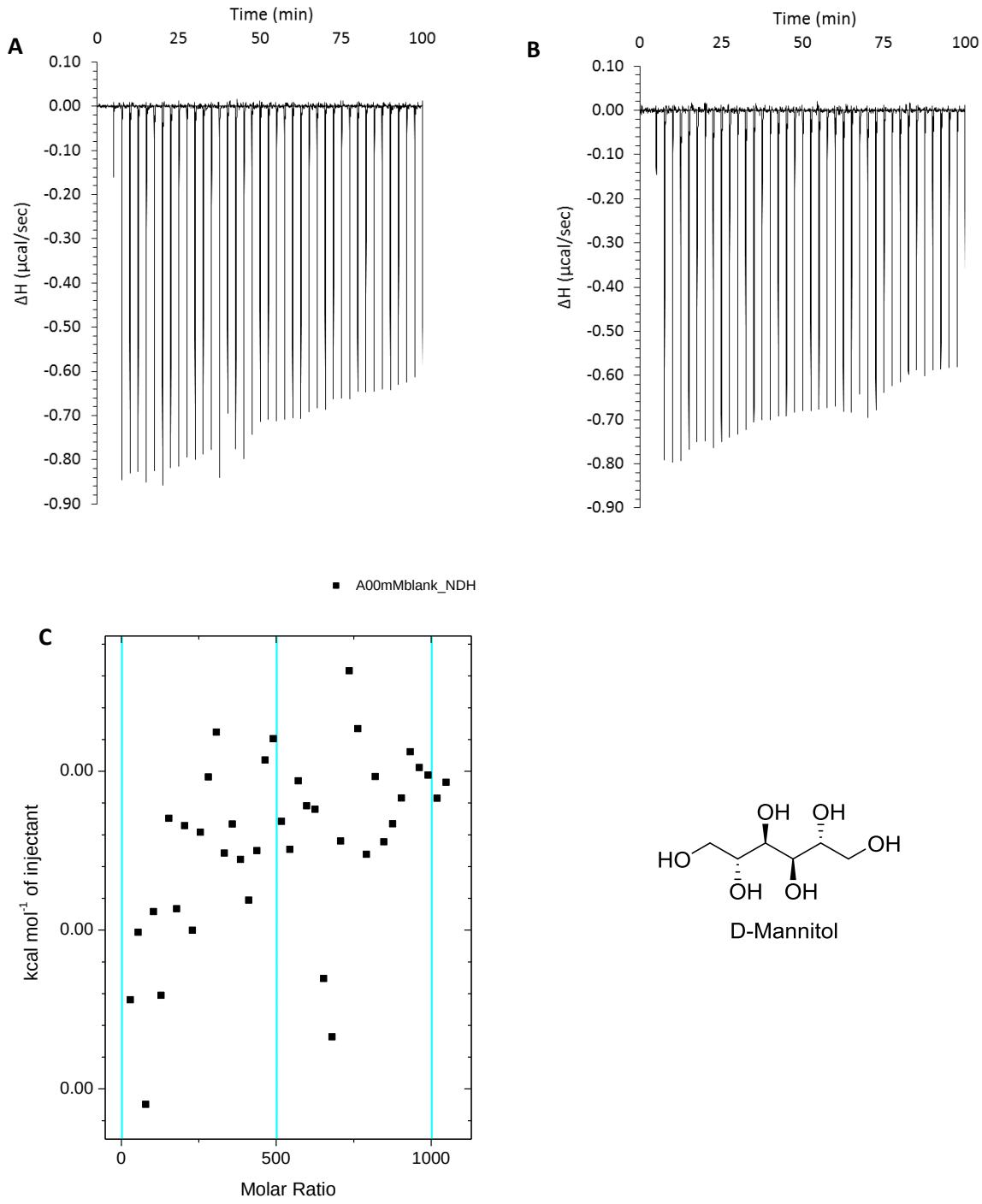

Supplementary Figure 61 | ITC binding results for receptor **2** (0.1 mM) titrated with D-mannitol (500 mM) in 10 mM phosphate buffer solution (pH 7.4) in which: A) shows the blank run (addition of substrate into medium); B) shows the titration (substrate into receptor **2**); C) shows the plotted change in enthalpy vs molar ratio. The experiment was performed 2 times with similar results.

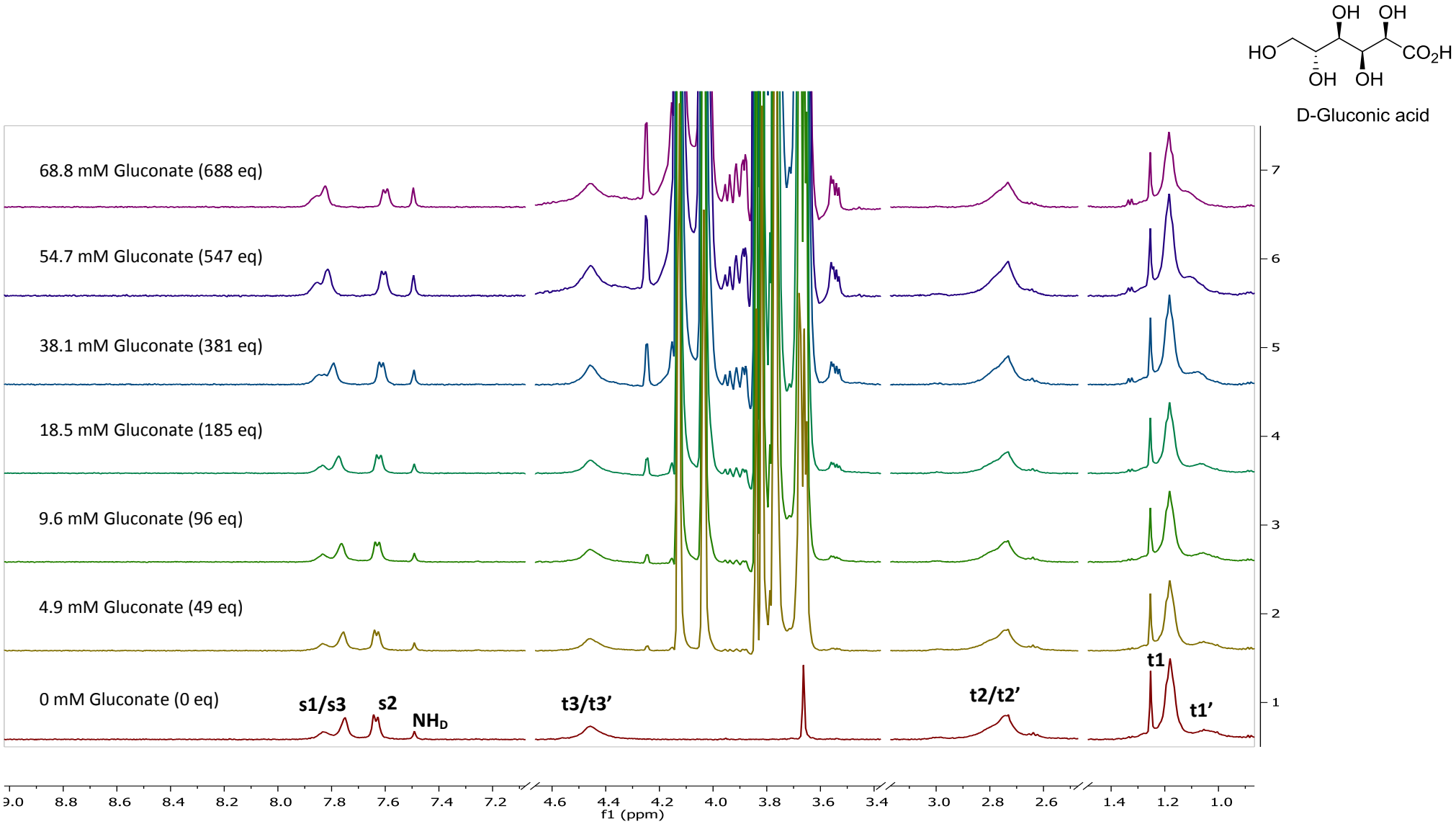

Supplementary Figure 62 | ^{1}H NMR spectra for receptor **2** (0.1 mM) titrated with a combined solution of D-gluconate (250 mM) and receptor **2** (0.1 mM), in D_2O with 10 mM phosphate buffer (pH 7.4) at 298 K. Spectra imply no significant binding, despite some movement and broadening of peaks at high concentrations of guest. The experiment was performed 2 times with similar results.

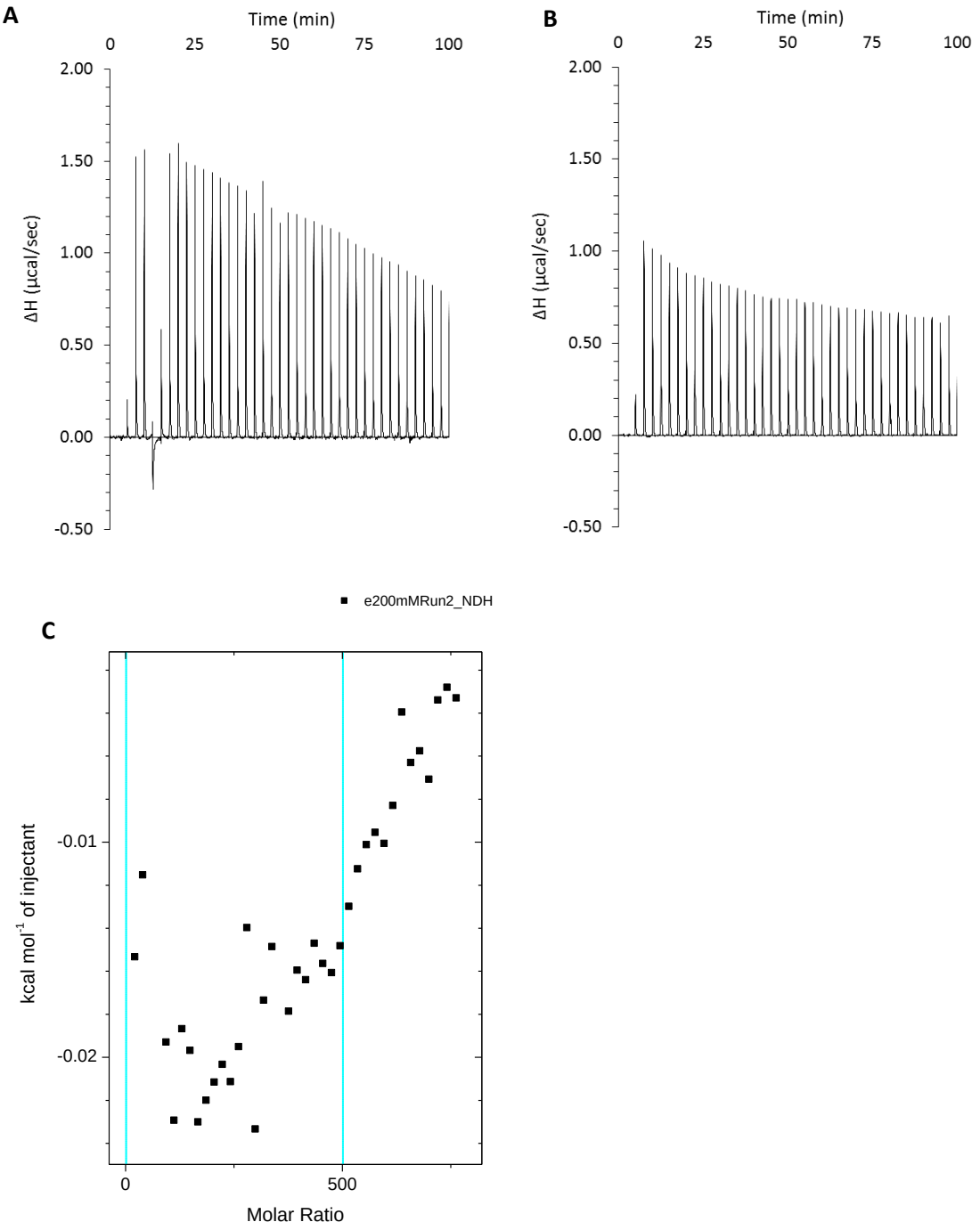

Supplementary Figure 63 | ITC binding results for receptor **2** (0.06 mM) titrated with D-gluconate (200 mM) in 10 mM phosphate buffer solution (pH 7.4), in which: A) shows the blank run (addition of substrate into water); B) shows the titration (substrate into receptor **2**); C) shows the plotted change in enthalpy vs molar ratio. The experiment was performed 3 times with similar results.

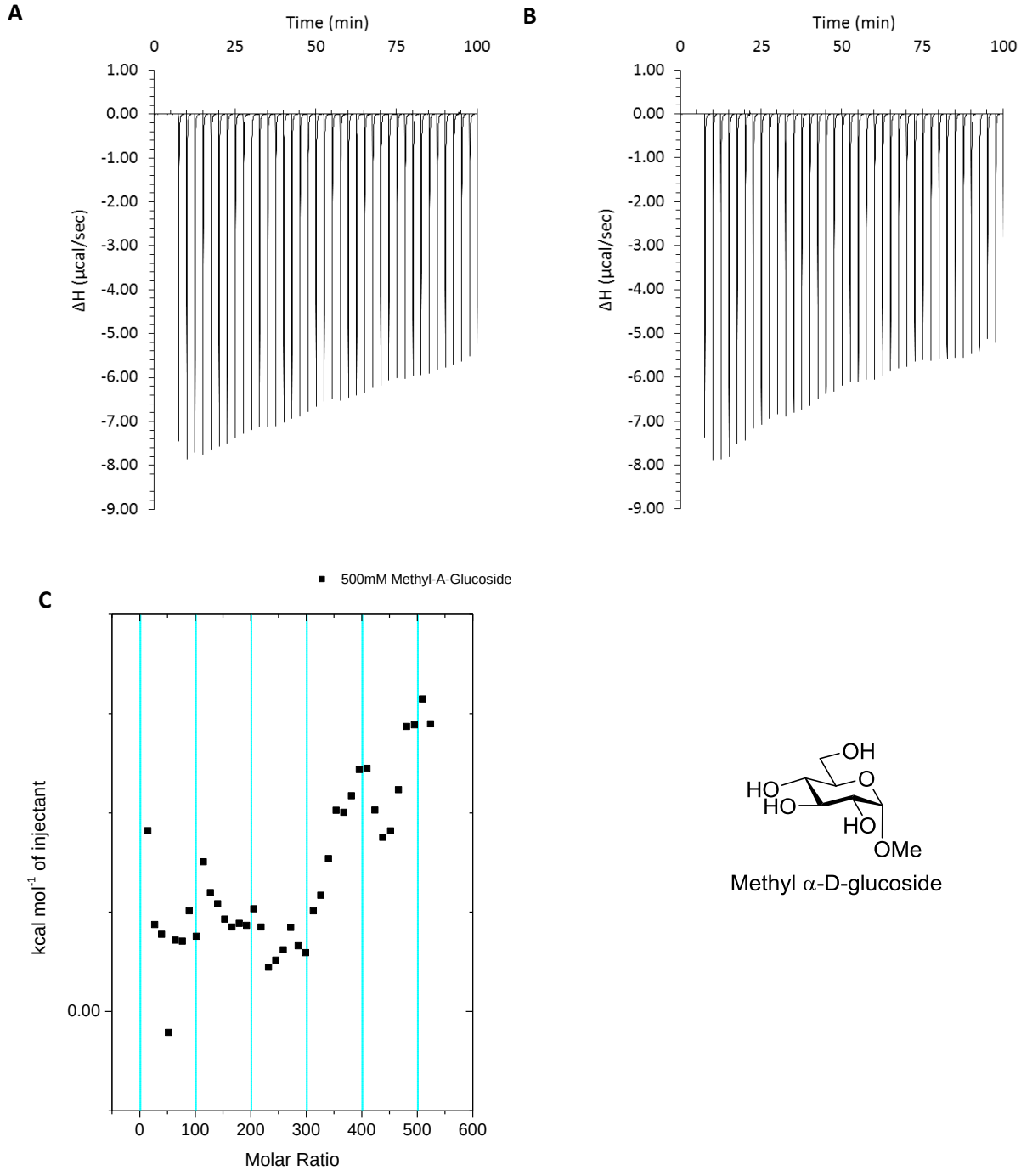

Supplementary Figure 64 | ITC binding results for receptor **2** (0.06 mM) titrated with methyl α-D-glucoside (500 mM) in 10 mM phosphate buffer solution (pH 7.4), in which: A) shows the blank run (addition of sugar into water); B) shows the titration (sugar into receptor **2**) and C) shows the plotted change in enthalpy vs molar ratio. The experiment was performed once.

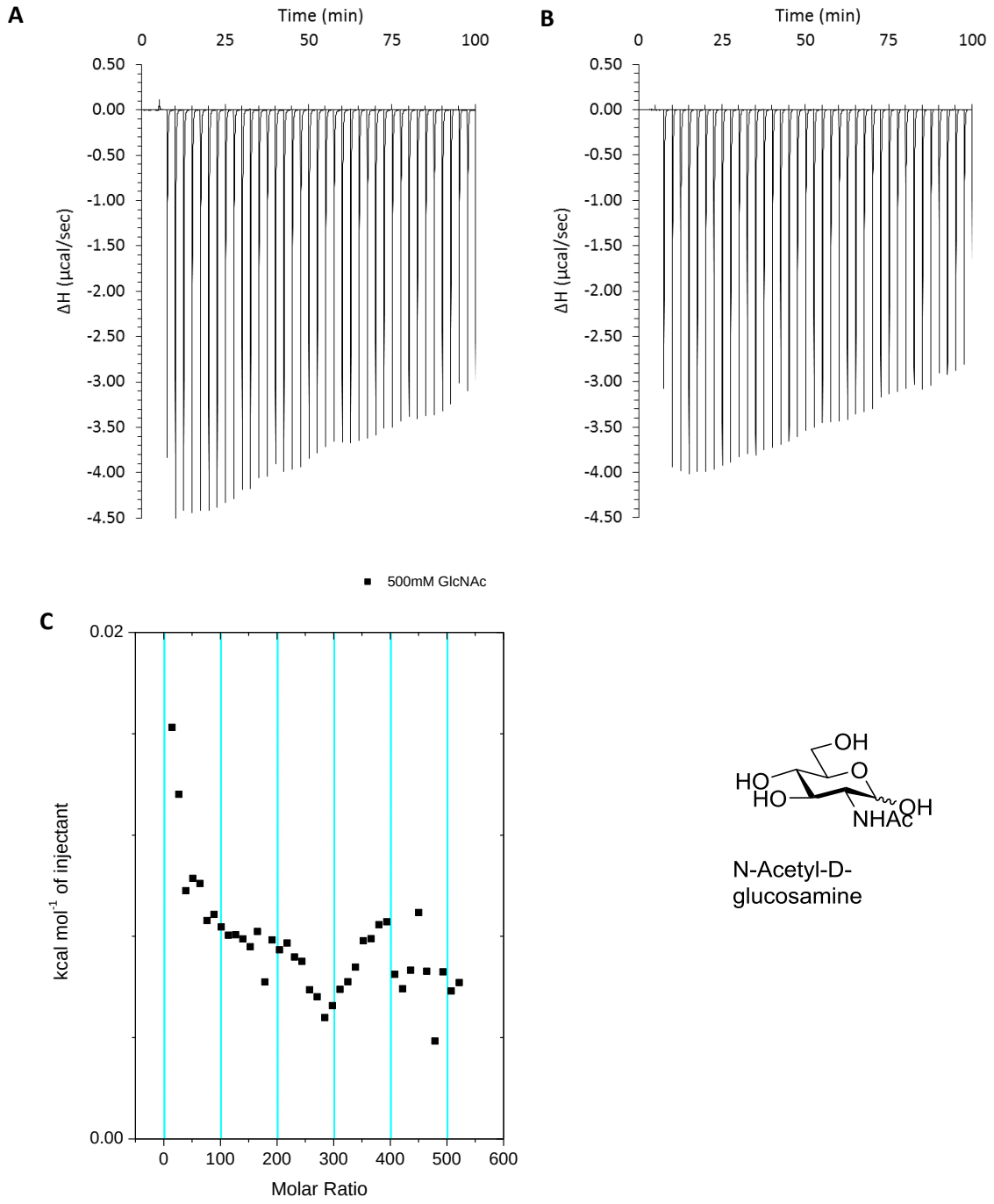

Supplementary Figure 65 | ITC binding results for receptor **2** (0.06 mM) titrated with *N*-acetyl-D-glucosamine (498 mM) in 10 mM phosphate buffer solution (pH 7.4), in which: A) shows the blank run (addition of sugar into water); B) shows the titration (sugar into receptor **2**) and C) shows the plotted change in enthalpy vs molar ratio. The experiment was performed 2 times with similar results.

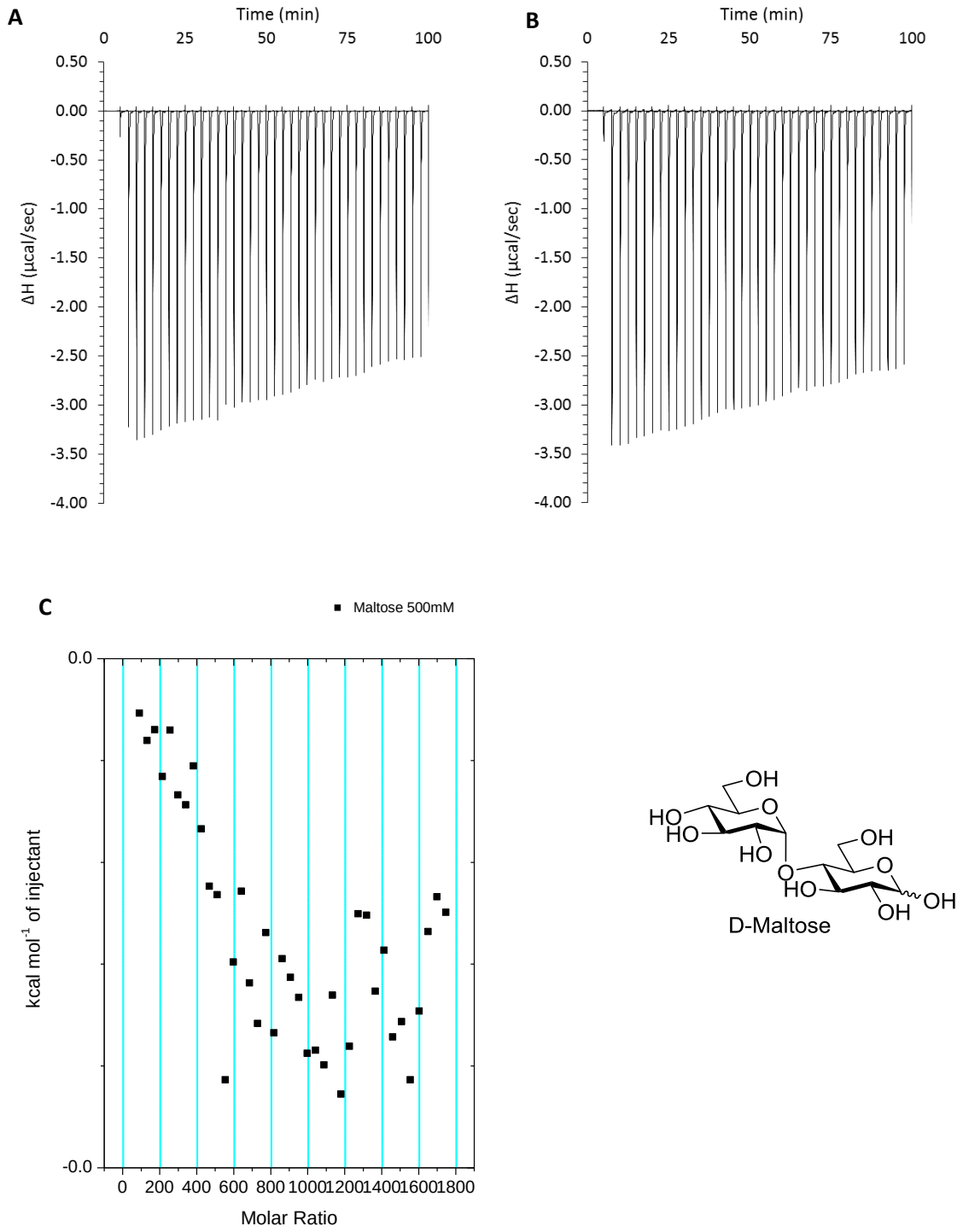

Supplementary Figure 66 | ITC binding results for receptor **2** (0.06 mM) titrated with maltose (500 mM) in 10 mM phosphate buffer solution (pH 7.4), in which: A) shows the blank run (addition of sugar into water); B) shows the titration (sugar into receptor **2**) and C) shows the plotted change in enthalpy vs molar ratio. The experiment was performed once.

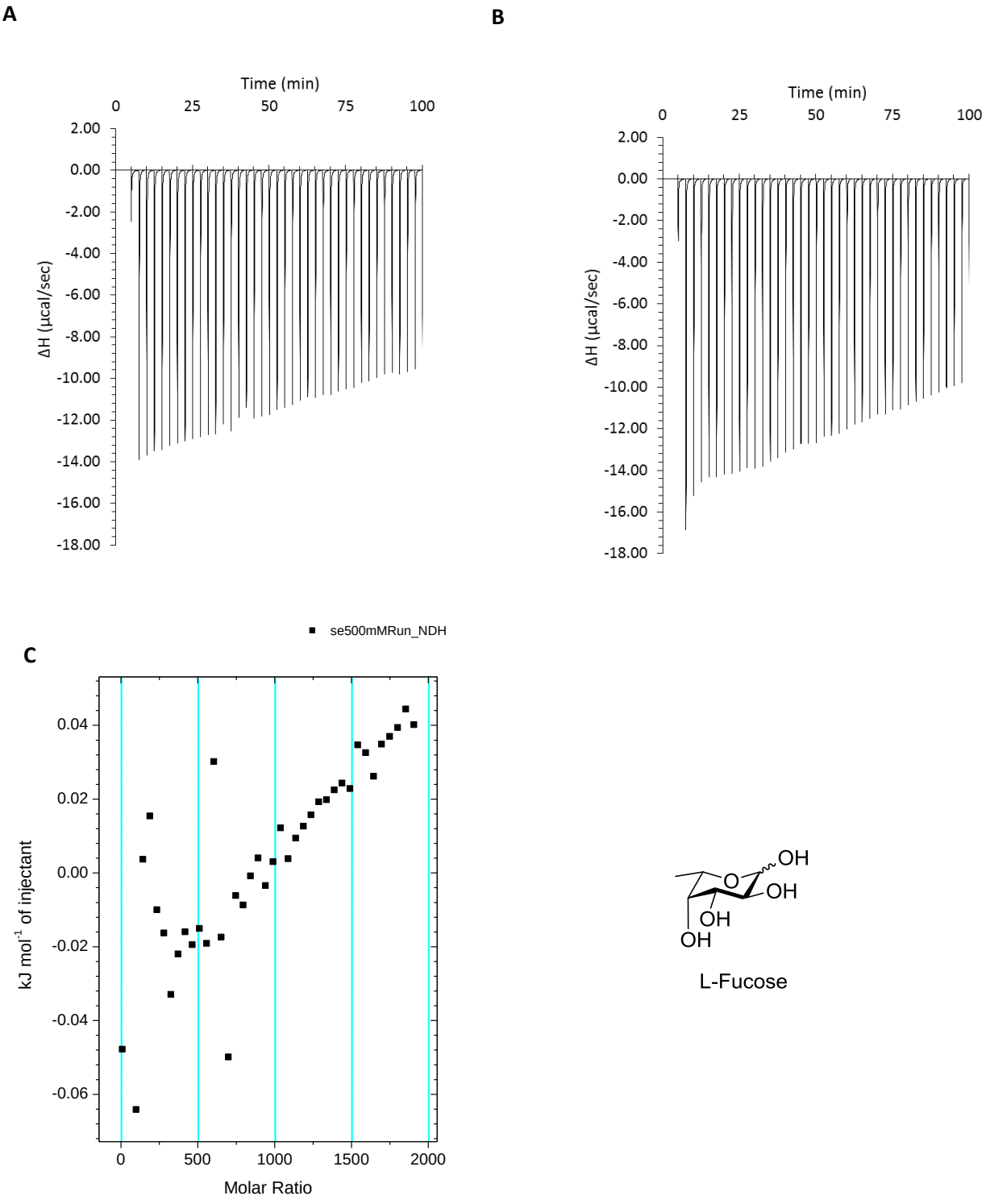

Supplementary Figure 67 | ITC binding results for receptor **2** (0.06 mM) titrated with L-fucose (500 mM) in 10 mM phosphate buffer solution (pH 7.4), in which: A) shows the blank run (addition of substrate into water); B) shows the titration (substrate into receptor **2**); C) shows the plotted change in enthalpy vs molar ratio. The experiment was performed once.

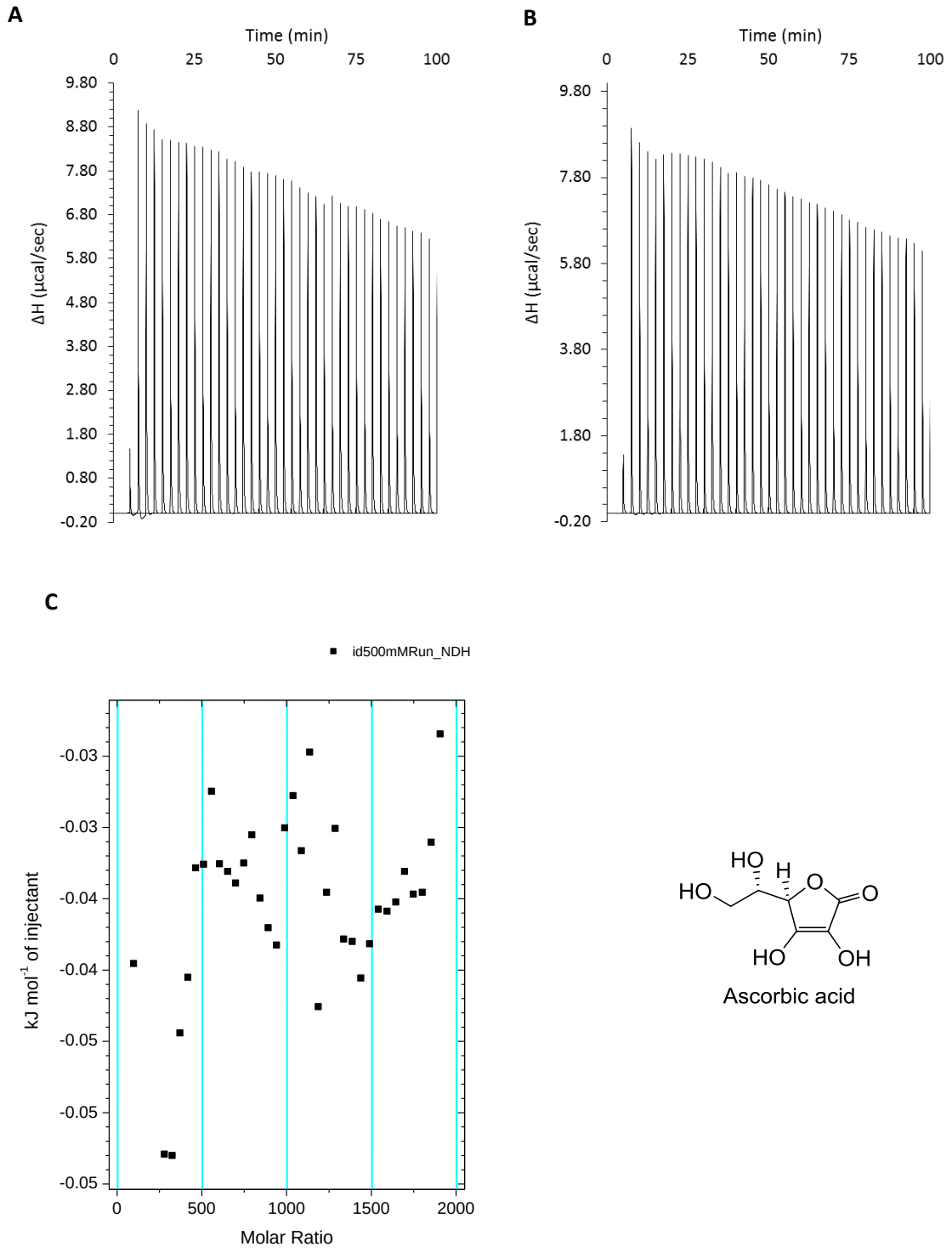

Supplementary Figure 68 | ITC binding results for receptor **2** (0.06 mM) titrated with ascorbic acid (500 mM) in 10 mM phosphate buffer solution (pH 7.4), in which: A) shows the blank run (addition of substrate into water); B) shows the titration (substrate into receptor **2**); C) shows the plotted change in enthalpy vs molar ratio. The experiment was performed once.

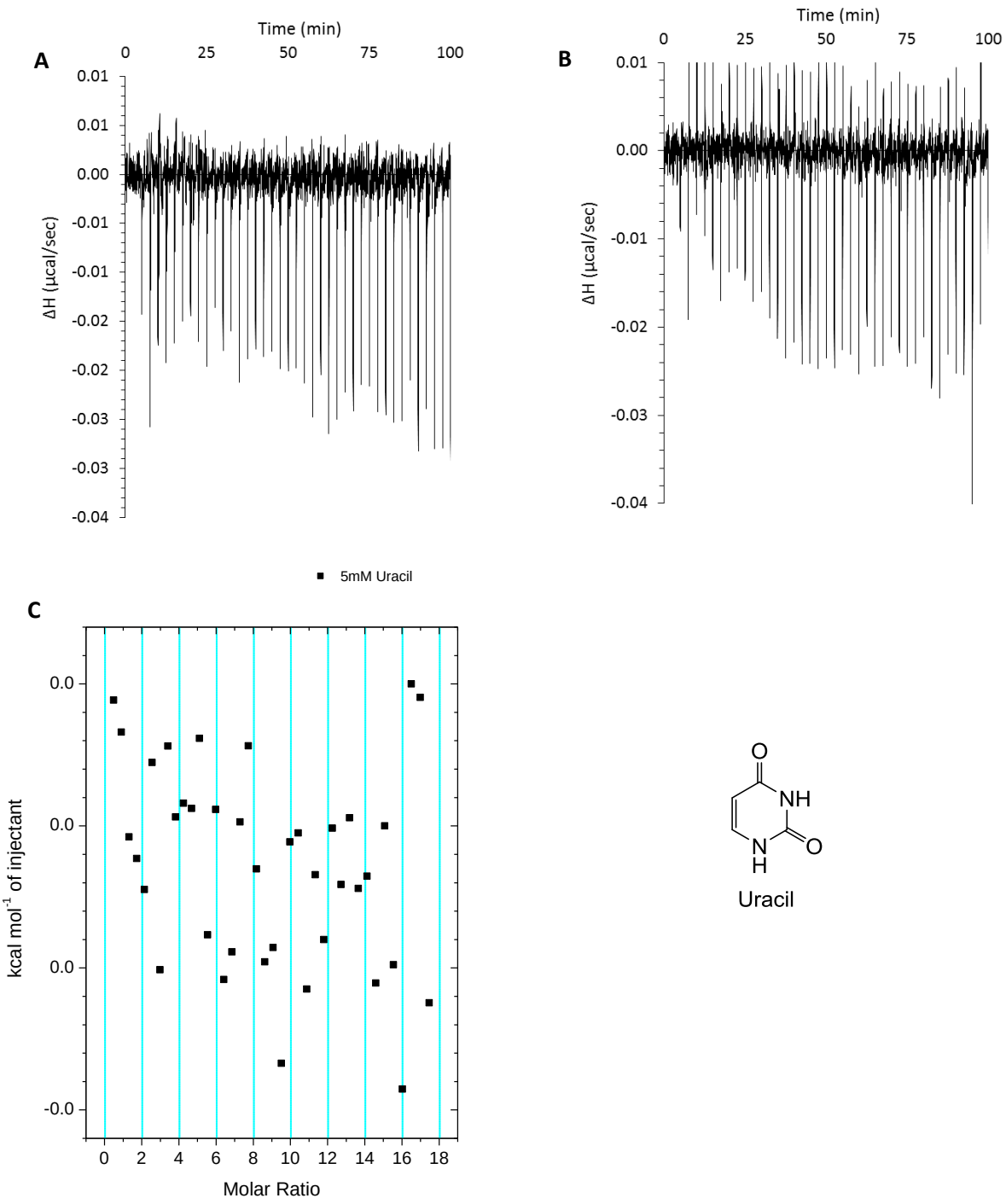

Supplementary Figure 69 | ITC binding results for receptor **2** (0.06 mM) titrated with uracil (5 mM, limit of solubility) in 10 mM phosphate buffered saline (pH 7.4), in which: A) shows the blank run (addition of uracil into water); B) shows the titration (uracil into receptor **2**) and C) shows the plotted change in enthalpy vs molar ratio. The experiment was performed once.

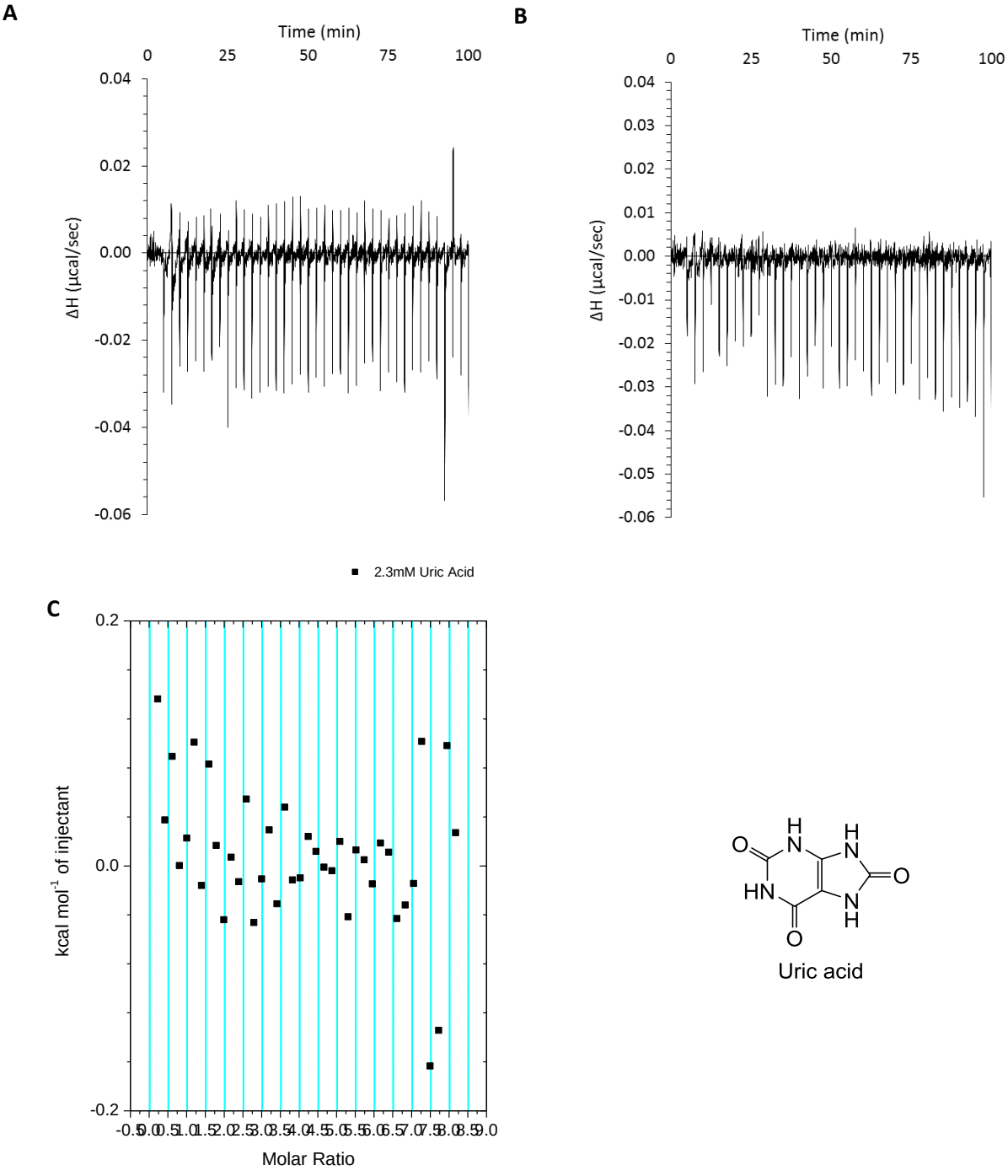

Supplementary Figure 70 | ITC binding results for receptor **2** (0.06 mM) titrated uric acid (2.34 mM, limit of solubility) in 10 mM phosphate buffered saline (pH 7.4), in which: A) shows the blank run (addition of uric acid into water); B) shows the titration (uric acid into receptor **2**) and C) shows the plotted change in enthalpy vs molar ratio. The experiment was performed once.

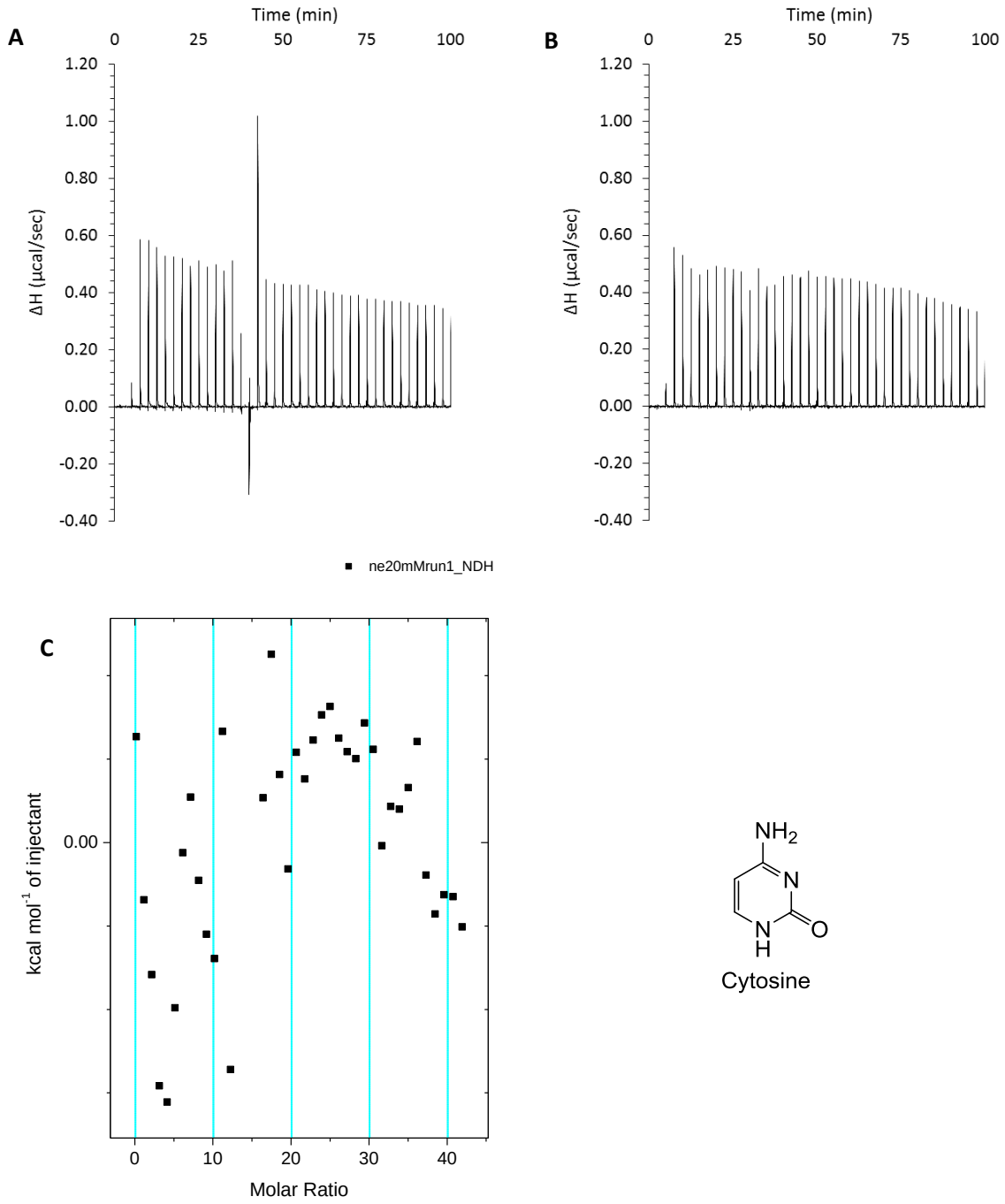

Supplementary Figure 71 | ITC binding results for receptor **2** (0.1 mM) titrated with cytosine (20 mM) in 10 mM phosphate buffer solution (pH 7.4) in which: A) shows the blank run (addition of substrate into medium); B) shows the titration (substrate into receptor **2**); C) shows the plotted change in enthalpy vs molar ratio. The experiment was performed 3 times with similar results.

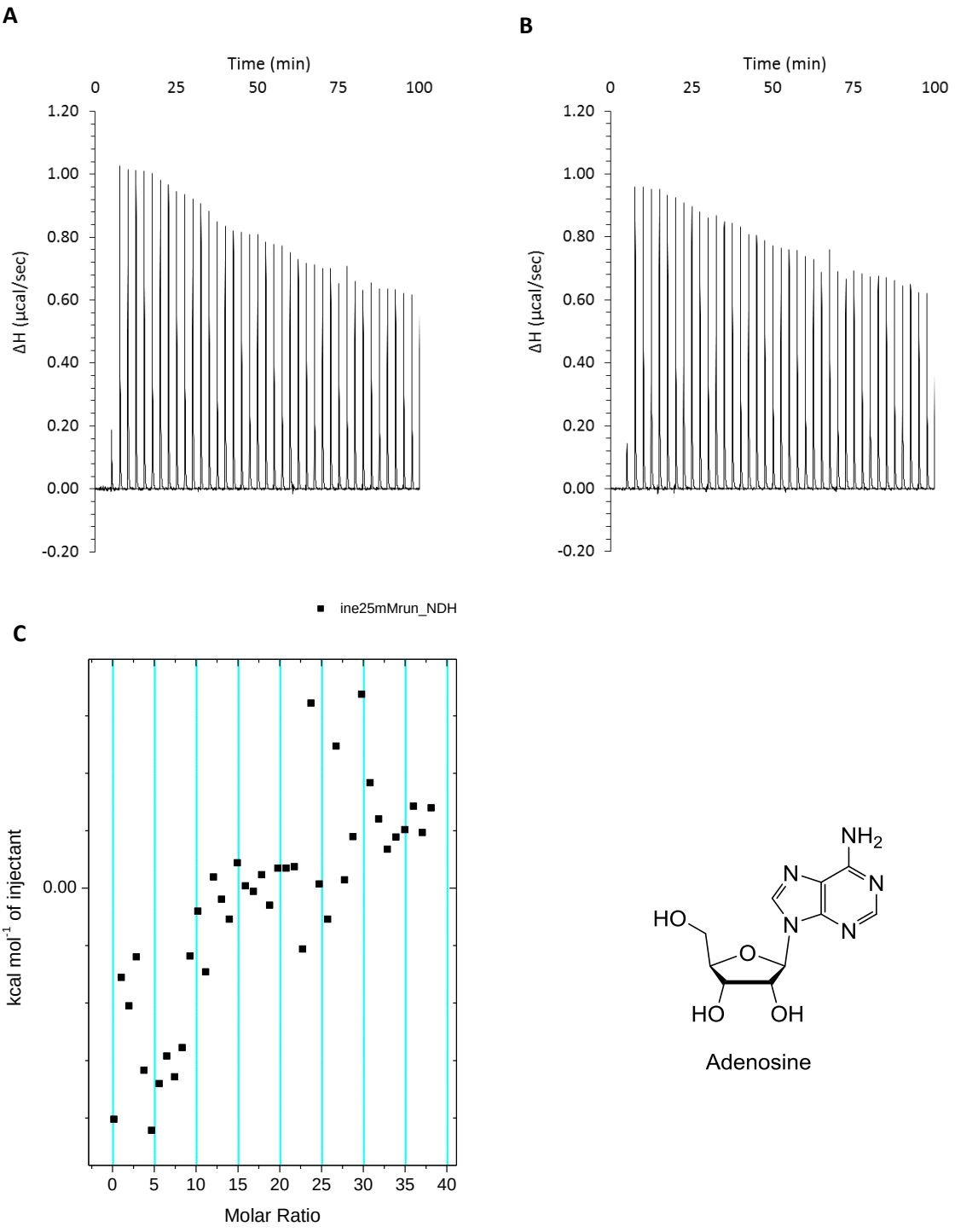

Supplementary Figure 72 | ITC binding results for receptor **2** (0.1 mM) titrated with adenosine (500 mM) in 10 mM phosphate buffer solution (pH 7.4) in which: A) shows the blank run (addition of substrate into medium); B) shows the titration (substrate into receptor **2**); C) shows the plotted change in enthalpy vs molar ratio. The experiment was performed once.

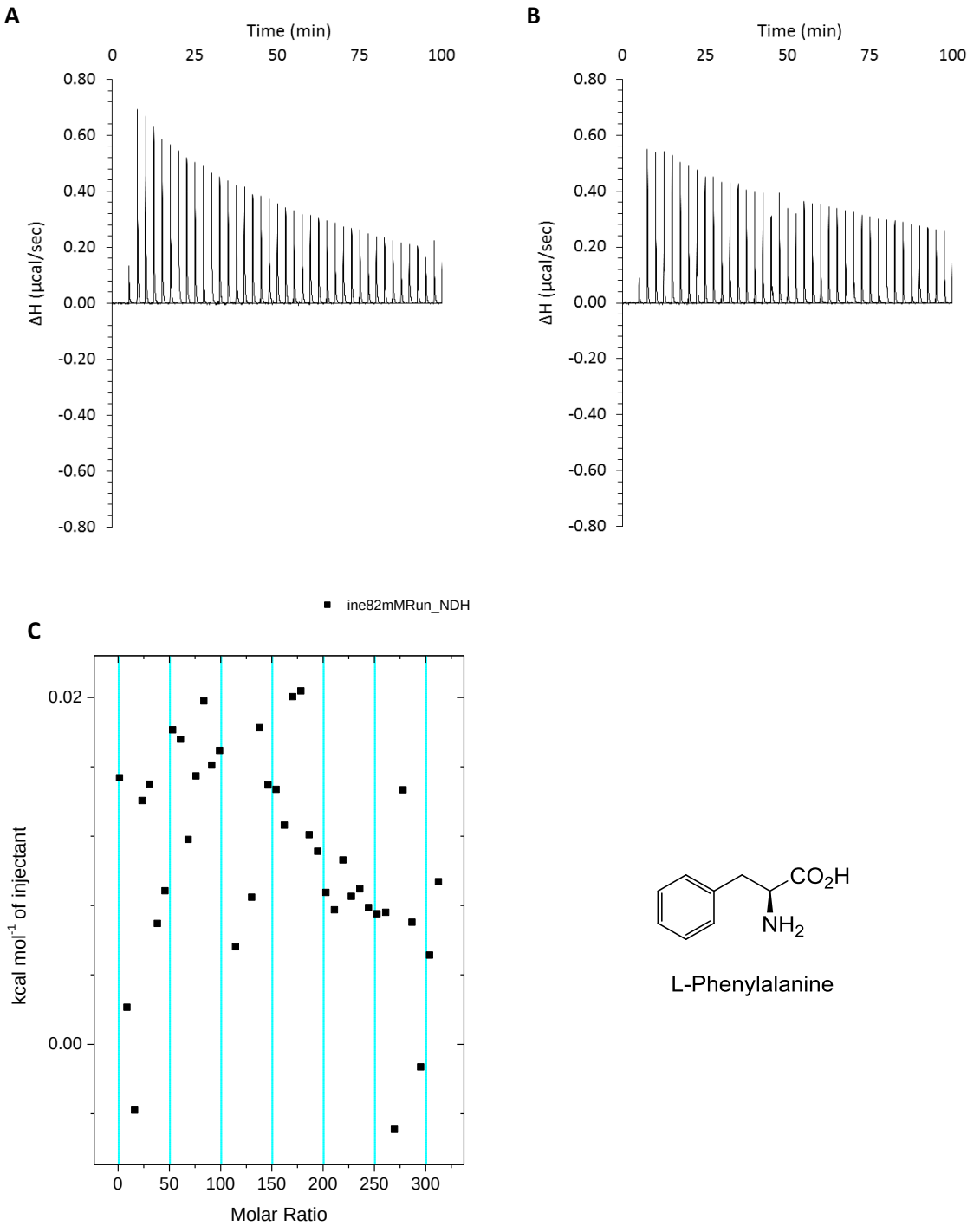

Supplementary Figure 73 | ITC binding results for receptor **2** (0.06 mM) titrated with L-phenylalanine (82 mM) in 10 mM phosphate buffer solution (pH 7.4), in which: A) shows the blank run (addition of substrate into medium); B) shows the titration (substrate into receptor **2**); C) shows the plotted change in enthalpy vs molar ratio. The experiment was performed 2 times with similar results.

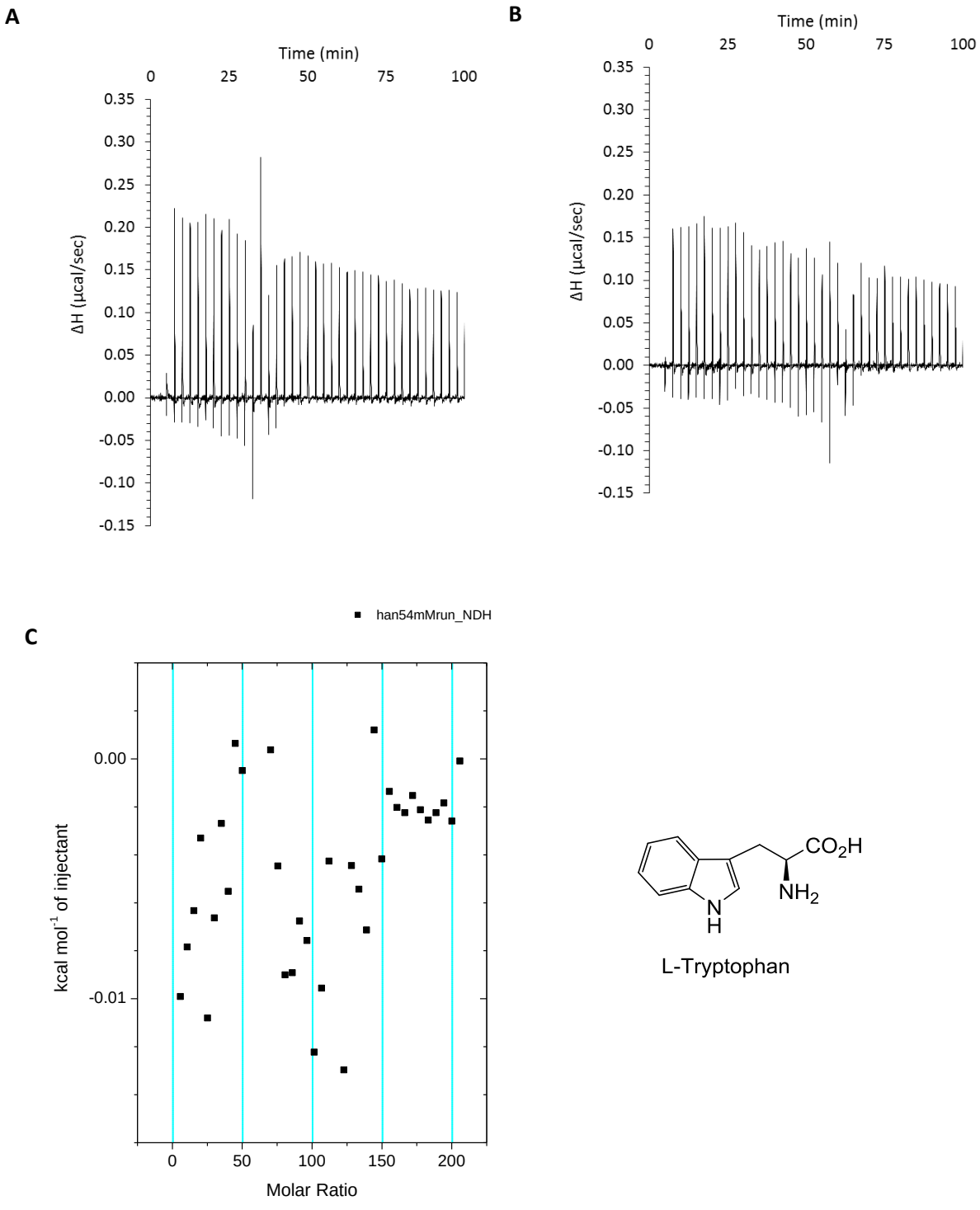

Supplementary Figure 74 | ITC binding results for receptor **2** (0.06 mM) titrated with L-tryptophan (54 mM) in 10 mM phosphate buffer solution (pH 7.4), in which: A) shows the blank run (addition of substrate into medium); B) shows the titration (substrate into receptor **2**); C) shows the plotted change in enthalpy vs molar ratio. The experiment was performed once.

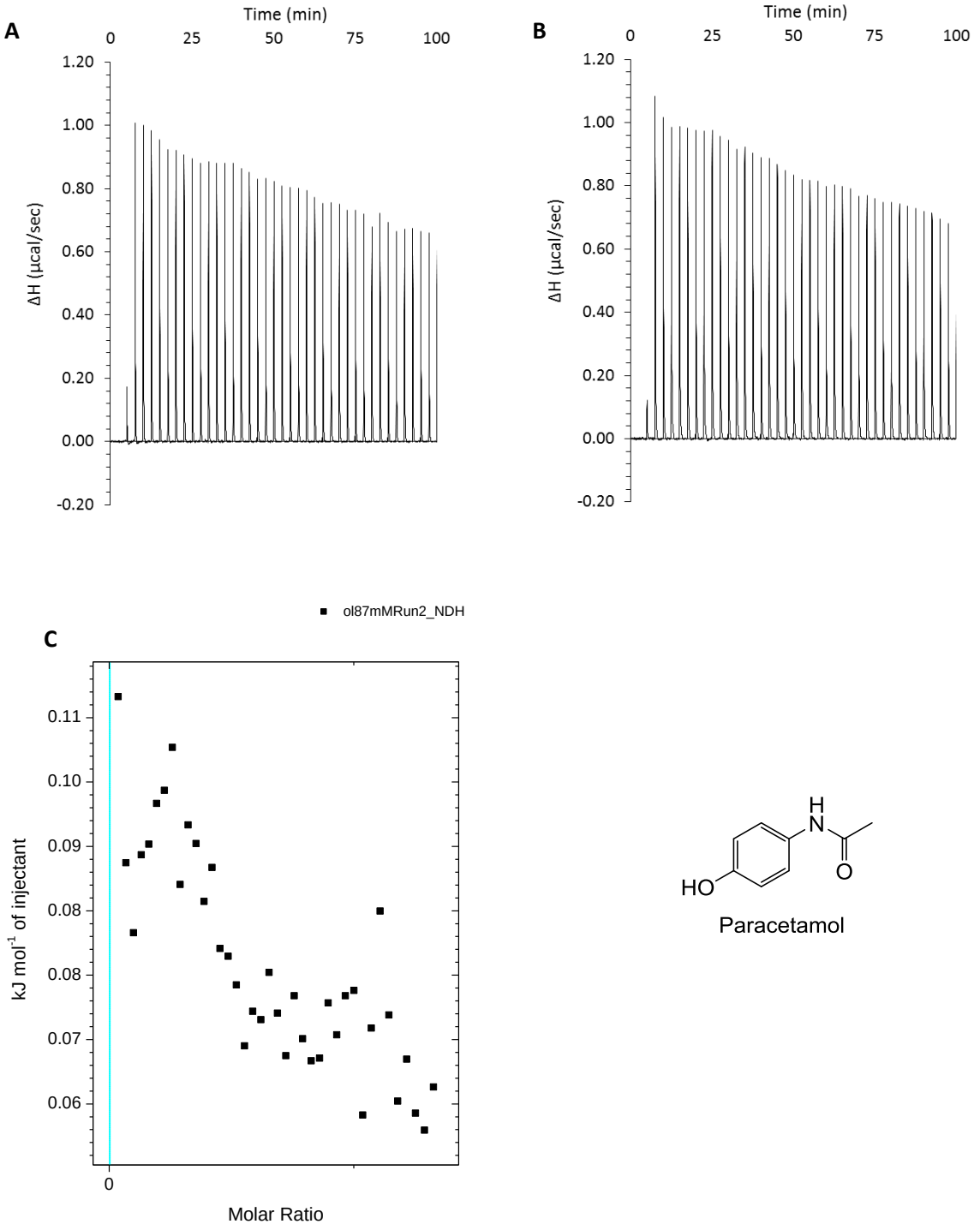

Supplementary Figure 75 | ITC binding results for receptor **2** (0.06 mM) titrated with paracetamol (87 mM) in 10 mM phosphate buffer solution (pH 7.4), in which: A) shows the blank run (addition of substrate into water); B) shows the titration (substrate into receptor **2**); C) shows the plotted change in enthalpy vs molar ratio. The experiment was performed 2 times with similar results.

3. Modelling Studies

Free Receptor

Modelling studies employed Maestro Version 10.4.018, using Batchmin V11.0 for energy minimisation. The nonacarboxylate **D** was employed as a surrogate for **2**, as the full receptor structure generated software errors. Monte Carlo Molecular Mechanics (MCMM) simulations were undertaken allowing rotations around all non-aromatic bonds in the bicyclic system and also the Ar-Et bonds. The calculations employed both MMFFs and OPLS2005 force fields force-fields, aqueous GB/SA solvation, and 2000 MCMM steps. The two force fields gave similar ground state structures with inward-directed NH groups and outward-directed methyl groups. The structure resulting from the OPLS2005 calculation is shown in Supplementary Supplementary Figure **76**. It is notable that, in work on eariler synthetic carbohydrate receptors, the MMFFs and OPLS2005 force fields have given qualitatively different structures. The similar results in this case suggest a clear preference for open conformations with inward-directed NH groups.

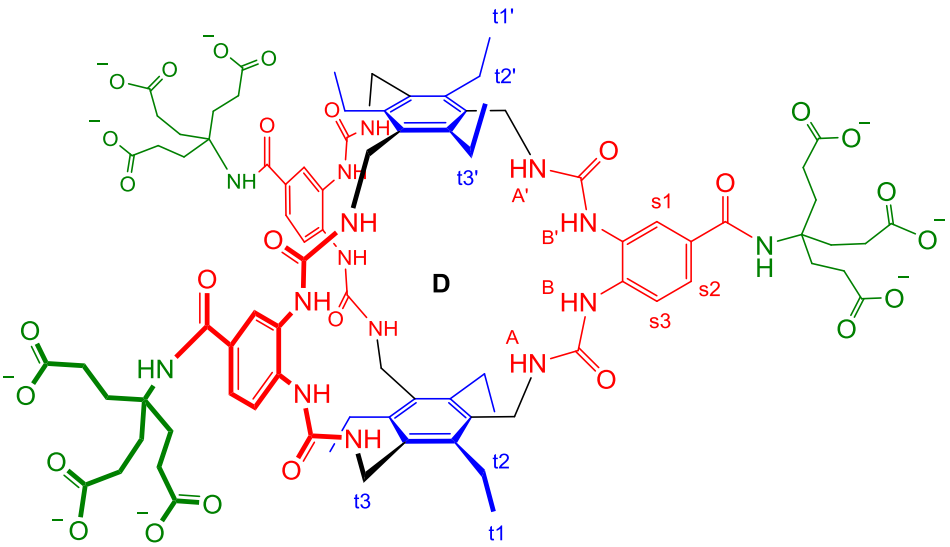

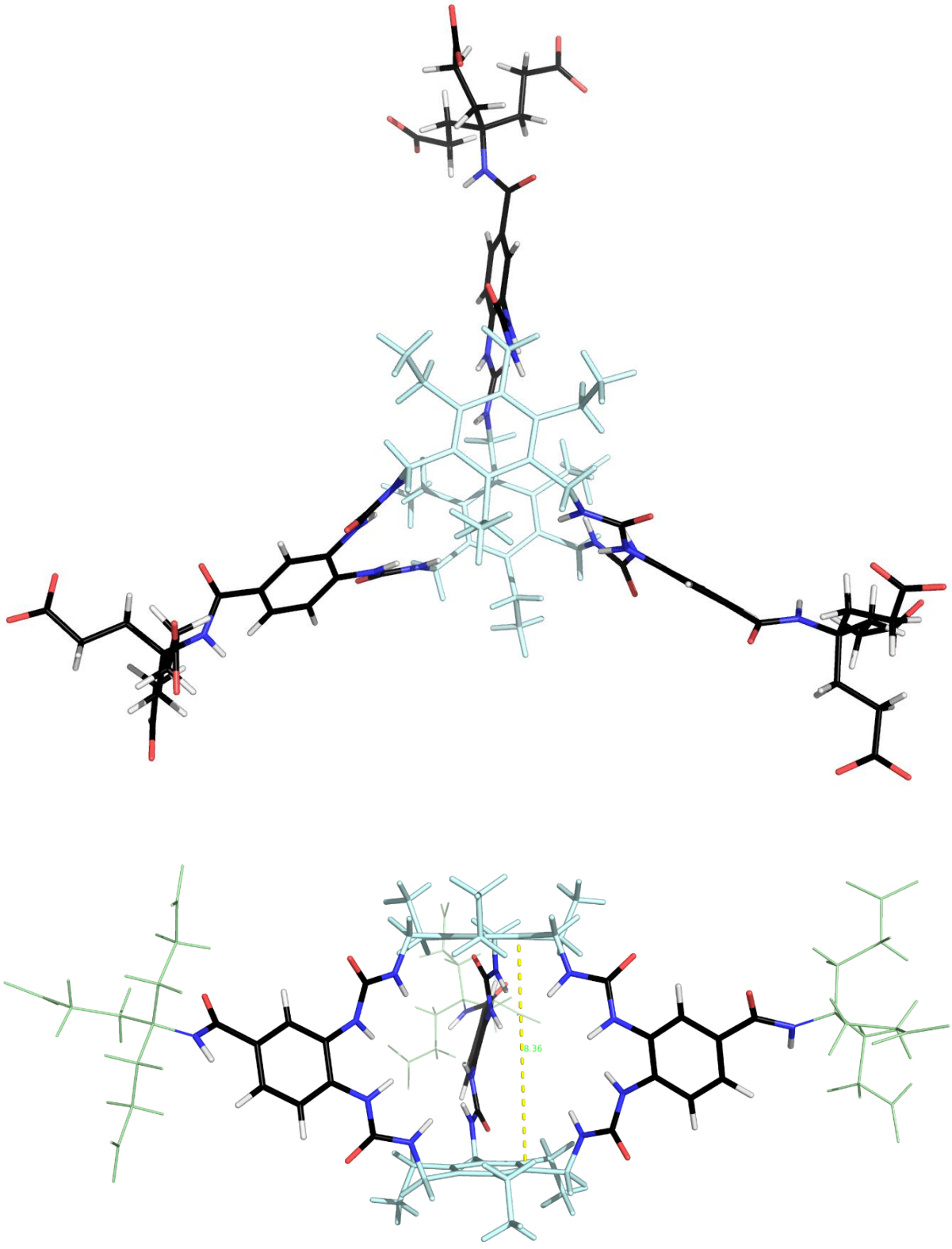

Supplementary Figure 76 | Ground state structure from the MCMM simulation of model receptor **D**, OPLS2005 force field, shown from two perspectives. The triethylmesitylene (TEM) units are highlighted in pale blue and tricarboxylate side-chains in pale green. The inter-TEM distance is 8.36 Å (yellow broken line).

Complex with β-D-Glucose 1

The complex **D.1** was modelled using the same software and force fields as employed for **D** above. The initial structures were generated by placing the glucose in the centre of the ground state receptor conformations from the above calculations, lying parallel to the triethylbenzene aromatic surfaces. MCMM calculations (1000 steps) were then performed allowing the acyclic bonds in the glucose to rotate and the glucose itself to rotate and move (max. distance 0.5 Å). The result for the OPLS2005 force field is shown in Supplementary Supplementary Figure **77**and Supplementary Supplementary Figure **78** (also Figure 1d in the paper), and that for the MMFFs force field in Supplementary Supplementary Figure **79** and Supplementary Supplementary Figure **80**. As reported in the paper, the OPLS2005 calculation predicted 10 intermolecular hydrogen bonds of length 1.95 - 2.48 Å. The MMFFs method appears to give shorter and stronger hydrogen bonds, finding 11 in the range 1.81 – 2.47 Å; the extra H-bond arises because three are predicted between a spacer diurea and the glucose 4-OH. In the discussion we prefer to use the OPLS2005 structure, as the more conservative option.

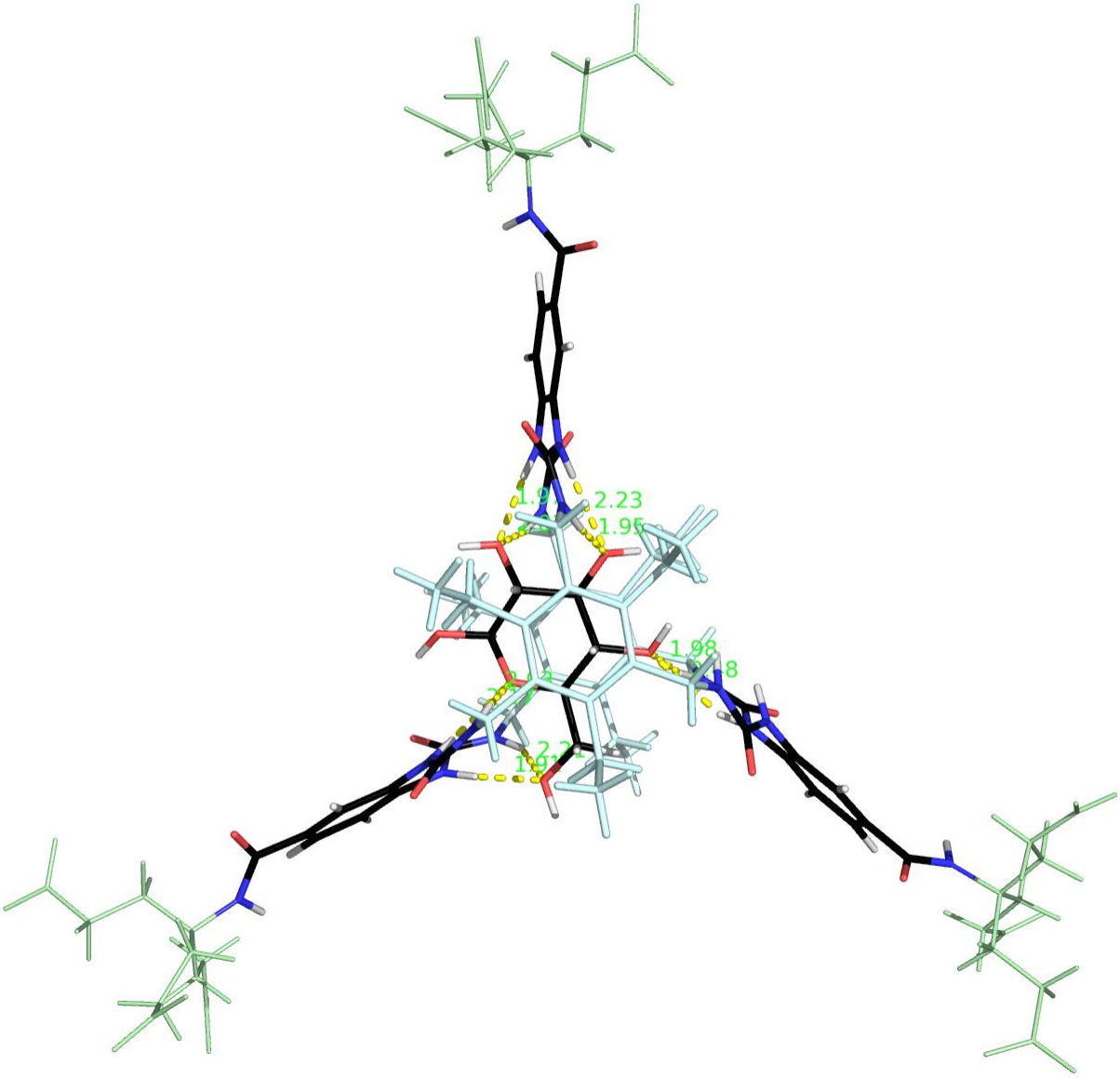

Supplementary Figure 77 | Ground state structure from the MCMM simulation of model receptor **D**, OPLS2005 force field, shown from above. The triethylmesitylene (TEM) units are highlighted in pale blue and tricarboxylate side-chains in pale green. Ten intermolecular hydrogen bonds are shown as yellow broken lines.

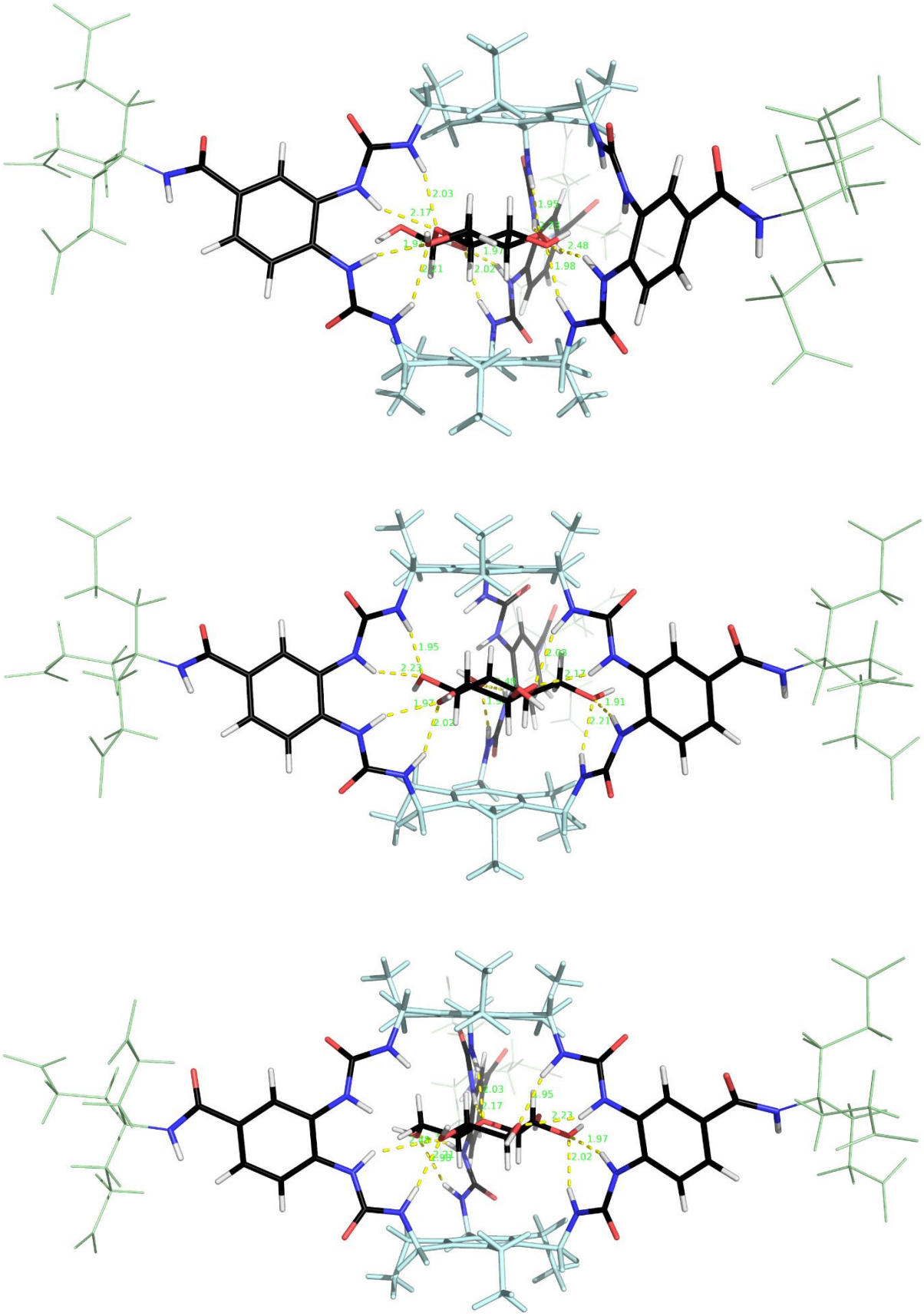

Supplementary Figure 78 | As Supplementary Supplementary Figure **77** (OPLS2005 structure) shown side-on from three perspectives. Top: Glucose CH_2OH points towards viewer. Middle: CH_2OH points right. Bottom: CH_2OH points left.

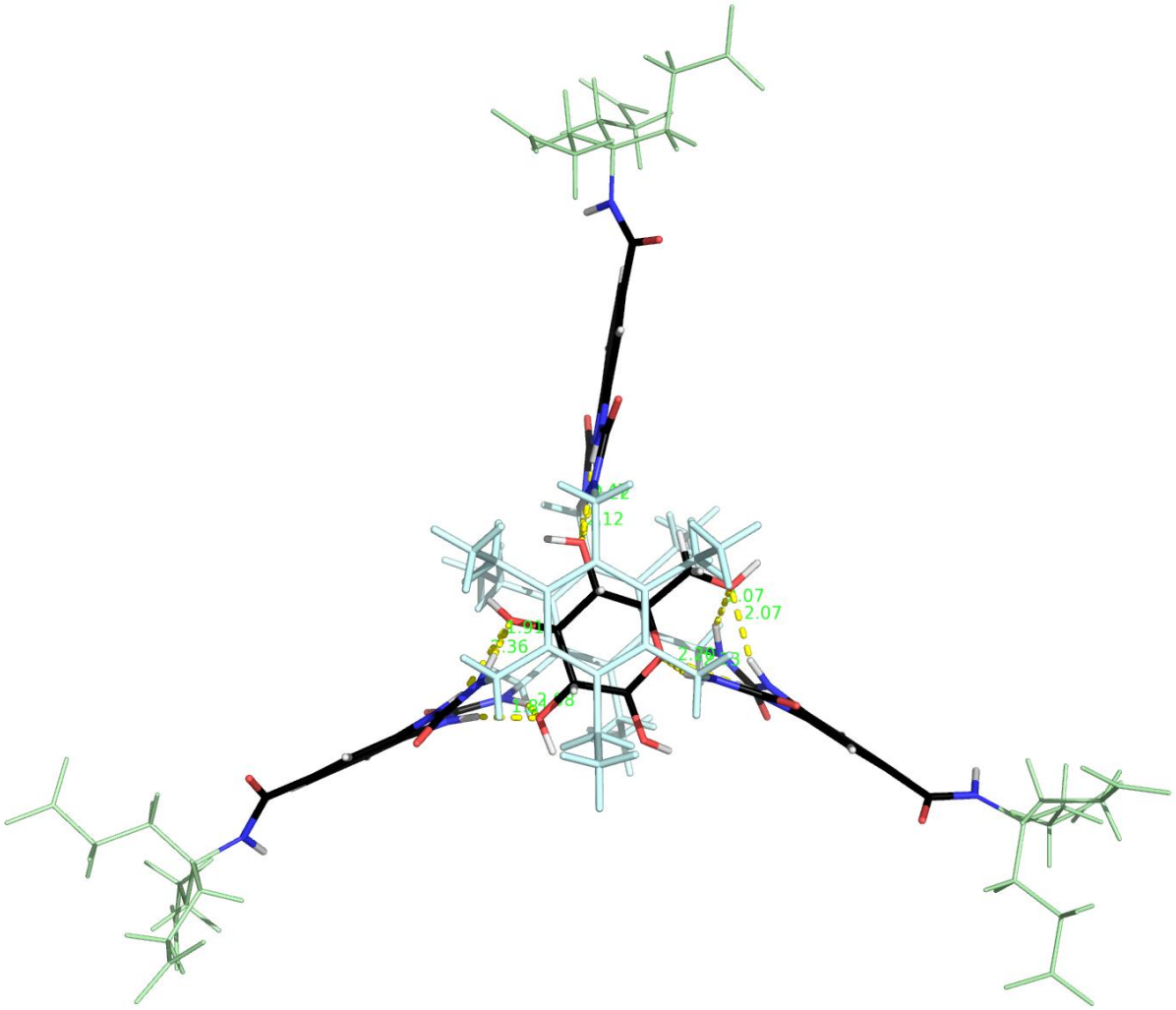

Supplementary Figure 79 | Ground state structure from the MCMM simulation of model receptor **D**, MMFFs force field, shown from above. The triethylmesitylene (TEM) units are highlighted in pale blue and tricarboxylate side-chains in pale green. Eleven intermolecular hydrogen bonds are shown as yellow broken lines.

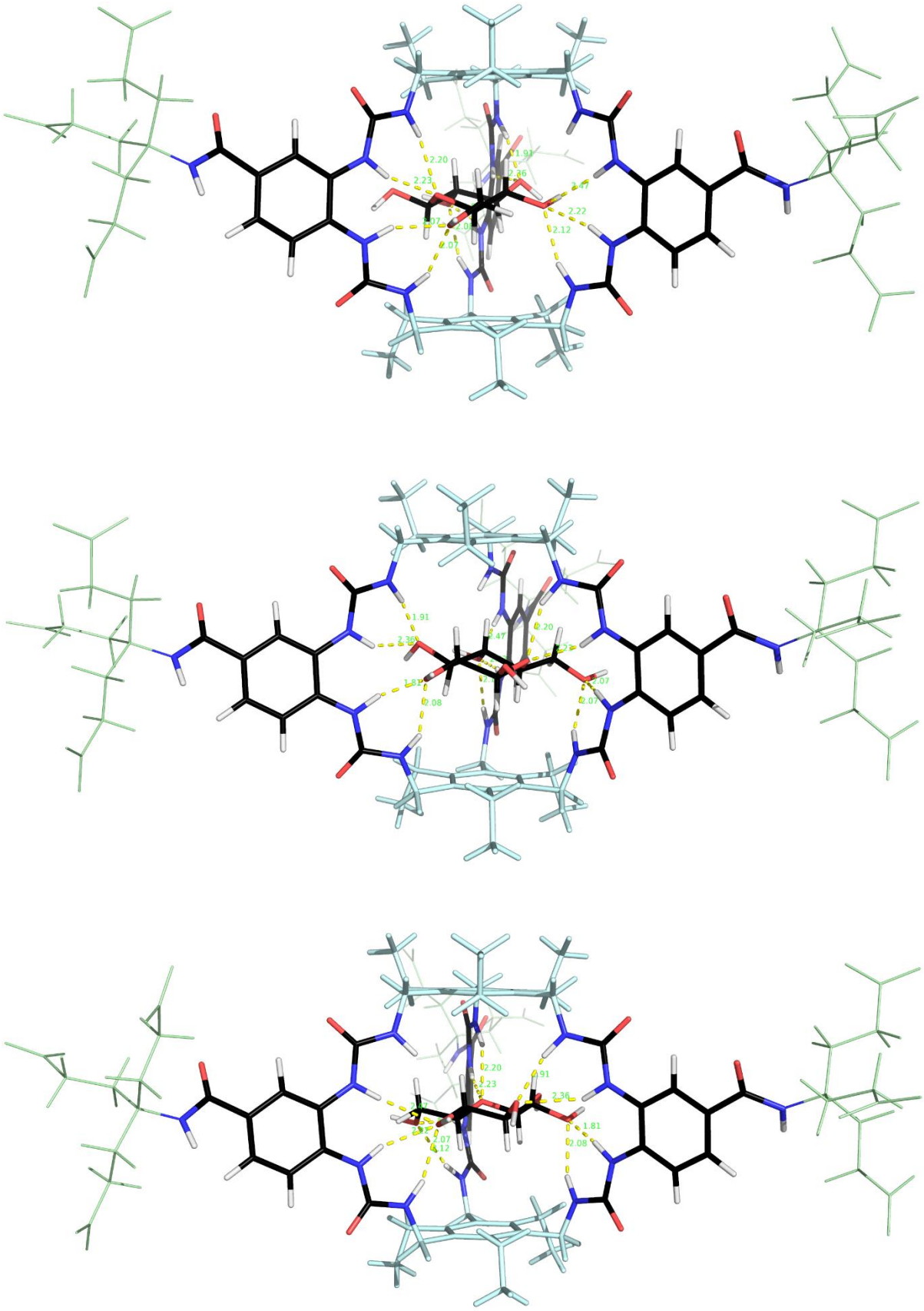

Supplementary Figure 80 | As Supplementary Supplementary Figure **79** (MMFFs structure) shown side-on from three perspectives. Top: Glucose CH_2OH points towards viewer. Middle: CH_2OH points right. Bottom: CH_2OH points left.